Quest for Peptidase Activity Modifiers: Benefits of Kinetic Strategies

Dissertation

zur

Erlangung der naturwissenschaftlichen Doktorwürde
(Dr. sc. nat.)

vorgelegt der
Mathematisch-naturwissenschaftlichen Fakultät

der

Universität Zürich
von

Patricia Schenker
von Walterswil, SO

Promotionskomitee

Prof. Dr. Amedeo Caflisch (Vorsitz)
Prof. Dr. Antonio Baici (Leitung der Dissertation)
Prof. Dr. Brigita Lenarčič
Prof. Dr. Ben Schuler

Zürich, 2009

To Stefan

Acknowledgements

First of all, I would like to thank Prof. Dr. Antonio Baici for giving me the opportunity to work in his lab and introducing me in the beautiful world of enzyme kinetics. I am, and I always will be fascinated about what one can see with carefully performed kinetic measurements.
I am thankful to Prof. Dr. Brigita Lenarčič for being in my thesis committee and the unfortunately not many but interesting discussions we had. Also I would like to thank Prof. Dr. Amedeo Caflisch and Prof. Dr. Ben Schuler for their acceptance in being in my thesis committee.

Besides, I would like to thank my collaborators, Pietro Alfarano, Peter Kolb, Michael Wächter and Peter Rüedi for working with me on interesting topics. A special thank goes to Pietro Alfarano, with whom I shared most time at the Institute. He gave me support not only in scientific related issues and has always been a very good and honest friend to me.

Furthermore I would like to thank Heidi Roschitzki-Voser, Beatrice Paoli, Michaela Kramer, Steve Rast and Sara Züger for their encouragement, the talks we had and the nice time spent together. Also my current lab member Marko Novinec for discussions and keeping me company.

A special thank goes to Alexandra Altorfer with whom I shared most of the time in the lab. She gave me fundamental backup during the last part of my thesis and always found the right encouraging words to keep me going on. Not least, I am deeply grateful for her efforts that made running fun again for me.

Finally I am truly thankful to my family, their support and encouragement over all these years. Above all, Stefan, the man by my side.

Summary

Peptidases are indispensable for physiological activation and turnover of proteins but in the extracellular space they may escape control and be harmful to the organism. This thesis focuses on the mechanism of interaction between peptidases and modifiers taking into account the peculiar microenvironment concerned with cells, enzymes, inhibitors and activators.

The insoluble nature of extracellular matrix components, which build up connective tissues, is a central point in the pharmacological management of pathological peptidases, for which adequate investigation tools are necessary. The kinetic mechanism of inhibition of enzyme modifiers designed for pharmacological applications has been considered so far only marginally but is nevertheless of paramount importance. Indeed, ascribing modifiers to their correct inhibition/activation category by kinetic studies carefully performed *in vitro*, provide support to the interpretation of pharmacokinetic and pharmacodynamic issues.

We performed a systematic re-evaluation of enzyme inactivators using acetylcholinesterase as a model enzyme. Considering a comprehensive collection of common and rare mechanisms of action, we set up diagnostic tools for model discrimination, which were tested and validated with practical examples.
Conventional, competitive inhibitors carrying warheads directed to the active center of extracellular matrix degrading peptidases may experience serious difficulties in reaching and effectively controlling their targets. This occurs because the enzymes are tightly bound to their insoluble substrates and virtually do not detach during their permanence in the tissues. We identified a compound that binds outside the catalytic center of cathepsin B and controls the flexibility of a key structural element, which is responsible for the exo- and endopeptidase activity of the enzyme. This and similar inhibitors possessing engineered structures that bind to accessible sites of the target enzymes, even when these are tightly bound to their substrates, represent valuable candidates for the pharmacological control of pathological peptidases.

Artificially designed modifiers target outside the active site of enzymes may be engaged in multiple interactions with naturally occurring inhibitors as well as with unspecific ligands such as components of the extracellular matrix. We elaborated a kinetic model for describing double interaction between modifiers and enzymes, which assists in making predictions of synergy, zero-interaction and antagonism between inhibitors and/or activators and can be used for non-linear regression analysis of experimental data as well.
Ordinary, uncommon and even bizarre effects brought about by the combination of two modifiers, such as reactivation at high effector concentration following inhibition at low concentration, can be quantitatively interpreted with the aid of easy-to-use kinetic equations. The theoretical treatment could be used for interpreting puzzling results obtained with elastase-2 in interaction with sulfated glycosaminoglycans.

Zusammenfassung

Peptidasen sind für die physiologische Aktivierung und den Umsatz von Proteinen unabdingbar. Jedoch können sie in der extrazellulären Matrix der natürlichen Kontrolle entkommen und in der Folge für den Organismus schädlich wirken. Die vorliegende Arbeit fokussiert sich auf die Interaktionsmechanismen zwischen Peptidasen und ihren Modifiern unter Miteinbezug der auffälligen Mikroumgebung bestehend aus Zellen, Enzymen, Inhibitoren und Aktivatoren.

Die Unlöslichkeit der das Bindegewebe aufbauen extrazellulären Bestandteile, ist ein zentraler Punkt innerhalb der pharmakologischen Handhabung von pathologischen Peptidasen. Deshalb werden bei Untersuchungen von Peptidasen geeignete Werkzeuge benötigt. Bisher wurde der kinetische Mechanismus einer Enzyminhibition trotz seiner Wichtigkeit in pharmakologischen Anwendungen nur geringfügig in die Analysen miteinbezogen. Jedoch kann die Zuordnung eines Modifiers zu seinem Inhibitions-/Aktivationsmechanismus durch sorgfältige *in vitro* Messungen unterstützend bei der Interpretation von pharmakokinetischen und pharmakodynamischen Problemen wirken.

Wir führten eine systematische Neubeurteilung von Inaktivatoren durch unter Benutzung von Acetylcholinesterase als Modellenzym. In Anbetracht einer umfangreichen Kollektion von häufigen und seltenen Mechanismen stellten wir diagnostische Werkzeuge für die Modelldiskriminierung auf, die anhand praktischer Beispiele getested und validiert wurden.
Herkömmliche kompetitive Inhibitoren, die sogenannte 'warheads' gerichtet gegen das aktive Zentrum einer extrazellulären Matrix abbauenden Peptidase tragen, können ernsthafte Schwierigkeiten in der Erreichung und effektiven Kontrolle ihrer Targets erfahren. Der Grund liegt in der sehr starken Anbindung der Enzyme an ihre unlöslichen Substrate von denen sie während ihrer Zeit im Gewebe praktisch nicht weg dissoziieren. Wir identifizierten ein Molekül das ausserhalb der aktiven Stelle von Cathepsin B bindet und die Flexibilität eines strukturellen Schlüsselelementes, verantwortlich für die Exo- und Endopeptidaseaktivität des Enzyms, kontrolliert. Solche und ähnliche Inhibitoren welche konstruierte Strukturen besitzen die ausserhalb der

aktiven Stelle eines Enzyms binden auch wenn dieses fest an ein Substrat gebunden ist, repräsentieren wertvolle Kantidaten für die pharmakologische Kontrolle von pathologischen Peptidasen.
Künstlich hergestellte Modifier welche ausserhalb des aktiven Zentrums eines Enzyms binden, können mit den natürlich vorkommenden Inhibitoren wie auch unspezifischen Liganden, z.B. Komponeten der extrazellulären Matrix, in Wechselwirkung treten. Wir arbeiteten ein kinetischen Modell aus um die doppelte Interaktion zwischen Modifiern und Enzymen zu beschreiben, was in der Vorhersage von 'Synergy', 'Zero-Interaction' und 'Antagonism' zwischen Inhibitoren und/oder Aktivatoren benutzt werden kann, wie auch für die nicht-lineare Regressionsanalyse von experimentellen Daten.
Gewöhliche, ungewöhnliche aber auch sonderbare Effekte hervorgerufen durch die Kombination von zwei Modifiern, wie beispielsweise die Reaktivierung bei hoher Modifierkonzentration nach einer unsprünglichen Inhibition bei tiefen Modifierkonzentration, können quantitativ durch die Zuhilfenahme von einfach zu benützenden kinetischen Gleichungen interpretiert werden. Die theoretische Behandlung konnte für die Interpretation der rätselhaften Resultate eingesetzt werden, welche sich bei der Interaktion von Elastase-2 mit Glykosaminoglykanen zeigten.

Contents

Introduction

The Area Under Investigation

Hydrolytic enzymes, chiefly peptidases, are involved in tumor malignancy and invasion as well as in destruction of connective tissue in inflammatory and non-inflammatory rheumatic diseases. Cellular invasion characterizes many physiological (e.g. wound healing, uterine involution, tooth eruption) and pathological processes (e.g. tumor invasion, angiogenesis, inflammation), and the enzymatic mechanisms of all these situations are similar. Invasive cells produce enzymes which are able to degrade the barriers (basement membranes and extracellular matrices) they must cross.
The pharmacological inhibition of extracellular matrix degrading peptidases by exogenous modifiers is a delicate task, for which a solution has not yet been found. The obstacles to this goal must be sought in the peculiar nature of the substrates of these enzymes, which are insoluble macromolecular assemblies, and in the demanding properties exogenous inhibitors should possess for accomplishing their difficult mission.

Before describing the aims of this thesis, an overview of the extracellular matrix, of the cellular events responsible for matrix homeostasis and enzyme production, as well as a short portrait of the enzymes involved are presented below.

1.1 The Extracellular Matrix

Connective tissue consists of an extracellular matrix (ECM) and a cellular component. Here, the building blocks, the properties and the interactions between these structures, with focus on ECM remodeling and degradation, are discussed. Because of the possible harmful effects, caused by excessive or insufficient degradation of tissue matrix, the remodeling processes need to be tightly controlled. Thus, in the last part of this section a few pathologies relevant to the topic of this thesis are described and control failure is discussed.

1.1.1 Cells Involved in ECM Remodeling and Degradation

The cells responsible for the synthesis and maintenance of the ECM are of mesenchymal origin, fibroblasts, osteoblasts, chondrocytes, myocytes and adipocytes, which undergo developmental transformation until reaching a characteristic tissue-specific phenotype, which governs the correct expression of matrix components, such as the collagen types II, IX and XI in articular cartilage, the collagen types I and III in skin, as well as elastin and the proteoglycans.
Besides being involved in physiological remodeling, the cells mentioned above may also participate in pathological connective tissue degradation following failure of the natural control mechanisms.
Blood-borne cells sustain the role of resident cells in the ECM by participating in physiological remodeling, e.g. in bone fracture and wound healing, as well as in pathological situations, such as tumor invasion and cartilage degradation. Among the cells involved in the process of ECM remodeling are leukocytes and fibroblasts.

Leukocytes are part of the immune system and are further classified into lymphocytes, polymorphonuclear leukocytes (among which the neutrophilic granulocytes, 'neutrophils', play a leading role being the first cells recruited at inflammatory sites), platelets, monocytes and macrophages.
Fibroblasts, chondrocytes and osteocytes are the major cells in the synthesis and maintenance of ECM and produce the non-collagenous components, collectively called the *ground substance* that mainly comprise the proteoglycans, as well as elastic and collagen fibers, called the *fibrous substance*. Under homeostatic conditions they are found in their differentiated state, but upon stimulation these cells may undergo phenotypic transition, often towards a primitive fibroblast-like state. Following this transformation, the metabolic habits of the cells and their characteristic protein expression patterns change, including excessive synthesis of peptidases, which results in net degradation of the ECM.
Especially macrophages and neutrophils are involved in the degradation of matrix components. Tissue material that needs to be degraded is either phagocytosed and hydrolyzed intracellularly by these cells, or the degradation occurs in the extracellular space through the action of secreted/exocytosed peptidases.

Tissue remodeling by extracellular proteolysis is a vital process in the human organism. Alveolar macrophages for example, contain lysosomes with various hydrolytic enzymes, which digest most ECM components. Additionally, these cells use an oxygen-dependent mechanism to rapidly produce the superoxide radical and hydrogen peroxide (*respiratory burst*, p. 10) to destroy microorganisms which entered the upper respiratory airways. Also the neu-

trophils, besides exploiting oxygen-dependent mechanisms to kill microorganisms, possess a complete battery of hydrolases and bactericidal proteins stored in large amounts in specific and azurophil granules, which are used for both intracellular and extracellular tasks.

Not all cells that take part in the maintenance of the equilibrium between degradation and production of the tissue matrix are permanently in the matrix. Preservation of the equilibrium between degradation by proteolysis and synthesis of new extracellular structures by different cells is indispensable to life. Fixed structures in the matrix and second messengers, such as chemokines and cytokines, provide guidance in communication and migration of the cells involved in tissue remodeling.

1.1.2 Structural Components of the ECM

As mentioned before, the ECM is divided into fibrous substance and ground substance. Collagen and elastin contribute the fibrous substance of the extracellular matrix, proteoglycans and the ground substance. Depending on the tissue type, the proportion of the two substances fits to the properties required.

Fibrous Substance

Elastic fibers are composed of elastin, microfibrils as well as proteoglycans. Owing to their great elasticity, they are mainly found in organs subjected to stress, like lungs and aorta. Stability, organization and strength is supplied by collagen fibers, made up by over 20 different, genetically distinct collagen types. Collagen and elastin fibers are often interweaved to prevent rupture of the tissue. Imbalance in the proportion of either one of these fibers at the wrong place in the organism can cause severe pathologies [39, 97].

Ground Substance

Proteoglycan monomers, consisting of a core protein with covalently linked glycosaminoglycans (Figure 1.1a), which, in association with hyaluronan and linked proteins build large aggregates (Figure 1.1b), the main components of the ground substance.
We distinguish between extracellular proteoglycans (e.g. fibromodulin, lumican, decorin) and proteoglycans on the cell membrane (e.g. syndecan, CD44, perlecan). Decorin is the smallest proteoglycan with only one glycosaminoglycan side chain and aggrecan found in cartilages is the largest (up to 100MDa). The turnover of proteoglycans is relatively fast. Having a short half-life (e.g. around 20 days for aggrecan), they are continuously renewed and interactions between these structures and fibers of the ECM affect their dimension.

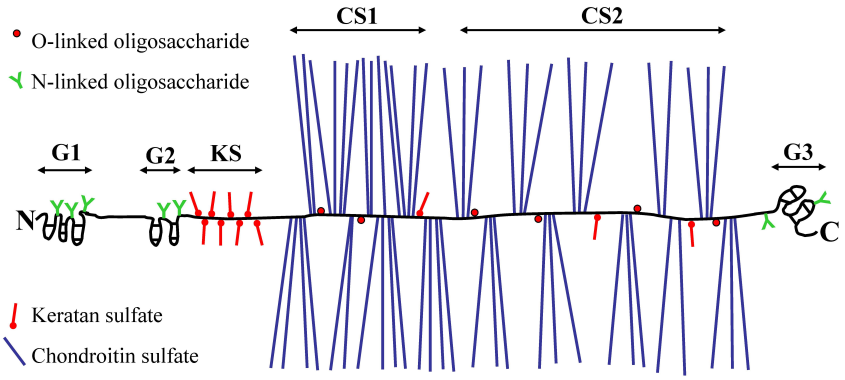

(a)

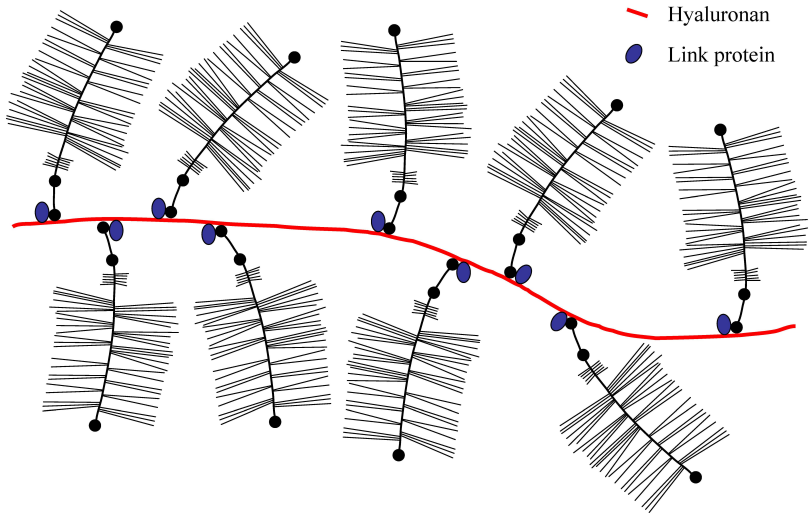

(b)

Figure 1.1: Structure of a proteoglycan. a) Proteoglycan monomer. G1, G2 and G3: Globular domains with disulfide bridges, KS: Keratan sulfate rich region, CS1 and CS2: Chondroitin sulfate rich region. N and C denote the amino and carboxy termini, respectively. b) Aggregate of a proteoglycan.

Since the composition of proteoglycans is very variable, their function is manifold: they act as lubricants, space fillers, impact absorbers and regulators of diffusion [52]. Because of their anionic character due to carboxyl residues (COO^-) and sulfate ester groups (OSO_3^-), cations such as potassium (K^+), sodium (Na^+) and calcium (Ca_2^+) are bound to these glycosaminoglycans. These osmotically active cations bind water to form hydrated gels. A proteoglycan can in fact bind up to 50 times its weight of water and thus participates in the transport of nutrients through the ECM.

The proteoglycans support and anchor cells within the ECM and interact with enzymes and chemokines in order to focus and increase their effects. Moreover, proteoglycans control the osmotic pressure within the connective tissues.
In articular cartilage for instance, the resulting 'Donnan effect' produces a pressure comparable to that present in the tires of an automobile conferring this tissue the necessary resilience and impact absorber properties.
The functional aspects of proteoglycans are depicted in the cartoon on the right, showing the reversible compressibility of articular cartilage with a) the unloaded cartilage, where water is structurally organized between negative charges of glycosaminoglycans. b) The cartilage experiences compressive load, which displaces water and the negative charges come closer. c) With the removal of cartilage compression water is restored within ordered domains between the negative charges.

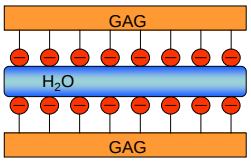

(a) unloaded cartilage

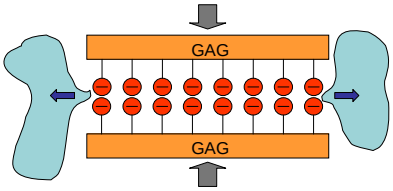

(b) cartilage under pressure

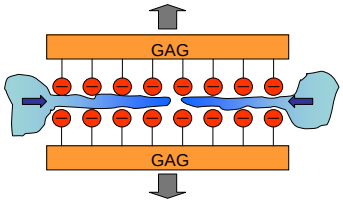

(c) removal of cartilage pressure

The glycosaminoglycans (chondroitin-, dermatan-, heparan-, keratan sulfate and hyaluronan) are highly negatively charged heteropolysaccharides of repeating disaccharide units with uronic acid and hexosamine (see below). They fill out most of the space in the ECM, even though they represent only 10% of the extracellular weight.
In virtue of its strong hydrophilic character and its stiffness, *hyaluronan* (or *hyaluronic acid*) is often used to create cell free environments. Abundant above all in brain, cartilage as well as bone is the glycosaminoglycan *chondroitin sulfate*. In most tissues an inhomogeneous sulfatation distribution of the disaccharide units, either at the C-4 or the C-6 position of the hex-

osamine ring, is found along the chondroitin sulfate chain. Even if labeled either chondroitin-4-sulfate or chondroitin-6-sulfate, commercially available chondroitin sulfates are always copolymers of the two isomers with intercalating sulfate-free sequences. The most common glycosaminoglycan in skin is *dermatan sulfate*, which is involved in processes of wound healing [107]. The chemical and physical properties of dermatan sulfate are due to the presence of iduronic acid in place of glucuronic acid found in chondroitin sulfates. This uronic acid confers dermatan sulfate additional molecular flexibility to adapt and favor binding to several proteins.

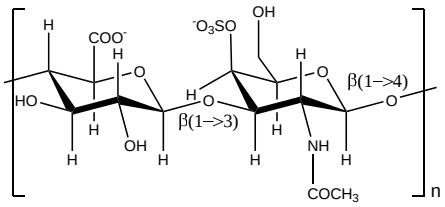

Chondroitin-4-sulfate

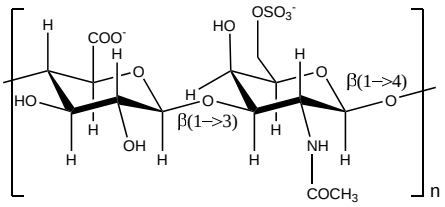

Chondroitin-6-sulfate

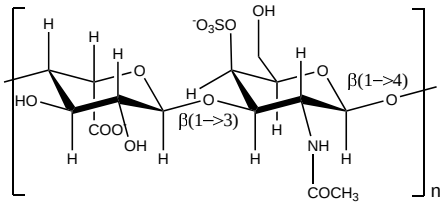

Dermatan sulfate

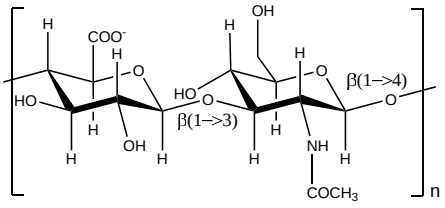

Hyaluronan

Heparan sulfate plays a key function in the kidney, where it takes part in glomerular filtration. Additionally, it binds several proteins, such as the fibroblast growth factor (FGF), a mediator in the stimulation of fibroblast proliferation. Chemokines are also immobilized by heparan sulfates, resulting in chemotactic activity for leukocytes. Because of its large hydration *keratan sulfate* is suitable for the absorption of mechanical shock. It is predominantly found in the cornea and cartilage [47].
Heparin has a structure similar to that of heparan sulfate and acts indirectly as anticoagulant by preventing the formation of blood clots interacting with antithrombin III. Following proteolytic activation of the precursor prothrombin, fibrinogen is degraded by thrombin and as a result, fibrin polymers are formed. After binding to heparin, antithrombin III (the true anticoagulant) undergoes a conformational change, which increases its binding affinity to thrombin and thus inhibits the coagulation cascade. The following irreversible formation of the antithrombin-thrombin complex, through cleavage of the antithrombin molecules, decreases the affinity of heparin again [87, 88].

1.1.3 Interactions Between Cells and the ECM

Communication between the ECM-resident cells and between cells and the matrix assures regular tissue remodeling. This exchange of information is carried out by cell-cell interactions (such as cadherins, or members of the immunoglobulin (Ig) family), cell-matrix interactions (via integrins, keratin filaments, selectins, glycoproteins), and through the mediation of second messengers (e.g. cytokines, interferons).
Remodeling of the tissue matrix beyond the normal processes resulting in local tissue destruction may be caused by infection or mechanical injury. In such situations, the immune system and especially inflammatory processes play an important role in establishing the success or failure of ECM remodeling.

The Immune System

A distinction is made between the innate and the adaptive immune system. The innate immune system, comprising the complement system, is antigen independent, whereas the adaptive immune system is characterized by its high specificity and antigen dependency.
Decisive for a fast initial reaction of the organism facing an invading pathogen, is the innate system as a 'first line of defense' with its defensive anatomic, physiologic, phagocytic and inflammatory barriers. The adaptive system, which is able to recognize and selectively eliminate specific antigens and microorganisms, needs more time to act effectively.
The internalization and degradation of pathogens is primarily performed by antigen presenting cells such as macrophages, B-cells and dentritic cells. The peptide fragments resulting from intracellular degradation of the pathogen are complexed with the major histocompatibility complex (MHC) II and presented on the surface of the cells. Intracellular antigens, such as viruses or tumor proteins, are also degraded by these cells but are presented with the MHC I complex.
The cell-mediated response includes the recognition of these antigens by T-cell (*thymus*), more specifically T_H-cells (*helper*) and T_C-cells (*cytotoxic*). Antigens bound to MHC II complexes are recognized by T_H-cells, MHC I complexed peptides by T_C-cells.
Once the interaction between a T_H-cell and a MHC II complex has occurred, the T-cell starts to produce cytokines and interleukins such as IL-2 that stimulates B-cells as well as T_C-cells. Upon cytokine stimulation, T_C-cells transform into cytotoxic T_C-cells enabling them to recognize and eliminate antigen-bearing cells more efficiently. T_H-cells also stimulate their clonal selection by the secretion of IL-1.
When B-cells interact with an antigen over cell membrane-bound antibodies, a humoral response takes place. The interaction causes the B-cell to

differentiate into an antibody-secreting plasma cell. The secreted antibodies facilitate the recognition and elimination of the corresponding antigen by phagocytosis.
In contrast to the cell-mediated response, most suitable for endogenous antigens, the humoral response is more suitable for exogenous antigens. Nevertheless, for an effective defense both systems are necessary.

Inflammation

Inflammation is a complex response of the organism triggered by local injury or infection and includes five development stages: 1) Tissue injury, followed by the release of inflammation mediators, such as histamine and cytokines. 2) Circulation disturbance resulting from a defective microcirculation (rubor, calor, dolor). 3) Exudation (tumor), as a result of the increased migration of inflammation mediators into the injured tissue. 4) Proliferation of cells and matrix components. 5) Healing and scarring.
In the first phase of inflammation, secreted mediators such as thrombin, histamine, IL-1 and the tumor necrosis factor-α (TNF-α) increase the production of cell adhesion molecules (CAMs), such as selectins, in local blood vessels. Following cell binding and with the aid of other cytokines (e.g. IL-8), the cell adhesion molecules control transendothelial migration.
In the tissue itself, neutrophils, the first cells migrated to an inflammatory site, develop more receptors for chemoattractants and Fc receptors for the recognition of immunoglobulin's. By chemotaxis, promoted by chemokines and prostaglandins, the neutrophils are guided to the site of inflammation.
The phagocytic activity of macrophages and neutrophils triggers a metabolic pathway, the *respiratory burst*, where reactive oxygen species (ROS) and reactive nitrogen intermediates (RNIs) are produced inside the cells. These products are partially secreted in the extracellular space, as are peptidases from neutrophil granules. Besides killing pathogens, the ROS inactivate certain peptidase inhibitors by oxidation and the peptidases that escape natural controls degrade the ECM. Collagen for example is degraded by matrix metallopeptidase-1 (interstitial collagenase) [49], fibronectin, an important protein in cell-matrix communication [91], is hydrolyzed by cathepsin B [48], elastin by human elastase-2 (human leukocytes elastase) [95].

1.1.4 Control of Matrix Remodeling and its Failure

In situations like inflammation, it is essential to strictly control the whole process, for example the action of the peptidases secreted by neutrophils. Two strategies to control the activity of secreted peptidases are the use of endogenous inhibitors (Table 1.1, p. 16) and the local restriction of less specific enzymes, like elastase-2 or cathepsin B, by binding them to the cellular membrane. Any failure in the control of peptidases results

in excessive pathological degradation of the ECM as seen for instance in lung fibrosis [65], osteoarthritis [14], and tumor progression and metastasis [71, 76, 101, 114].

Typical characteristics of *chronic inflammation* are the persistent accumulation of active macrophages that secrete peptidases, which in turn degrade matrix components, and reactive oxygen species that damage the surrounding tissue. Furthermore, the activity of macrophages stimulates the proliferation of fibroblast and the production of extracellular matrix components (*stroma reaction*). At sites of chronic inflammation, granulomas with a central part of macrophages surrounded by lymphocytes are often formed. During the development of chronic inflammation, mediators such as interferon γ released by T-cells, and tumor necrosis factor secreted by macrophages, play an important role. These cytokines stimulate the production of cell adhesion molecules, which results in the recruitment of even more inflammatory cells.

In *lung emphysema*, the alveolar septum is destroyed by chronic cough, asthma attacks, oxidants from smoke [111] or air pollution. Following inflammation of the lung tissue, flow resistance increases and aggravates expiration resulting in overload and hyperdistension of the lung. Because of the tissue damaged, neutrophils are attracted and stimulated to secrete proteolytic enzymes.
Another severe pulmonary pathology is *lung fibrosis*, in which fibroblasts proliferate and large amounts of collagen fibers are stored in the alveolar septum. As a consequence, the lung loses its elasticity and the ability to expand reversibly.

Various risk factors such as age, sex, trauma, overuse, genetics determinants contribute to the onset of *osteoarthritis*. Following initial weakening in the collagen network, proteoglycans absorb more water molecules, which results in a more nutrient-rich and oxygen containing environment. Chondrocytes within this new environment change their metabolism from anaerobic to aerobic and are subjected to phenotypic transition characterized by swelling, proliferation and the production of collagen types I and III, which are otherwise typical of skin, instead of collagen type II. The stiff collagen types I and III can not sustain the mechanical requirements of articular cartilage.
A marker of this characteristic osteoarthritic phenotype is cathepsin B, perhaps the most destructive enzyme in the affected joints [20, 64, 79, 116]. This phase may last several years until physical stress becomes important for joint stability. The synoviocytes are then induced to produce and secrete interleukin-1 and tumor necrosis factor, which in turn stimulate chondrocytes to express and secrete matrix degrading peptidases such as matrix metallopeptidases and ADAMTS (a disintegrin and metallopeptidase with thrombospondin motifs). Moreover, the production of different glycosamino-

glycans is impaired [14].
In *rheumatoid arthritis* enzymatic destruction of cartilage is associated with an autoimmune response, which is responsible for the chronic character of the pathology.

One of the most intensively investigated fields in the context of pathological ECM degradation is *tumor invasion* and *metastasis*. The pathology of malignant tumors is characterized by two critical steps: local invasion around the primary tumor and the following metastatic spread to distant sites in the organism, where new tumor cell colonies grow up. To accomplish this tasks tumor cells secrete hydrolytic enzymes, among which several peptidases are the mediators of ECM degradation.
Endopeptidases favor the detachment of cells from the primary tumor mass and degrade proteoglycans, collagen, elastic fibers as well as basal membranes promoting intravasation of tumor cells into blood vessels. Extravasation at remote sites is sustained enzymatically as well. Cysteine peptidases, notably the cathepsins B, H, L and S [60, 76], but also serine and metallopeptidases are the protagonist enzymes in this complex scenery.

1.2 Control of Peptidases in ECM Remodeling and Degradation

Peptidases are implicated in a multitude of events in an organism, from its development (fertilization, implantation, embryogenesis, morphogenesis, differentiation), over healing (inflammation, wound repair) to pathological events (arthritis, lung emphysema, tumor). A relevant function of peptidases is the processing of precursor proteins to their active forms by limited proteolysis [21, 59]. A detailed analysis of the life cycle of these enzymes in the context of ECM degradation is a prerequisite for the development of efficient strategies against the pathologies in which they are involved.
The peptidases involved in tissue remodeling and degradation, their function and the problems encountered while planning their control by exogenous inhibitors are discussed in this section.

1.2.1 The Peptidases Involved

The pathologically relevant peptidases are exactly the same enzymes needed by cells for their regular functions. The enzymes are either stored in the lysosomes or secreted in the extracellular space. The matrix metallopeptidases such as MMP-1 (EC 3.4.24.7) also known as interstitial collagenase 1, MMP-2 (EC 3.4.24.24), formerly known as gelatinase A or MMP-3 (EC 3.4.24.17) (stromelysin 1), cleave, as their name implicates, collagen and

other important proteins in the matrix. The activation of these matrix metallopeptidases is achieved by limited proteolysis.
Common to all these enzymes is their need of zinc, cobalt or maganese for their catalytic activity and some of them require also calcium. Besides matrix proteins, which among other functions mediate cell attachment to the ECM (e.g. integrin, perlecan, and syndecan), also cytokines and the tumor necrosis factor as well as the endogenous α_1-peptidase inhibitor are hydrolyzed by MMPs.
Often, a teamwork is needed between different enzymes, as for example between MMP-1 and ADAMTS. Most of the different collagen types are degraded by MMP-1 but before this can happen, the aggrecanases ADAMTS4 (EC 3.4.24.82) and ADAMTS5 (3.4.24.-) are required to degrade proteoglycans and to demask the collagen fibrils embedded therein. As their practical name indicates, the substrate of these enzymes is aggrecan, the large proteoglycan typically found in hyaline cartilage [82].

Within the serine peptidase family S1 (trypsin family) three enzymes emerge for their participation in remodeling and degradation of tissue matrix, namely elastase-2 (EC 3.4.21.37), cathepsin G (EC 3.4.21.20) and myeloblastin (EC 3.4.21.76), also known as leukocyte proteinase 3. When these enzymes are secreted into the extracellular space they are extremely destructive enzymes for the human body.
Elastase-2 and myeloblastin have a similar specificity for substrates and hydrolyze among other proteins elastin, collagen, fibronectin as well as plasma proteins. Cathepsin G is structurally related to elastase-2 and degrades besides matrix components [57], also immunoglobulin G and M [11, 12], a property shared with elastase-2. The three leukocyte peptidases are also involved in the digestion of bacteria and are collectively named *serprocidins* (serine proteinases with bactericidal activity) to underline this fact [30].
An interesting feature of the three enzymes is their basic isoelectric point and their highly positive charged surface due to the numerous arginines residues (Figure 1.2) [85]. These charges are responsible for electrostatic interactions with different glycosaminoglycans, such as chondroitin-4-sulfate and dermatan sulfate [6, 7]. The strength of the interaction and the resulting modification of the enzyme activity depends above all on the chain length of the glycosaminoglycans, the position of the carboxyl groups, the sulfatation isomerism and sulfatation degree [63], as well as their flexibility [32]. Additionally, it was shown that, depending on the substrate (peptide or protein substrate), the interaction of glycosaminoglycans with myeloblastin results either in an increase or decrease in the enzyme activity [46].

A further group of enzymes strongly involved in tissue remodeling and degradation are some cathepsins of the cysteine peptidases. These enzymes are not only responsible for intracellular digestion of proteins but also engaged in extracellular proteolysis [17, 75, 110].

Figure 1.2: Surface representation of elastase-2 (PDB code 1HNE), 'front' (left) and 'back' (right). All 18 (of totally 19) arginines on the surface are colored in blue. Active site (His57, Asp102, Ser195) is colored in red.

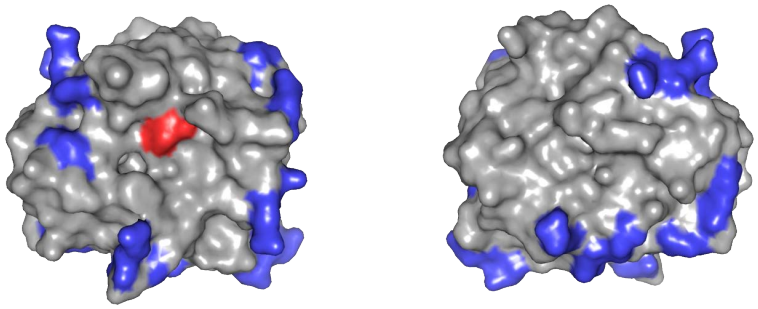

Cathepsins L (EC 3.4.22.15) and B (EC 3.4.22.1) degrade extracellular matrix proteins such as collagen [70], fibronectin [16, 27, 105], link protein of proteoglycan [29, 78], glucagon [5] and cytosolic proteins [38]. Cathepsin B regulates the activity of aldolase [24], converts prorenin to renin [2] and trypsinogen to trypsin [51]. Additionally, cathepsin B is involved in processing the prohormone thyroglobulin [26] and in the presentation of antigen via MHC complexes [74]. Cathepsin K (EC 3.4.22.38) is typically found in osteoclasts, where it is the major peptidase involved in bone resorption, besides cathepsin B, L and S [54]. Glycosaminoglycans are essential for the collagenolytic activity of cathepsin K under acidic conditions [68].
Procathepsin L also interacts with different glycosaminoglycans such as dextran sulfate, heparan sulfate and chondroitin sulfate, which promote autocatalytic activation of the proenzyme [73]. These interactions do not impair the ability of cathepsin L to degrade matrix proteins [56].
Cathepsin S (EC 3.4.22.27) is present in all MHC II positive cells, where it is involved, besides in the degradation of matrix proteins [36], in degrading the invariant chain of MHC II molecules and subsequent proper antigen presentation [96].
The aspartic peptidase cathepsin D (EC 3.4.23.5) is found in the lysosomes of various cells and degrades several chemokines released by activated macrophages during inflammation [112].

1.2.2 The Life Cycle and Control of the Peptidases

Knowing the life cycle of an enzyme is essential for identifying potential targets for therapeutic intervention. The mentioned peptidases show the following course until they reach their mature form and degrade ECM structures: Stimulation → Biosynthesis → Inactive enzyme → Activation → Active enzyme → Storage or release as active enzyme → Degradation of the ECM. In

case of extracellular activation the inactive enzyme is released as a precursor into the extracellular space.
Theoretically, each of these steps offers a potential target for intervention, including modulation of stimuli that govern the rate of biosynthesis, inhibition of intra-/extracellular activators, intra-/extracellular inhibition of the enzyme, promotion of intracellular storage and protection of the extracellular matrix. Not all of these interventions may be equally effective and, above all, feasible.

Considering the life cycle of an enzyme, it is essential to know the properties of its mature form as well as its relationships with the surroundings in the extracellular space. These include interactions with matrix molecules, which may affect enzyme activity. In the specific case of cathepsin B it was shown that its survival in the extracellular space depends on the local pH [13, 108, 109].

In a healthy organism, it is the duty of specific and effective endogenous inhibitors to control the action of peptidases [69]. Table 1.1 contains a few examples of naturally occurring protein inhibitors with their major target enzymes. A comprehensive treatment of peptidases and their inhibitors can be found in the MEROPS database [94] (http://merops.sanger.ac.uk).
Proteinaceous inhibitors are often unspecific towards a peptidases [40, 89]. For example, being present in functionally unrelated proteins, thyropins, thyroglobulin type-1 domains with inhibitory activity, can interact with members of both cysteine and aspartic peptidases [66].
Additionally, many hundreds of synthetic inhibitors are known, such as the group of the epoxysuccinyl derivatives for the cysteine peptidases [45, 90] or the pyrrolidine scaffold-based metallopeptidases inhibitors [113].

In pathological situations, extracellularly acting peptidases are insufficiently controlled by their endogenous inhibitors, and their continuous secretion leads to excessive local accumulation of unwanted enzyme activities, which eventually results in pathological ECM turnover.
There are three main reasons why the naturally occurring inhibitors are unable to efficiently control the system [10, 31]:

- *Imbalance* between enzymes and their inhibitors. As a result of the continuous secretion of peptidases into the extracellular space, their concentration is much higher than the concentration of natural inhibitors.
- Formation of a *microenvironment* between the peptidase-secreting cell and the ECM, which hinders natural inhibitors to reach their target enzymes.
- *Inactivation of inhibitors* by reactive oxygen species produced by phagocytic cells during the respiratory burst.

Table 1.1: Peptidases and their natural inhibitors. MEROPS [94] identifier in parenthesis. SLPI; secretory leukocyte proteinase inhibitor, timp; tissue inhibitor of metallopeptidase.

Endogenous inhibitor	**Main natural peptidases**
α-1 peptidase inhibitor (I04.001)	elastase-2 (S01.131), cathepsin G (S01.133)
α-2 macroglobulin (I39.001)	elastase-2 (S01.131), cathepsin B (C01.060), cathepsin D (A01.009), cathepsin G (S01.133), cathepsin H (C01.040)
cystatin A (I25.001)	cathepsin S (C01.034), cathepsin H (C01.040)
cystatin B (I25.003)	cathepsin S (C01.034), cathepsin H (C01.040)
elafin (I17.002)	elastase-2 (S01.131), myeloblastin (S01.134)
SLPI domain 1 (I17.950)	elastase-2 (S01.131), cathepsin G (S01.133)
timp-1 (I35.001)	matrix metallopeptidase-1 (M10.001)
timp-2 (I35.002)	matrix metallopeptidase-2 (M10.003)
timp-3 (I35.003)	matrix metallopeptidase-3 (M10.005)

The following are possible explanations why synthetic inhibitors are inefficient against their putative target peptidases:

- Peptidases have high affinities to their natural substrates and therefore they do not dissociate easily. Acting on the ECM these enzymes are continuously faced with a virtually infinite concentration of substrate and, assuming the simple Michaelis-Menten mechanism to be valid, their rate of substrate turnover corresponds to the limiting rate.
  Thermodynamically, concentration of any solid (insoluble) molecule is considered to be 1M by convention, which in the case of ECM components means infinite, i.e. enzymes engaged in ECM turnover are always saturated with respect to substrate. The competition by any inhibitor needs a particularly strong interaction between enzyme and inhibitor.

- Peptidases secreted into the ECM are surrounded by a multitude of potential interacting partners, such as the ECM itself, endogenous inhibitors or cell membrane receptors. Single or multiple binding to any of these interaction partners may induces conformational changes in the enzymes and affect the binding affinity of an exogenous inhibitor.

- Considering that several peptidases may be engaged in ECM turnover at the same time and in the same environment, enzyme-enzyme interactions, as well as enzyme-inhibitor interactions are plausible.
  A few examples illustrate the complex network of interactions that may occur: Elastase-2 activates other peptidases such as matrix metallopeptidases [81] and procathepsin B [37] and inactivates peptidase inhibitors (timp-1 [83], cystatin C [29]). Cathepsin B, L and S inactivate the SLPI domain 1 [106], an inhibitor of elastase-2. Elastase-2 preadsorbed on elastin is no longer efficiently inhibited by α_1-peptidase inhibitor [95]. Besides elastase-2, also the cathepsins K, L and S interact with elastin by a two step binding mechanism resulting in a tightly bound enzyme-elastin complex [86]. Glycosaminoglycans, such as heparan sulfate, bind enzymes (e.g. cathepsin B [1]) but also inhibitors (e.g. timp-3 [115]), which results in the alteration of enzyme activity. Polynucleotides, present in the bronchial fluid of patients with lung diseases, bind elastase-2 [18, 19, 67], cathepsin G [42] and myeloblastin [41] affecting their inhibition by endogenous inhibitors.

1.2.3 New Trends in the Control of Peptidases

A common strategy in industrial and academic research on synthetic inhibitors of peptidases, has been, and continues to be, targeting the inhibitors to the active center of the enzymes. While this is an excellent approach for inhibiting enzymes acting on soluble substrates, it did not prove to be effective when the substrates are insoluble [10]. In recent years, the concept of targeting enzymes with molecules binding outside the active center, has become increasingly popular [53, 58]. The concept of allosteric control of enzyme activity, widely exploited in nature (e.g. HIV-1 reverse transcriptase, fructose-1,6-bisphosphatase), is receiving great attention and represents a challenging alternative to classical inhibitors for pharmacological applications. Thus, targeting a peptidase that is tightly bound to insoluble components of the ECM by allosteric effectors represents a new, stimulating and still little explored trend.

A promising approach is represented by 'designed ankyrin repeat proteins' (DARPins) [23], purposely *in vitro* engineered proteins for specific, high-affinity target binding [22, 43, 98]. This approach consists in the random and unspecific search for good binders at the surface of a protein. The probability of finding good binders is very high but serendipitous, because the binding portion at the surface of the target protein can not be predicted. Nevertheless, the hitherto known examples are amazing for their efficiency, such as the allosteric inhibition of human caspase-2 [98] and of aminoglycoside phosphotransferase [61].

A specific approach on the search of potential allosteric sites in proteins, is the screening of evolutionarily conserved residues in whole protein families. Allosteric communication is an important process during cell signaling and there is evidence that conserved residues are the structural motifs for this communication [50, 102]. Proteins such as myoglobin [44] and serine peptidases related to chymotrypsin, unsuspected to be capable of allosteric regulation, revealed to be true allosteric proteins. Mutation of the conserved residues responsible for long-range communication in allosteric enzymes could provide valuable information on the possible use of hot spots for targeting modifying agents.

A widely exploited and fully computational screening method for predicting the binding mode of small molecules to proteins as well as the affinity of the interaction is the 'docking' procedure, a method that is particularly useful in the development of new drugs. Calculations are performed with a large amount of virtual molecules to pick out only the most promising binders. After the establishment of putative binding pockets on the surface of the target protein, a library of molecules (e.g. the ZINC database [55]) is prepared for the actual docking procedure by conversion of the 2D molecules to 3D compounds and the addition of water molecules (Figure 1.3).

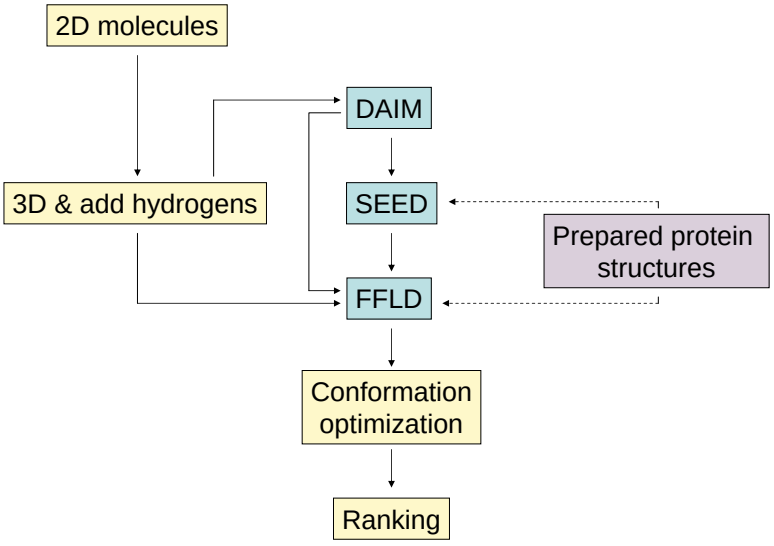

Figure 1.3: Docking procedure. DAIM: Decomposition and Identification of Molecules, SEED: Solvation Energy for Exhaustive Docking, FFLD: Fragment-based Flexible Ligand Docking.

The fragment-based docking procedure can be summarized in three steps: 1) Decomposition of the molecule into small rigid fragments [62]. 2) The fragments are docked into the putative binding pocket using an accurate scoring function, which not only considers the internal energies of the two interacting molecules but also the basic terms of their interactions [72]. 3) The original structure is re-merged so that the positions with the most favorable interaction energies can be used as anchors for deciding the definite position of the ligands [28, 33]. The following two final steps consist of the conformational optimization and the ranking of the compounds.
The docking method has been used in this thesis for purposely targeting an inhibitory ligand to the characteristic peptide extension of human cathepsin B known as the occluding loop. The flexibility of this structure is manifested after removal of the propeptide [80, 92, 93]. In mature cathepsin B, endo- and exoproteolytic activity depend on the conformation of the occluding loop [84]: In the 'closed' conformation, the primed subsites of the substrate binding sites are obstructed and therefore only exoproteolytic cleavage takes place. In the 'open' conformation, the primed subsites are free and the enzyme acts as endopeptidase. Theoretically, following fixation of the occluding loop in its closed position with a ligand, the exopeptidase activity should be retained and the endopeptidase should be hindered.

1.3 Properties of an Ideal Modifier of Peptidases in a Pathological Environment

Besides being specific and efficient against their target enzymes, therapeutically useful modifiers should possess additional properties: an effective overall mechanism of action, low toxicity and antigenecity, and good bioavailability. Thus, technically precise studies of the modifiers *in vitro* can suggest their possible effectiveness *in vivo*. The successful use of enzyme inhibitors *in vivo* depends on the fulfillment of six criteria listed on the right side of Figure 1.4.
From a theoretical point of view, the best inhibitor of any unwanted enzyme activity will be the substance possessing a favorable set of all six properties (Figure 1.4, right side). A critical analysis of the impact of these criteria in the particular field of inhibition of ECM-degrading peptidases has shown that some of the six properties of the inhibitors are mutually dependent when considered in the light of seven properties of the target enzymes and of the diseases with which they are associated (Figure 1.4, left side).

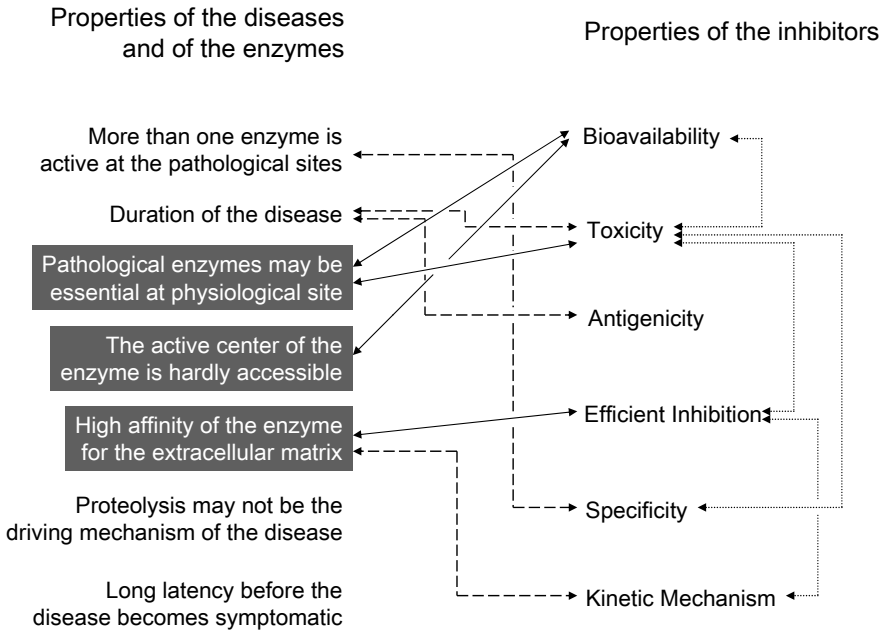

Figure 1.4: Properties of diseases with involved enzymes (natural factors) and of inhibitors aimed at attenuating the adverse affects (adapted from [10]). The objective is to inhibit the enzymes by making the best use of the six properties of the inhibitors shown on the right side. Dotted arrows join those properties of the inhibitors that are logically dependent from one another. The central dashed and full-line arrows denote the problems arising with the practical use of the inhibitors: full lines represent critical tasks and dashed lines indicate problems for which individual solutions are theoretically possible. The grey underscored properties represent three serious drawbacks in the pharmacological management of ECM-degrading peptidases.

1.3.1 Bioavailability, Toxicity and Antigenecity of the Inhibitor

The pharmacokinetic concept of bioavailability includes all processes responsible for the presence of a drug at the target site and is a complex function concerned with drug resorption and metabolism. This property describes the quantity of a substance, which is actually available to the organism. In the case of ECM-degrading peptidases, drugs must be able to effectively reach their final target site. A modern approach to this difficult task is the delivery of peptidase inhibitors incorporated in nanoparticles [34, 35].
Toxicity relates to both the bioavailability and the efficiency of drugs. The most common warheads used to inactivate peptidases include alkylating or acylating chemical groups attached to recognition elements specific for the target enzymes. Unfortunately, while the recognition elements may be specific for the enzymes, this is not the case of the warheads, which my react non-specifically with essential metabolites.
The lack of antigenecity (= capacity to induce an immune response), an obvious requirement for the use of drugs, paradoxically conflicts with the notion that most physiological inhibitors of endopeptidases are proteins as well. These inhibitors have the function of defending the organism form excessive proteolysis due to leakage of the enzymes from dead cells or accidentally liberated in the extracellular space. The use of heterologous macromolecular inhibitors is restricted to substances with structural identity or similarity with the corresponding human inhibitors. In any case, they should not elicit immunological reactions.
Hence, many macromolecular substances occurring in plants and animals, e.g. the elastase-2 inhibitor eglin from the leech *Hirudo medicinalis* [15, 100] can not be used in humans.

1.3.2 Efficiency, Specificity and Kinetic Mechanism of the Inhibitors

Avoiding side effects in enzyme inhibition also means conservation of the activities of beneficial non-target enzymes while suppressing undesired effects, and the specificity for the target enzymes is an obvious requirement. Thus, efficient (potent) inhibition is a welcome property denoted by a large second-order association constant for enzyme inactivators (irreversible inhibitors), or low K_i values for reversible inhibitors[1].
The progress made in the production of specific and efficient inhibitors of peptidases is considerable and modern medicinal chemistry excellently handles these two properties. However, the kinetic mechanism of the inhibitors

[1] Although not universally accepted, the term 'efficiency' applies to reversible inhibitors, while 'potency' is preferred to describe the action of inactivators.

plays a decisive role for their practical use. Unfortunately, highly efficient peptidase inhibitors may present the drawback of low rates of complex formation with the target enzymes resulting in insufficient protection [9, 10]. We can postulate a satisfactory management of the chemical and pharmacokinetic requirements of peptidase inhibitors such as to justify their use as drugs (Figure 1.4, right side). However, the properties of the diseases and of their associated enzymes (Figure 1.4, left side) represent natural factors, which are intrinsic to the system and, therefore, not modifiable by external intervention.
Three aspects are particularly problematic: the double identity of peptidases in their physiological and pathological function, the frequently inaccessible active center of the enzymes at their pathological site, and the tight binding mode of the enzymes to their substrates, insoluble components of the ECM. Figure 1.4 indicates with connecting double headed arrows the multiple relationships existing between the properties of the enzymes, of the diseases and the inhibitors. These render the pharmacological management of ECM-degrading peptidases remarkably problematic.

The three relationships marked in Figure 1.4 by full-line arrows deserve a few comments. There is a relationship between the bioavailability and the toxicity of a drug when reactions occur at non-target sites. To be effective, inhibitors of ECM-degrading peptidases should be transported to and interact with the enzymes only at their pathological site, while preserving their physiological activity. Moreover, enzymes embedded in the ECM are generally hardly accessible by excellent inhibitors.

The description of a modifier's mechanism contains not only the interactions between enzyme and modifier dictated by their chemical structure, but also the steps and rates with which they react with each other. Knowledge of the interaction mechanism and its effects on the enzyme activity, which depend on the inhibitor and substrate concentrations, is very important in the development of therapeutically useful compounds. The appendix A.1 and B.1 list the classification of inhibition and activation mechanisms.
It is important to note that the interaction mechanism of a modifier with an enzyme may depend on the nature of the substrate. In fact, analysis of the reaction mechanism of inhibitors with peptidases involved in pathological ECM-degradation, reveals quantitative differences in the behavior of the modifier depending on whether low-molecular-mass substrates or macromolecular substrates are considered. In particular, there is experimental evidence that linear competitive inhibitors (classical and tight binding) found to be effective at given concentrations in presence of low-molecular-mass substrates, must be used at much higher concentrations to obtain the same effects with macromolecular substrates [3, 4].
As mentioned above, peptidases acting on insoluble substrates of the ECM are faced with saturating substrate concentrations and a large concentration

of inhibitors is needed to gain satisfactory effects. Much more promising are therefore, linear or hyperbolic mixed-type inhibitors with a high proportion of uncompetitive character, even if at saturating concentrations hyperbolic inhibitors will not completely abolish enzyme activity. However, inhibitors like these are efficient even at saturating substrate concentrations.

1.4 Aim of the Thesis

The control of proteolytic activity in the extracellular space by means of exogenous enzyme modifiers requires specific strategies, which must cope with the insoluble nature of the ECM. Three main goals of this thesis were:

- to develop new criteria for peptidase inhibition as an alternative to classical approaches based on targeting the active sites of the enzymes
- to re-evaluate kinetic diagnostic tools and mathematical models for analyzing enzyme-modifier interactions
- to explore the interaction mechanisms between enzymes and modifiers in an experimental system that considers the natural environment.

In this context, the human cysteine peptidase cathepsin B was chosen as a target for its recognized involvement in key pathophysiological processes. The particular structure of cathepsin B known as 'occluding loop' was screened with a computational approach for selecting binders that would interfere with this site. The sought 'proof of principle' was inhibition of enzyme activity without interference with the catalytic site.
Exogenous modifiers of peptidase activity are likely to interfere with naturally occuring inhibitors and components of the ECM, and these interactions are expected to generate effects ranging from synergy to antagonism. In this framework, a reassessment of the theory of multiple enzyme-modifier interactions was compelling. The validation of a general mathematical model for double interaction between an enzyme and two modifiers, and an exhaustive screening of plausible interactions, constituted a major task of this thesis.
Furthermore, kinetic mechanism and diagnostic tools for irreversible enzyme modification were in need of re-evaluation to facilitate mechanism discrimination by combined graphical and mathematical methods.
The setup of improved methods was aimed at supporting the interpretation of puzzling effects, such as the interaction between the serine peptidase elastase-2 with naturally occurring glycosaminoglycans, which results in inhibition at low concentrations and reactivation at higher concentrations of these ECM components.

These methods should not only allow quantitative predictions of interferences occurring between endogenous and exogenous inhibitors of peptidases involved in degradation and remodeling of the ECM, but also in other enzyme systems.

Publications

A double-headed cathepsin B inhibitor devoid of warhead

Protein Science, 2008, 17:2145−2155

Abstract

Synthetische Inhibitoren der Peptidasen zielen bei der Inhibition der Katalyse oftmals auf die aktive Stelle ab, sei dies durch reversible Verdrängung des Substrats oder durch kovalente Modifikation der katalytischen Gruppen des entsprechenden Enzyms. Cathepsin B besitzt als einzige Cysteinpeptidase ein flexibles Segment, den sogenannten 'occluding Loop', welcher den C-terminalen Teil der Substratbindungsstelle blockieren kann. Ist dieser Loop in einer offenen Stellung, agiert das Enzym als Endopeptidase, entsprechend in der geschlossenen Loopstellung als Exopeptidase.
Wir fokussierten uns unter Anwendung einer Dockingprozedur auf den sich an der Oberfläche von Cathepsin B und damit ausserhalb des katalytischen Zentrums befindenden occluding Loops. Ziel war es, Inhibitoren zu identifizieren, welche mit dem occluding Loop interagieren und dadurch die Enzymaktivität modulieren, jedoch ohne direkt gegen die katalytischen Gruppen zu wirken.
Aus einer umfangreichen Bibliothek von Compounds konnte durch die *in silico* Annäherung [2-[2-(2,4-dioxo-1,3-thiazolidin-3- yl)ethylamino]-2-oxoethyl] 2-(furan-2-carbonylamino)acetat identifiziert werden, der die Arbeitshypothese erfüllte. Das Molekül besitzt zwei individuelle Bindungseinheiten und verhält sich gegenüber Cathepsin B als reversibler, 'doppelköpfiger' kompetitiver Inhibitor, der synthetische Substrate wie auch Proteinsubstrate vom aktiven Zentrum ausschliessen kann. Der Inhibitionsmechanismus deutet darauf hin, dass der occluding Loop mit dem Inhibitor vor allem über Wasserstoffbrücken interagiert und so in seiner geschlossenen Konformation stabil-

isiert wird, wobei die Endopeptidaseaktivität des Enzyms eingeschränkt ist. Ausserdem hindert der Dioxothiazolidinteil des Compounds sterisch die Anbindung der C-terminalen Einheit des Substrats, was zu einer Inhibition der Exopeptidaseaktivität von Cathepsin B in einem physiopathologisch relevanten pH Bereich führt.

A double-headed cathepsin B inhibitor devoid of warhead

PATRICIA SCHENKER, PIETRO ALFARANO, PETER KOLB, AMEDEO CAFLISCH, AND ANTONIO BAICI
Department of Biochemistry, University of Zurich, CH-8057 Zurich, Switzerland

(RECEIVED July 2, 2008; FINAL REVISION August 21, 2008; ACCEPTED August 21, 2008)

Abstract

Most synthetic inhibitors of peptidases have been targeted to the active site for inhibiting catalysis through reversible competition with the substrate or by covalent modification of catalytic groups. Cathepsin B is unique among the cysteine peptidase for the presence of a flexible segment, known as the occluding loop, which can block the primed subsites of the substrate binding cleft. With the occluding loop in the open conformation cathepsin B acts as an endopeptidase, and it acts as an exopeptidase when the loop is closed. We have targeted the occluding loop of human cathepsin B at its surface, outside the catalytic center, using a high-throughput docking procedure. The aim was to identify inhibitors that would interact with the occluding loop thereby modulating enzyme activity without the help of chemical warheads against catalytic residues. From a large library of compounds, the in silico approach identified [2-[2-(2,4-dioxo-1,3-thiazolidin-3-yl)ethylamino]-2-oxoethyl] 2-(furan-2-carbonylamino) acetate, which fulfills the working hypothesis. This molecule possesses two distinct binding moieties and behaves as a reversible, double-headed competitive inhibitor of cathepsin B by excluding synthetic and protein substrates from the active center. The kinetic mechanism of inhibition suggests that the occluding loop is stabilized in its closed conformation, mainly by hydrogen bonds with the inhibitor, thus decreasing endoproteolytic activity of the enzyme. Furthermore, the dioxothiazolidine head of the compound sterically hinders binding of the C-terminal residue of substrates resulting in inhibition of the exopeptidase activity of cathepsin B in a physiopathologically relevant pH range.

Keywords: cysteine peptidases; inhibition; enzyme kinetics; occluding loop; docking; endopeptidase; exopeptidase

Supplemental material: see www.proteinscience.org

Cathepsin B, a cysteine peptidase of the papain family (EC 3.4.22.1, identifier C01.060 in the Merops database) (Rawlings et al. 2004), has been classically ranked among the lysosomal enzymes and implicated in intracellular protein digestion. Physiologically, cathepsin B is also involved in antigen processing (Matsunaga et al. 1993), in the activation of thyroglobulin, the precursor of thyroid hormones (Friedrichs et al. 2003), and in the maturation of beta-galactosidase (Okamura-Oho et al. 1997). From a pathological point of view, cathepsin B activates trypsinogen in hereditary pancreatitis (Kukor et al. 2002) and participates in apoptosis (Bröker et al. 2005), tumor progression and malignancy (Yan and Sloane 2003; Mohamed and Sloane 2006), and rheumatic diseases (Lenarcic et al. 1988; Baici et al. 1995a,b). Particular extralysosomal functions of cathepsin B are due to altered expression at the gene level and/or atypical trafficking (Müntener et al. 2003, 2004; Zwicky et al. 2003; Baici et al. 2006).

Reprint requests to: Antonio Baici, Department of Biochemistry, University of Zurich, Winterthurerstrasse 190, CH-8057 Zurich, Switzerland; e-mail: abaici@bioc.uzh.ch; fax: 41-44-6356805.

Abbreviations: Abz, ortho-aminobenzoyl; AMC, 7-amino-4-methylcoumarin; DTT, dithiothreitol; Z, benzyloxycarbonyl; Dnp, Nε-2,4-dinitrophenyl; FRET, Förster resonance energy transfer; DOFA, [2-[2-(2,4-dioxo-1,3-thiazolidin-3-yl)ethylamino]-2-oxoethyl] 2-(furan-2-carbonylamino)acetate; MALDI, matrix-assisted laser desorption/ionization; MS, mass spectrometry; LC, liquid chromatography; SDS-PAGE, sodium dodecyl sulfate, polyacrylamide gel electrophoresis.

Article and publication are at http://www.proteinscience.org/cgi/doi/10.1110/ps.037341.108.

Cathepsin B is capable of endopeptidase (Mort 2004), peptidyl-dipeptidase (Aronson Jr. and Barrett 1978; Bond and Barrett 1980), and carboxypeptidase activities (Takahashi et al. 1986; Rowan et al. 1993). Among the cysteine peptidases, it owns a unique structural element, called an occluding loop, which comprises residues Ile^{105}–Pro^{126} (Fig. 1; Musil et al. 1991). At low pH, two salt bridges, His^{110}–Asp^{22} and Arg^{116}–Asp^{224}, hold the loop in a closed position over the primed subsites of the substrate binding cleft, thus preventing extended binding of polypeptides and endoproteolytic activity. The closed conformation, through the engagement of His^{111} in a hydrogen bond with the C-terminal carboxylate of the substrate and the loose specificity in P2′, is responsible for the peptidyl-dipeptidase activity of cathepsin B (Illy et al. 1997; Quraishi et al. 1999; Krupa et al. 2002). As mutations of the amino acids His^{110} and Asp^{22} have shown, removal of the salt bridges induces endopeptidase activity, attributed to increased flexibility of the loop (Nägler et al. 1997). This concept agrees with higher endopeptidase activity and with the competition between the occluding loop and the propeptide following deprotonation of His^{110} changing the pH from 4.0 to 6.0 (Quraishi et al. 1999). The flexibility of the loop was further demonstrated by the fact that cystatins A and C were able to displace the loop (Nycander et al. 1998; Pavlova et al. 2000), and deletion of residues 108–119 abolished the exopeptidase activity of cathepsin B (Illy et al. 1997).

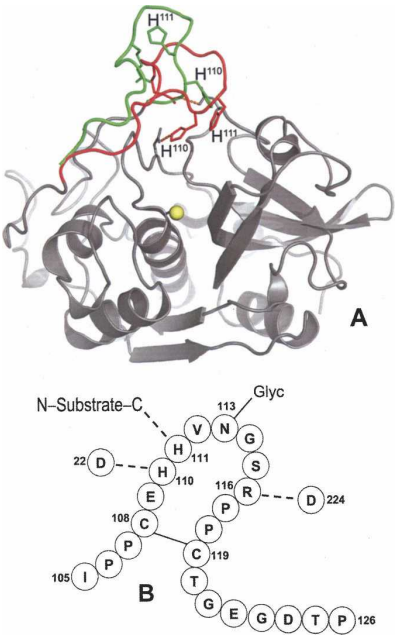

Figure 1. The occluding loop of human cathepsin B. (*A*) Closed conformation (red) in the mature enzyme (Musil et al. 1991), where a hydrogen bond is made between His^{110} and Asp^{22}. The conformation seen in procathepsin B with the occluding loop lifted (green) to accommodate the propeptide, which is not shown for clarity (Turk et al. 1996). Image generated with PyMOL software (http://www.pymol.org). (*B*) Scheme of the occluding loop with hydrogen bonds present in the closed conformation. The symbol Glyc attached to Asn^{113} indicates the N-linked oligosaccharide.

A large number of synthetic compounds behave as inhibitors of cathepsin B. Most of them are either reversible or irreversible competitive inhibitors acting ''inside the active center'' (Otto and Schirmeister 1997; Michaud and Gour 1998; Frlan and Gobec 2006). The practical use of these inhibitors is in most cases difficult for reasons analyzed elsewhere (Baici 1998). In the present study we target cathepsin B ''from the outside,'' i.e., at the surface of the molecule excluding any direct interference with catalysis. Our strategy aims at proving the concept that latching the occluding loop in its closed conformation may possibly hinder the endo- and/or exopeptidase activities of the enzyme. The approach consists of computational analysis by docking a large number of compounds to the surface of cathepsin B in the occluding loop region. From 40 compounds matching the working hypothesis, 29 are commercially available and one of them inhibits at low micromolar concentration the endo- and exoproteolytic activities of cathepsin B. We analyze the kinetic mechanism of inhibition, from which we propose a model for the interaction between the compound and the enzyme.

Results

Kinetic mechanism of inhibition with synthetic substrates

Z-RR↓AMC and Abz-GIVR↓AK(Dnp)-OH were used as substrates for monitoring the endo- and exoproteolytic activity of cathepsin B, respectively. Arrows in the substrate acronyms indicate the scissile bonds. Forty of 47,878 compounds screened in the docking approach were selected as candidate binders of human cathepsin B. Twenty-nine of them were commercially available and were tested as modifiers of enzyme activity, and one of them, DOFA (Fig. 2), behaved as a true inhibitor. Two compounds out of 29 were scarcely soluble in DMSO (Zinc-2005 codes 1271923 and 2990182; Supplemental Table 1). Five of them were soluble in DMSO but were prone to aggregation under the assay conditions for cathepsin B giving rise to modest and inconsistent inhibition between different assays. We considered these five compounds (958753, 1837733, 1871954, 3247330, and 1581881) as promiscuous inhibitors (Shoichet 2006). None of the compounds tested was a covalent inactivator of cathepsin B. DOFA did not inhibit human cathepsin L, and papain was only partially inhibited at millimolar concentrations (assays with Z-FR↓AMC; data not shown). A

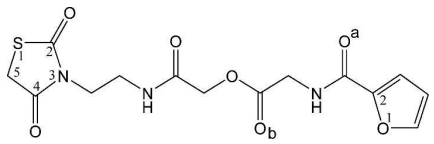

Figure 2. Structure of the inhibitor. The IUPAC name of the compound is [2-[2-(2,4-dioxo-1,3-thiazolidin-3-yl)ethylamino]-2-oxoethyl] 2-(furan-2-carbonylamino)acetate (abbreviated DOFA; Zinc-2005 code: 2616818). Numbering and lettering used as aid for the description in the main text.

previous report of high-throughput screening classified DOFA inactive against cathepsin B (http://pubchem.ncbi.nlm.nih.gov/, CID 2078629, AID 453). Reasons can be sought in either too strict criteria or in the occasional failure of high-throughput screening methods in detecting hits (Buxser and Vroegop 2005). DOFA behaved as a reversible inhibitor of cathepsin B and manifested neither tight-binding nor slow-binding inhibition behavior. Reaction traces were linear from the very beginning of the reaction, i.e., from 3–4 ms onward, as measured with a stopped-flow apparatus. Therefore, initial velocities at variable substrate and modifier concentrations were treated as steady-state rates. In control experiments we checked the possibility that any inhibitory effect of DOFA was not due to aggregation of the compound. For this purpose 0.01% Triton X-100 was added to buffers and the DTT concentration was increased to 5 mM. In comparison with buffer not containing detergent and with DTT = 2 mM, the basal activity of cathepsin B was higher by ~40%. However, inhibition profiles for increasing DOFA concentration, percentages of inhibition, and inhibition constants were the same.

The kinetic results in this study refer to those obtained with the enzyme purified from human liver. Nevertheless, we confirmed inhibition mechanisms and kinetic parameters also with recombinant cathepsin B. The reason was to ascertain any influence of glycosylation at N^{113}, which is located at the tip of the occluding loop, on the binding of potential inhibitors. Both kinetic and modeling results discussed below suggest that N^{113} glycosylation possibly occurring in the wild-type enzyme does not affect inhibition of cathepsin B by DOFA.

The kinetic mechanism was analyzed by a combination of graphical and regression methods to discriminate between models of enzyme–modifier interaction (Fig. 3). With the Abz-GIVR↓AK(Dnp)-OH exoproteolytic substrate at pH 4.5, the best fitting model for cathepsin B inhibition by DOFA was linear competitive inhibition with $I_{90/10} = 81$ and $K_i = 6.7$ μM (Fig. 4A). The specific velocity plot, typical for this mechanism, is shown in the inset of Figure 4A. With this substrate, data at pH 6.0 could not be obtained because of its scarce solubility. DOFA inhibited the endoproteolytic cathepsin B activity (Z-RR↓AMC as substrate) at pH 4.5 and 6.0. The specific velocity plot (not shown) established the linear nature of the inhibition

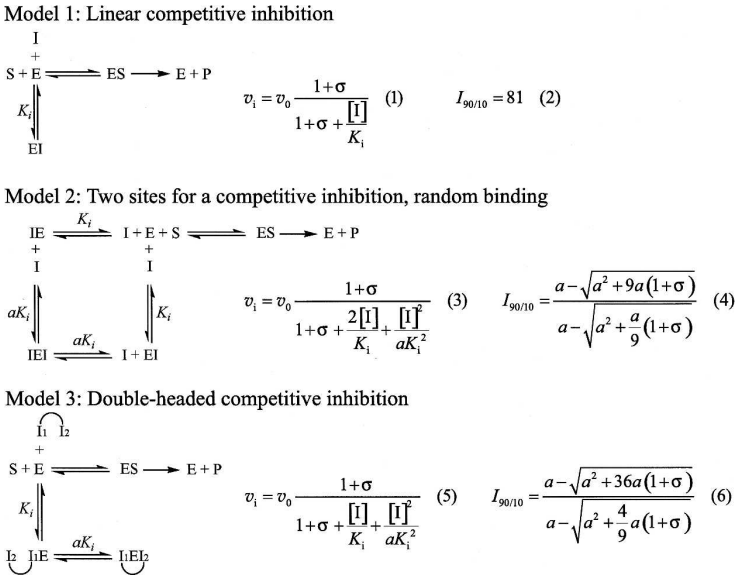

$$v_i = v_0 \frac{1+\sigma}{1+\sigma+\frac{[I]}{K_i}} \quad (1) \qquad I_{90/10} = 81 \quad (2)$$

$$v_i = v_0 \frac{1+\sigma}{1+\sigma+\frac{2[I]}{K_i}+\frac{[I]^2}{aK_i^2}} \quad (3) \qquad I_{90/10} = \frac{a-\sqrt{a^2+9a(1+\sigma)}}{a-\sqrt{a^2+\frac{a}{9}(1+\sigma)}} \quad (4)$$

$$v_i = v_0 \frac{1+\sigma}{1+\sigma+\frac{[I]}{K_i}+\frac{[I]^2}{aK_i^2}} \quad (5) \qquad I_{90/10} = \frac{a-\sqrt{a^2+36a(1+\sigma)}}{a-\sqrt{a^2+\frac{4}{9}a(1+\sigma)}} \quad (6)$$

Figure 3. Kinetic models for the inhibition of cathepsin B. v_i and v_0 represent reaction rates in the presence and in the absence of inhibitor, respectively. $\sigma = [S]/K_m$; $I_{90/10}$ = ratio of the inhibitor concentrations, which give 90% and 10% inhibition. The double-headed inhibitor possesses two distinct binding moieties that sequentially bind the enzyme.

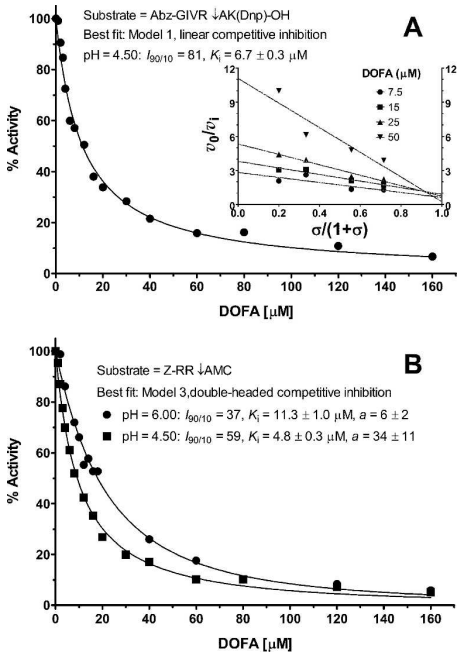

Figure 4. Inhibition profiles of human cathepsin B by DOFA. Main conditions and best-fit kinetic parameters are shown. (*A*) Inhibition profile using the FRET substrate Abz-GIVR↓AK(Dnp)-OH (pH 4.5), [S] = K_m = 9.7 μM; data were obtained fluorimetrically with $\lambda_{ex}/\lambda_{em}$ at 320/420 nm. The *inset* shows the specific velocity plot at four substrate and four inhibitor concentrations. (*B*) Inhibition profiles with Z-RR↓AMC as substrate; [S] = K_m = 0.47 mM at pH 6.0 (black circles) and [S] = K_m = 1.54 mM at pH 4.5 (black squares). Data at pH 6.0 were collected photometrically at 360 nm and those at pH 4.5 were obtained fluorimetrically with $\lambda_{ex}/\lambda_{em}$ at 383/455 nm. Fluorescence readings in *A* and *B* were corrected for the inner filter effect.

process, i.e., enzyme activity was driven to zero at saturating inhibitor concentration, and diagnosed competitive-type inhibition. However, the specific velocity plot would not be able to discriminate between Models 1–3 in Figure 3. The activity profiles obtained at a fixed substrate concentration and variable inhibitor concentrations revealed the $I_{90/10}$ ratio to be less than 81, which can be estimated by inspection to be around 60 at pH 4.5 and around 40 at pH 6.0 (Fig. 4B). This suggests that the inhibition mechanism was not of the classical competitive type, for which $I_{90/10} = 81$ (Model 1 in Fig. 3). On the other hand, Models 2 and 3 in the same figure predict $I_{90/10}$ values less than 81. For discriminating between models with Z-RR↓AMC as substrate, we set its concentration equal to K_m so that $\sigma = [S]/K_m = 1$ in the activity profiles in Figure 4B (thereby it was imperative to carefully measure the substrate concentration and K_m). In Models 2 and 3, when the factor $a = 1$, $I_{90/10}$ depends only on σ, whereas for $a \neq 1$ the $I_{90/10}$ ratio depends both on a and σ (Fig. 5A,B). Model 2 was ruled out as redundant, and Model 3 was preferred on the basis of the following quantitative and logical observations. In Model 2, two inhibitor molecules should bind to different places at the surface of the cathepsin B molecule with almost the same affinity, i.e., with the a value between 1 and 2, as shown in Figure 5A. The double-headed competitive inhibitor (Model 3 in Fig. 3) was superior also on the basis of the following quantitative observations. For Model 3, the squared symbol with dashed arrows in Figure 5B indicates the best-fit value for $a = 6$ at pH 6.0, which corresponds to $I_{90/10} = 37$ and $K_i = 11.3$ μM (Fig. 4B). Similarly, at pH 4.5, Model 3, with $a = 34$ (the black circle in Fig. 5B), $I_{90/10} = 59$, and $K_i = 4.8$ μM, produced a better fit to experimental data (Fig. 4B) than Model 2.

Inhibition of endo- and exoproteolysis using protein substrates

While low molecular mass oligopeptides are indispensable tools for determining inhibition mechanisms, they do not represent typical substrates for evaluating true endo- and exoproteolytic activities. Therefore, inhibition of cathepsin B endo- and exoproteolysis by DOFA was further

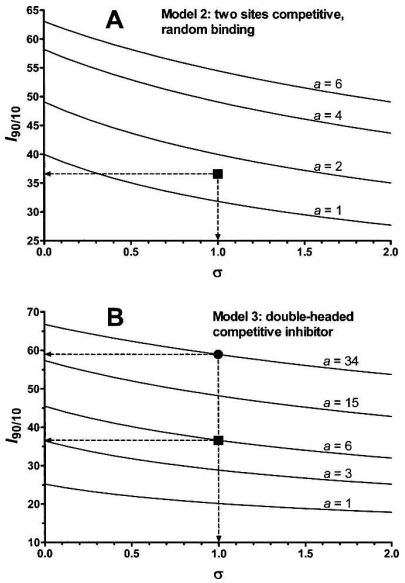

Figure 5. Ratios of inhibitor concentrations that give 90% and 10% inhibition. For Models 2 and 3 in Figure 3 the $I_{90/10}$ ratio depends on a and σ = $[S]/K_m$. Curves were generated with Equations 4 and 6 shown in Figure 3. (*A*) Curves for Model 2; (*B*) curves for Model 3. The black squares in panels *A* and *B* correspond to the best-fit value of the coefficient a, which coincides with the value obtained by inspection of the inhibition profiles at pH 6.0 in Figure 4B. The black circle in panel *B* shows the best-fit value of the coefficient a (34), close to the value obtained by inspection of the inhibition profiles at pH 4.5 in Figure 4B.

investigated with two protein substrates: rabbit muscle aldolase and the oxidized β-chain of bovine insulin. Peptide-bond hydrolysis on both proteins at pH 6.0 was inhibited in a concentration-dependent manner by DOFA (Fig. 6) and was almost complete at saturating inhibitor concentration. As commonly observed when switching from oligopeptide to polypeptide substrates, the modifier concentrations needed for achieving inhibition were higher.

Cathepsin B has been previously reported to sequentially remove up to nine dipeptide units from the C terminus of aldolase with peptidyl-dipeptidase activity (Bond and Barrett 1980). Aldolase incubated with cathepsin B in the presence or absence of DOFA was subjected to SDS-PAGE under reducing conditions. The bands excised after electrophoretic separation were N-terminally sequenced and the masses of the polypeptides determined by mass spectrometry. The SDS gels shown in Figure 7 were purposely overloaded to reveal the less prominent bands numbered 2, 3, and 4. The N-terminal sequence of the polypeptides in bands 1 and 2 was PHSHPAL, which corresponds to positions 2–8 of aldolase. Mass analysis of the whole broad band 1 revealed the presence, besides intact aldolase with amino acids 2–364 and a mass of 39,216 Da, C-terminally degraded fragments corresponding to sequences 2–362, 2–360, and other masses down to 2–352 that were generated by the sequential removal of six dipeptide units from the C terminus. The significant presence of the 2–351 peptide indicates that aldolase degradation also comprises carboxypeptidase activity of cathepsin B. The tiny band 2 contained the polypeptide 2–347, which was the smallest fragment obtained under the described conditions and corresponded to the removal of 17 amino acids from the C terminus, i.e., 8 dipeptide units (peptidyl–dipeptidase activity) plus one amino acid (carboxypeptidase activity). Bands 3 and 4 had the common N terminus SIGTENT (positions 46–52), suggesting their generation by a minor (but very useful for the purposes of this test) endoproteolytic cleavage between Gln^{45} and Ser^{46}. Band 3 corresponded to the 46–364 sequence and band 4 corresponded to sequence 46–347. Comparison of the relative intensities of bands 3 and 4 in lanes B and C (Fig. 7) suggests that DOFA inhibited the exopeptidase activity of cathepsin B on the macromolecular substrate aldolase, while the inhibitor was less or not active against the endoproteolytic activity of cathepsin B, as shown by the persistence of band 3 in lane C.

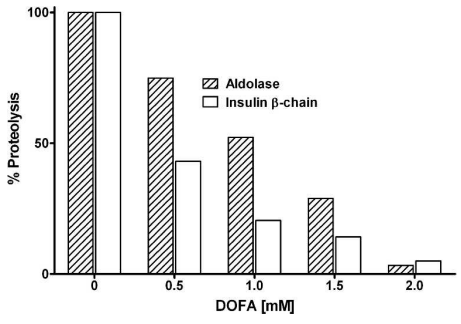

Figure 6. Inhibition of cleavage of rabbit muscle fructose 1,6-bisphosphate aldolase and of the bovine insulin β-chain by cathepsin B. Concentration-dependent inhibition by DOFA at pH 6.0. Released peptides were quantified fluorimetrically by the fluorescamine method.

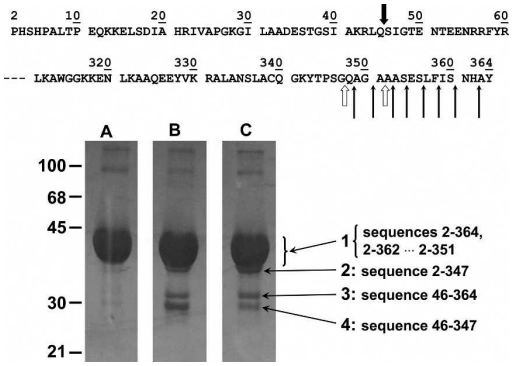

Figure 7. Proteolysis of rabbit muscle fructose 1,6-bisphosphate aldolase by cathepsin B. Aldolase was incubated 4 h at 25°C with cathepsin B at pH 6.0, and products were separated by SDS-PAGE. (Lane *A*) Aldolase alone run in parallel as control; (lane *B*) aldolase plus cathepsin B; (lane *C*) aldolase with cathepsin B and DOFA. The N- and C-terminal parts of the rabbit aldolase sequence, with numbered amino acid residues, are shown at the *top* of the figure. Thin arrows indicate sequential peptidyl-dipeptidase cleavages by cathepsin B. The two open thick arrows show carboxypeptidase cleavages. The black thick arrow indicates a minor endoproteolytic attack site. Numbers on the *left* side indicate the molecular masses of markers in kilodaltons. Numbers 1–4 with long pointing arrows are assigned to the bands for referencing in the main text, and the peptides identified within the bands are shown next to the band numbers. Peptides were identified in the excised bands by N-terminal sequencing and MALDI analysis.

The bovine insulin β-chain is a helpful substrate for exploring the specificity of peptide-bond cleavage by peptidases, including human cathepsin B (McKay et al. 1983). The cleavage at multiple sites of the insulin β-chain by cathepsin B was almost completely inhibited by a saturating concentration of DOFA at pH 6.0 (Fig. 6). Samples of insulin β-chain incubated with cathepsin B in the presence and absence of DOFA were separated by liquid chromatography, and the eluted peaks were analyzed by mass spectrometry. We confirmed most of the cathepsin B cleavages previously described (McKay et al. 1983). Additional cleavages, which depended on the incubation time and the relative enzyme to substrate concentrations, were identified. Each of the chromatographic peaks in Figure 8 contained only one (e.g., peptides 1–13, 1–14, and 6–28) or more proteolytic fragments (e.g., peptides 20–30 plus 1–11). Only a few of them will be discussed to demonstrate the inhibitory activity of DOFA. The generation of peptides 1–11 and 20–30 by endoproteolysis was inhibited by

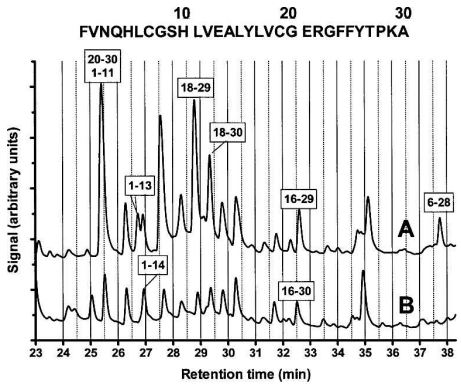

Figure 8. Proteolysis of the bovine insulin β-chain by cathepsin B. Incubation at pH 5.5 and 25°C in the absence (*A*) and in the presence (*B*) of DOFA. Peptides released by enzymatic digestion were characterized by LC/MALDI/MS. The sequence at the *top* of the figure shows the sequence of bovine insulin, β-chain with amino acid numbering. Boxed numbers, e.g., 6–28, indicate peptides released by the endo- and exoproteolytic action of cathepsin B.

DOFA. Fragment 1–13 was a product of carboxypeptidase activity on peptide 1–14: While DOFA completely inhibited this exoproteolytic event, endoproteolytic cleavage between residues 14 and 15 was unaffected, as shown by comparing the chromatographic profiles in the absence (Fig. 8, profile A) and in the presence of DOFA (Fig. 8, profile B). Fragment 18–29, generated by endoproteolysis at position 17–18 and exoproteolysis at position 29–30, was strongly decreased in the presence of DOFA. Comparison of the areas of fragments 18–29 and 18–30 after inhibition shows that both the exo- and the endoproteolytic events concerned with them were affected by the inhibitor. Carboxypeptidase activity inhibition is also shown by comparing the disappearance of fragment 16–29 and the appearance of fragment 16–30. Finally, the peptidyl–dipeptidase cleavage shown by fragment 6–28 disappeared in the presence of DOFA. Since the 6–30 peptide in Figure 8, profile B could not be unambiguously assigned, inhibition could be ascribed to endoproteolytic cleavage at positions 5–6, peptidyl–dipeptidase inhibition at position 28–29, or both.

Discussion

The docking approach used in this study aimed at identifying compounds that bind to the occluding loop of human cathepsin B and thereby modulate its enzymatic activity. Considering that no other means are available for selecting small molecules for a rather flexible protein segment, the most diverse compound library was used. There is a fundamental difference between our methodology and previous approaches to inhibitors that might interact with parts of the occluding loop of cathepsin B (Murata et al. 1991; Michaud and Gour 1998; Cathers et al. 2002). These studies exploited the properties of the fungal inhibitor E-64 (Hanada et al. 1978) and the crystal structure of cathepsin B (Musil et al. 1991). New inhibitors, such as CA-074, were designed by modification of the E-64 structure to create interactions with the primed sites of the substrate binding cleft and thus with the occluding loop (Murata et al. 1991). In this approach the epoxy moiety of the modifiers acted as a warhead against the active site cysteine to produce potent irreversible inhibition (Matsumoto et al. 1999). Conversely, we did not target the active site, and the molecules selected by docking were devoid of chemically active warheads. The finding of only one active compound out of 29 substances is in line with previous studies, which showed that candidate inhibitors predicted by docking algorithms are not necessarily active in vitro (Huang et al. 2005).

In agreement with published data (Illy et al. 1997; Nägler et al. 1997; Quraishi et al. 1999; Krupa et al. 2002) our results support the notion that the occluding loop of cathepsin B is a highly flexible segment. Short episodes of opening and closing govern endo- and exoproteolysis, which thus occur intermittently in the pH range 4.5–6.0. The compound identified by docking, DOFA, behaves as a reversible competitive inhibitor of the exo- and endopeptidase activities of cathepsin B with no involvement of a substrate-like binding mode in the active center of the enzyme. It can inhibit endoproteolysis most likely by forcing the loop in the closed conformation, and exoproteolysis by disturbing the accommodation of the C terminus of polypeptides in the primed side of the binding cleft. Docking calculations suggest that the dioxothiazolidine moiety of DOFA is located in the binding pocket of the side chain of the substrate C-terminal residue when the loop is closed. It makes a hydrogen bond with $N\delta^1$ of His^{110} and sterically hinders substrate binding for exoproteolytic activity (Fig. 9A,B). In this figure, the structures of DOFA and the four amino acids VRAK, which are part of the FRET substrate used for measuring exoproteolytic activity, were modeled on the known structure of human cathepsin B merely to show their spatial relationship. In fact, such a ternary ESI complex does not exist according to the kinetic mechanism; only the ES and EI complexes exist. This structural arrangement is consistent with the kinetic mechanism of inhibition: At pH 4.5 the exoproteolytic activity of cathepsin B is inhibited in a linear competitive manner by virtue of the dioxothiazolidine ring. Docking suggests that DOFA binds at the surface of the occluding loop and is involved in three hydrogen bonds with the enzyme (Fig. 9A). Of particular interest is that the carbonyl oxygen involved in a hydrogen bond with the amide of His^{111} occupies the place of the oxygen of a conserved water molecule present in the crystal structures of human cathepsin B. This position is shown as a red sphere in Figure 9B. Together with the favorable van der Waals interactions, three hydrogen bonds stabilize the loop in

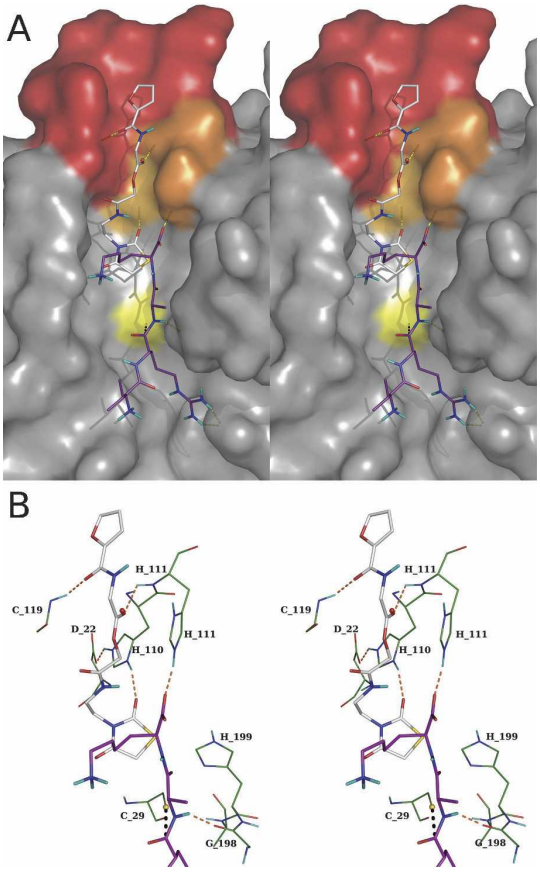

Figure 9. Stereoview of inhibitor and substrate within the structure of human cathepsin B. (*A*) The protein surface is shown with the occluding loop in red, His^{110} and His^{111} in orange, and the catalytic Cys^{29} in yellow. The substrate (carbon atoms in purple) is shown as residues VR↓AK, which is part of the FRET substrate used in this study to monitor peptidyl–dipeptidase activity. The Dnp group, which is exposed to the solvent, was omitted for clarity. The pose of DOFA obtained by docking (carbon atoms in gray) is visible in the *upper* part with the furan moiety in the occluding loop and the dioxothiazolidine ring sterically interfering with the lysine side chain of the substrate. (*B*) Details of the presumed interactions between DOFA and cathepsin B residues (carbon atoms in green). The inhibitor makes three hydrogen bonds with residues of the occluding loop: carbonyl group labeled "a" in Figure 2 with amide nitrogen of Cys^{119}, carbonyl group labeled "b" in Figure 2 with amide nitrogen of His^{111}, and 2-oxo group of the dioxothiazolidine ring with $N\delta^1$ of His^{110}. The hydrogen bonds of the occluding loop in the closed conformation, His^{110}–Asp^{22} and His^{111} with the C-terminal carbonyl of the substrate, are also shown. The red sphere indicates the position of a water molecule in the cathepsin B crystal structure. Images generated with PyMOL software (see Fig. 1).

the closed conformation (Fig. 9B). These structural properties are reflected in the kinetic mechanism observed with Z-RR↓AMC. Despite not being a complete model for endoproteolysis, the dipeptide is unquestionably cleaved by cathepsin B in the endo-, not in the exoproteolytic mode. The double-headed competitive kinetic mechanism diagnosed for DOFA on Z-RR↓AMC, and the changes in the kinetic parameters observed when going from pH 4.5 to 6.0, insinuate cooperation between the furan and the dioxothiazolidine moieties. Kinetic measurements alone would be unable to identify which element makes the stronger contribution to binding energy. However, with the support of structural information from modeling discussed above, we suggest that the dioxothiazolidine moiety takes the leader function. In the double-headed mechanism at pH 4.5, the K_i value of 4.8 μM is thus ascribed to the dioxothiazolidine part of the molecule and $K_i \approx 160$ μM to the furan part (factor $a = 34$ in Model 3, Fig. 3). The increase of pH to 6.0 disfavors the K_i of the dioxothiazolidine portion, which becomes 11.3 μM and favors binding of the furan moiety, decreasing its K_i to 68 μM.

The measurements with protein substrates, aldolase and the insulin β-chain, confirm the results just discussed with synthetic substrates, as well as the previously recorded ability of cathepsin B to exert peptidyl–dipeptidase and carboxypeptidase activity in the pH range 5.5–6.0 (Mort et al. 1998). While efficiently inhibiting these two exoproteolytic activities, DOFA was not able to inhibit all endoproteolytic events. For instance, the minor endoproteolytic action at position 45–46 of rabbit muscle aldolase was only moderately or not affected by DOFA, as was not position 14–15 of the insulin β-chain. Yet, other endoproteolytic attacks on the insulin β-chain were efficiently inhibited.

The pooled experimental evidence from the above described properties of DOFA inhibition strengthens the notion that not only pH dependent, intermittent closing and opening of the occluding loop, but also substrate structure determine together the susceptibility of particular peptide bonds. The binding affinity of DOFA is possibly not high enough to compete with a substrate, which optimally binds at both unprimed and primed sites. It appears that the occluding loop of cathepsin B can be assisted in assuming its closed or open conformation by particular polypeptides with an induced fit mechanism that promotes either exo- or endoproteolysis. This observation forms the basis of cathepsin B inhibition by its own propeptide (Quraishi et al. 1999) and its resistance to cystatin A and C inhibition (Nycander et al. 1998; Pavlova et al. 2000).

The above results draw attention to the physiopathological role of cathepsin B, which exerts its action in a relatively broad range of pH values, with exoproteolysis in the range 5–6 and endoproteolysis in the range 5–7.4. The pH in early endosomes is ~6.2 and drops to 5.0–5.5 in late endosomes and lysosomes (Gu and Gruenberg 2000). Extracellularly, the pH can vary from relatively acidic, e.g., at the periphery of solid tumors (Rofstad et al. 2006), to 7.4 in blood. Contrary to commonplace textbook information, proteolysis within phagolysosomes does not quite occur in a very acidic environment. For instance, 5 min after initiation of

phagocytosis in human polymorphonuclear leukocytes, the relatively acidic milieu of the lysosomes (pH ≈ 5) increases in the phagocytic vacuoles to a value of 7.8. It falls then to 7.4 after 15 min, to 6.4 after 30 min, and 5.7 after 60 min (rounded values from Cech and Lehrer [1984]). Various hydrolases are expected to find their optimal conditions of action during this forth and back excursion of pH (Baici et al. 1996).

It has been suggested that "targeting of the occluding loop of cathepsin B may be a poor inhibitor design strategy if the enzyme environment has a pH greater than 5.5" (Cathers et al. 2002). This statement refers to the above discussed approach "from inside." Since endo- and exoproteolysis by cathepsin B occurs in the physiologically and pathologically relevant pH range of 5–6, our approach of targeting the occluding loop from the enzyme surface may represent an alternative starting point for the development of clinically active compounds.

Materials and Methods

Materials and general methods

Recombinant human cathepsin B was prepared from *Escherichia coli* inclusion bodies (Kuhelj et al. 1995). Wild-type cathepsin B from human liver was obtained from Calbiochem. The synthetic substrates Z-FR↓AMC[2] and Z-RR↓AMC were purchased from Bachem and the internally quenched fluorogenic substrate Abz-GIVR↓AK(Dnp)OH from Merck. Rabbit muscle fructose-1,6-bisphosphate aldolase (EC 4.1.2.13) and fluorescamine were from Sigma-Aldrich Chemie and the oxidized bovine insulin β-chain from Serva Feinbiochemica. The putative binders/modifiers of cathepsin B activity determined by docking analysis and their sources are listed in Supplemental Table 1. The compound studied in detail, [2-[2-(2,4-dioxo-1,3-thiazolidin-3-yl)ethylamino]-2-oxoethyl] 2-(furan-2-carbonylamino)acetate (IUPAC name, here abbreviated DOFA; Fig. 2), Zinc-2005 code 2616818 (Irwin and Shoichet 2005) was obtained from Enamine. The compounds were dissolved as concentrated stock solutions in dimethyl sulphoxide, stored at 4°C, and diluted into the appropriate buffer at the moment of the assay. Photometric measurements were carried out with a Cary50 UV-visible spectrophotometer, and fluorescence was measured with an Aminco SPF-500 fluorimeter operating in the ratio mode. Reversed phase HPLC was performed in a Hewlett Packard Series 1100 apparatus with a Nucleosil 120-5 C18 column (4.0 × 250 mm). Matrix-assisted laser desorption/ionization mass spectrometry (MALDI-MS) and liquid chromatography followed by mass analysis, LC-MALDI/MS, was performed at the Functional Genomics Center in Zurich.

Docking

The A and B chains of the human cathepsin B structure, entry 1HUC in the Brookhaven database, were considered and all water molecules were removed. Hydrogens were added to side chains and termini of the protein to simulate conditions at pH 6–7. Cys^{29} was in the reduced form, and His^{110} was protonated at both imidazole nitrogen atoms. CHARMm atom types and force field parameters were assigned and used for both protein and ligands (Momany and Rone 1992), and hydrogens were minimized with the program CHARMM (Brooks et al. 1983). The search for a putative binding site focused on the occluding loop of the enzyme, for which no inhibitor has been reported to date. A benzene molecule was used as a probe with the program SEED (Solvation Energy for Exhaustive Docking) to identify possible binding pockets whose main interaction component is supposed to be hydrophobicity (Majeux et al. 1999). The surface tested by SEED consists of cathepsin B residues within a 9 Å distance from His^{110}, which locks the occluding loop in a closed position. The benzenes with the most favorable free energy of binding, excluding those in the catalytic site, were used to define the binding site for docking, which included all the 42 residues of the protein that had >50% of their atoms within 5 Å from the optimal poses of benzenes.

About 3 million compounds in the ZINC 2005 library (Irwin and Shoichet 2005) were clustered using a 17-field fingerprint by Decomposition and Identification of Molecules (Kolb and Caflisch 2006). Molecules with more than nine rotatable bonds were neglected. The resulting 48,026 cluster representatives were docked as in previous in silico campaigns (Huang et al. 2005, 2006; Kolb et al. 2008). For each molecule docked by the program FFLD (Fragment-based Flexible Ligand Docking) (Budin et al. 2001; Cecchini et al. 2004), the 300 most favorable poses were clustered with the leader algorithm yielding 764,776 poses (~17 poses per compound, 44,527 compounds). The cluster representatives were minimized in the rigid protein using CHARMM.

It is necessary to weed out unlikely poses to prevent a high number of false positives (Kolb et al. 2008). Suitable filters are cutoffs in the total van der Waals interaction energy and in the van der Waals efficiency (defined as the ratio between van der Waals energy and molecular mass). A cutoff of −30 kcal/mol for intermolecular van der Waals energy was selected by plotting a histogram of the van der Waals energies (Supplemental Fig. 1). Analogously, a cutoff of −0.09 kcal/g was chosen for the van der Waals efficiency (Supplemental Fig. 2). A total of 106,502 poses of 10,709 compounds survived both filters. Poses closer than 4 Å to Cys^{29} of the catalytic site and those with no hydrogen bond to the protein were neglected, yielding 25,178 remaining poses (5678 compounds).

The electrostatic contribution to the binding free energy was evaluated by the finite difference Poisson approach (module PBEQ of CHARMM) (Im et al. 1998). Poses were ranked for visual inspection according to most favorable van der Waals energy, van der Waals efficiency, electrostatics, and sum of van der Waals and electrostatic energy. Poses with high ranking in two lists or more were selected and visually inspected. Forty poses belonging to 40 different compounds were selected in this way. According to the predicted binding modes, three regions of the protein were exploited for binding: one on the occluding loop and one each on immediately adjacent regions. Twenty-nine out of the 40 candidate compounds were commercially available.

Kinetics

The peptide Z-RR↓AMC with 7-amino-4-methlycoumarin (AMC) as leaving group is a handy substrate for measuring the endopeptidase activity of cathepsin B (Barrett 1980), in which the two arginine residues correspond to the P_1 and P_2 positions (Schechter and Berger 1967). We preferred this substrate over Z-FR↓AMC for its slower hydrolysis that allowed long measuring times with low substrate consumption. The buffer for measurements at pH 6.00 was 50 mM sodium phosphate

containing 2 mM EDTA and 2 mM dithiothreitol (DTT), hereafter referred to as pH 6.0 buffer. For measurements at pH 4.50, 0.1 M sodium acetate, 0.2 M NaCl, 2 mM EDTA, and 2.5 mM DTT were used (hereafter referred to as pH 4.5 buffer). In control experiments aimed at ascertaining any aggregation phenomena on the part of the putative inhibitors, the DTT concentration was increased to 5 mM and the buffer included 0.01% (v/v) of hydrogenated Triton X-100, which does not absorb light in the ultraviolet range and is not fluorescent. The buffers were prepared and used at the same temperature of the kinetic assays, 25 ± 1°C. The final concentration of dimethyl sulphoxide, used for preparing stock solutions of the compounds, was 0.2% (v/v) in experiments with synthetic substrates and 1% (v/v) in those with protein substrates. Reaction progress with Z-RR↓AMC at pH 4.5 and 6.0 was followed by either measuring the change in absorbance at 360 nm, with $\Delta\varepsilon = 11{,}400\ M^{-1}cm^{-1}$ as the difference absorption coefficient between free and bound AMC or fluorimetrically with excitation and emission wavelengths, λ_{ex} and λ_{em}, set at 383 and 455 nm, respectively. Exopeptidase activity was continuously monitored fluorimetrically with the Förster resonance energy transfer (FRET) labeled substrate Abz-GIVR↓AK(Dnp)-OH (Cotrin et al. 2004). Appropriate corrections for inner filter effects were taken into account in fluorescence measurements considering the absorbencies of the substrates and of the tested compounds at λ_{ex} and λ_{em} (Palmier and Van Doren 2007). With the AMC-based substrate, λ_{ex} at 383 nm allowed high substrate concentrations to be used with small inner filter corrections. Since with the FRET substrate inner filter effects were more pronounced, λ_{ex} and λ_{em} were selected according to the compound being tested. The combination $\lambda_{ex}/\lambda_{em}$ 320/420 nm, often used in assays with this type of substrate, could not be utilized for the strong absorbance at 320 nm of one of the compounds (ZINC-2005 code 1797383), which simulated strong enzyme inhibition, whereas the combination $\lambda_{ex}/\lambda_{em}$ 370/430 nm revealed no inhibition. Any modifier-independent contribution to enzyme activity loss by denaturation, adherence to the vessel walls, or other causes was monitored in time-course assays by the Selwyn method (Selwyn 1965). Screening and primary analysis of the kinetic inhibition mechanism of the compounds was performed on initial velocity data obtained at various concentrations of substrate and compounds. The specific velocity plot, a sensitive tool for detecting mixed-type and/or hyperbolic mechanisms was routinely used in this phase (Baici 1981). The kinetic inhibition models considered and their related rate equations are shown in Figure 3. In Models 2 and 3, a is a coefficient, which is equal to 1 when the first binding process does not influence the second one. If the equilibrium constant of the vacant site is influenced after binding to the first site, $a \neq 1$. Kinetic analysis was performed by fitting the equations in Figure 3 to experimental data using GraphPad Prism version 5.00 for Windows. The runs test and analysis of residuals were performed to monitor deviations from a model, and discrimination between mechanisms was made by analysis of variance of the difference between the sum of squares (extra sum-of-squares test) and calculation of F ratios and p values. According to Occam's razor principle, the simplest mechanism describing experimental data was considered superior to a more complex (redundant) mechanism. Additionally, a powerful and decisive tool for model discrimination was the $I_{90/10}$ ratio, i.e., the ratio of inhibitor concentration necessary to achieve 90% and 10% inhibition. This parameter was determined experimentally and compared with values calculated from Equations 4 and 6 in Figure 3.

Protein substrates

The activity of cathepsin B on rabbit muscle aldolase was quantified by measuring primary amino groups derived from peptide-bond hydrolysis with fluorescamine (Schwabe 1975). Aldolase was dissolved in pH 6.0 buffer without DTT, incubated 3 h at 37°C with cathepsin B, which was pre-activated with DTT, and DOFA under vigorous shaking to prevent precipitation. Final concentrations were: aldolase = 3.5 mg/mL = 21.7 μM, cathepsin B = 2.3 μM, DOFA = 0.5, 1.0, 1.5, and 2.0 mM. The reaction was stopped with trichloroacetic acid, 5% (w/v) final concentration, and centrifuged. We added 0.1 mL of the clear supernatant to 2.0 mL 0.2 M sodium borate buffer (pH 8.50), and 1.0 mL of fluorescamine solution (15 mg/100 mL acetone). The fluorescence of labeled peptides was measured with $\lambda_{ex}/\lambda_{em}$ = 390/480 nm. Blanks were subtracted and controls compared with the samples containing the compounds. Measurements with the oxidized β-chain of bovine insulin as substrate were performed in pH 6.0 buffer using the same procedure. Final concentrations were: insulin β-chain = 72 μg/mL = 20.6 μM, cathepsin B = 2.3 μM, DOFA = 0.5, 1.0, 1.5, and 2.0 mM.

Endo- and exoproteolysis of protein substrates

Reaction products resulting from incubation of aldolase with cathepsin B and DOFA were also assessed by denaturing gel electrophoresis. Final concentrations in incubation mixtures at 25°C under continuous shaking for 4 h were: aldolase 3.5 mg/mL (21.7 μM) in pH 6.0 buffer without DTT, 2.3 μM of preactivated cathepsin B, and 1.0 mM DOFA. After centrifugation, the clear supernatant was analyzed by sodium dodecyl sulphated, polyacrylamide gel electrophoresis (SDS-PAGE) under reducing conditions with 12.5% polyacrylamide and silver stained. For N-terminal sequencing by Edman degradation, the bands were transferred to a polyvinylidene fluoride membrane. Peptides in the excised bands were also identified by MALDI analysis.

The oxidized β-chain of bovine insulin was incubated at a final concentration of 1.0 mg/mL (286 μM) in 0.1 M sodium acetate buffer containing 0.2 mM NaCl, 2 mM EDTA, and 2.5 mM DTT (pH 5.50) with 1.2 μM cathepsin B (control) or cathepsin B plus 1.0 mM DOFA. After 20 h at 25°C under shaking, solutions were centrifuged and the solvent removed in a Speed Vac concentrator. The residue was resuspended in 60 μL of deionized water containing 0.1% trifluoroacetic acid and centrifuged before analysis by LC/MALDI/MS.

Electronic supplemental material

Supplemental Table 1 shows the identification codes and the sources of the cathepsin B inhibitors. Supplemental Figure 1 presents the van der Waals interaction energies distribution used in the docking procedure and shows the cutoff of −30 kcal/mol for intermolecular van der Waals energy. Analogously, Supplemental Figure 2 shows the van der Waals interaction energy efficiencies distribution.

Acknowledgments

Docking calculations were performed on Matterhorn, a Beowulf Linux cluster at the University of Zurich, and we thank C. Bolliger, T. Steenbock, and A. Godknecht for computer support. We thank A. Widmer (Novartis Pharma, Basel, Switzerland) for providing the molecular modeling program Wit!P, which was used for preparing the structures. We also thank the staff at the

Functional Genomics Center in Zurich for expert assistance in LC/MALDI/MS measurements. This work was supported by grant 31-113345/1 of the Swiss National Foundation and by the Albert-Böni Foundation (to A.B.), and by a grant of the Hartmann-Müller Foundation (to A.C.).

References

Aronson Jr., N.N. and Barrett, A.J. 1978. The specificity of cathepsin B. Hydrolysis of glucagon at the C-terminus by a peptidyldipeptidase mechanism. *Biochem. J.* **171:** 759–765.

Baici, A. 1981. The specific velocity plot. A graphical method for determining inhibition parameters for both linear and hyperbolic enzyme inhibitors. *Eur. J. Biochem.* **119:** 9–14.

Baici, A. 1998. Inhibition of extracellular matrix-degrading endopeptidases: Problems, comments, and hypotheses. *Biol. Chem.* **379:** 1007–1018.

Baici, A., Hörler, D., Lang, A., Merlin, C., and Kissling, R. 1995a. Cathepsin B in osteoarthritis: Zonal variation of enzyme activity in human femoral head cartilage. *Ann. Rheum. Dis.* **54:** 281–288.

Baici, A., Lang, A., Hörler, D., Kissling, R., and Merlin, C. 1995b. Cathepsin B in osteoarthritis: Cytochemical and histochemical analysis of human femoral head cartilage. *Ann. Rheum. Dis.* **54:** 289–297.

Baici, A., Szedlacsek, S.E., Früh, H., and Michel, B.A. 1996. pH-Dependent hysteretic behaviour of human myeloblastin (leucocyte proteinase 3). *Biochem. J.* **317:** 901–905.

Baici, A., Müntener, K., Willimann, A., and Zwicky, R. 2006. Regulation of human cathepsin B by alternative mRNA splicing: Homeostasis, fatal errors and cell death. *Biol. Chem.* **387:** 1017–1021.

Barrett, A.J. 1980. Fluorimetric assays for cathepsin B and cathepsin H with methylcoumarylamide substrates. *Biochem. J.* **187:** 909–912.

Bond, J.S. and Barrett, A.J. 1980. Degradation of fructose-1,6-bisphosphate aldolase by cathepsin B. A further example of peptidyldipeptidase activity of this proteinase. *Biochem. J.* **189:** 17–25.

Bröker, L.E., Kruyt, F.A.E., and Giaccone, G. 2005. Cell death independent of caspases: A review. *Clin. Cancer Res.* **11:** 3155–3162.

Brooks, B.R., Bruccoleri, R.E., Olafson, B.D., States, D.J., Swaminathan, S., and Karplus, M. 1983. CHARMM: A program for macromolecular energy, minimization, and dynamics calculations. *J. Comput. Chem.* **4:** 187–217.

Budin, N., Majeux, N., and Caflisch, A. 2001. Fragment-based flexible ligand docking by evolutionary optimization. *Biol. Chem.* **382:** 1365–1372.

Buxser, S. and Vroegop, S. 2005. Calculating the probability of detection for inhibitors in enzymatic or binding reactions in high-throughput screening. *Anal. Biochem.* **340:** 1–13.

Cathers, B.E., Barrett, C., Palmer, J.T., and Rydzewski, R.M. 2002. pH Dependence of inhibitors targeting the occluding loop of cathepsin B. *Bioorg. Chem.* **30:** 264–275.

Cecchini, M., Kolb, P., Majeux, N., and Caflisch, A. 2004. Automated docking of highly flexible ligands by genetic algorithms: A critical assessment. *J. Comput. Chem.* **25:** 412–422.

Cech, P. and Lehrer, R.I. 1984. Phagolysosomal pH of human neutrophils. *Blood* **63:** 88–95.

Cotrin, S.S., Puzer, L., Judice, W.A.D., Juliano, L., Carmona, A.K., and Juliano, M.A. 2004. Positional-scanning combinatorial libraries of fluorescence resonance energy transfer peptides to define substrate specificity of carboxydipeptidases: Assays with human cathepsin B. *Anal. Biochem.* **335:** 244–252.

Friedrichs, B., Tepel, C., Reinheckel, T., Deussing, J., von Figura, K., Herzog, V., Peters, C., Saftig, P., and Brix, K. 2003. Thyroid functions of mouse cathepsins B, K, and L. *J. Clin. Invest.* **111:** 1733–1745.

Frlan, R. and Gobec, S. 2006. Inhibitors of cathepsin B. *Curr. Med. Chem.* **13:** 2309–2327.

Gu, F. and Gruenberg, J. 2000. ARF1 regulates pH-dependent COP functions in the early endocytic pathway. *J. Biol. Chem.* **275:** 8154–8160.

Hanada, K., Tamai, M., Yamagishi, M., Ohmura, S., Sawada, J., and Tanaka, I. 1978. Isolation and characterization of E-64, a new thiol protease inhibitor. *Agric. Biol. Chem.* **42:** 523–528.

Huang, D.Z., Lüthi, U., Kolb, P., Edler, K., Cecchini, M., Audetat, S., Barberis, A., and Caflisch, A. 2005. Discovery of cell-permeable non-peptide inhibitors of β-secretase by high-throughput docking and continuum electrostatics calculations. *J. Med. Chem.* **48:** 5108–5111.

Huang, D.Z., Lüthi, U., Kolb, P., Cecchini, M., Barberis, A., and Caflisch, A. 2006. In silico discovery of β-secretase inhibitors. *J. Am. Chem. Soc.* **128:** 5436–5443.

Illy, C., Quraishi, O., Wang, J., Purisima, E., Vernet, T., and Mort, J.S. 1997. Role of the occluding loop in cathepsin B activity. *J. Biol. Chem.* **272:** 1197–1202.

Im, W., Beglov, D., and Roux, B. 1998. Continuum solvation model: Computation of electrostatic forces from numerical solutions to the Poisson–Boltzmann equation. *Comput. Phys. Commun.* **111:** 59–75.

Irwin, J.J. and Shoichet, B.K. 2005. ZINC—a free database of commercially available compounds for virtual screening. *J. Chem. Inf. Model.* **45:** 177–182.

Kolb, P. and Caflisch, A. 2006. Automatic and efficient decomposition of two-dimensional structures of small molecules for fragment-based high-throughput docking. *J. Med. Chem.* **49:** 7384–7392.

Kolb, P., Huang, D., Dey, F., and Caflisch, A. 2008. Discovery of kinase inhibitors by high-throughput docking and scoring based on a transferable linear interaction energy model. *J. Med. Chem.* **51:** 1179–1188.

Krupa, J.C., Hasnain, S., Nägler, D.K., Menard, R., and Mort, J.S. 2002. S2′ substrate specificity and the role of His110 and His111 in the exopeptidase activity of human cathepsin B. *Biochem. J.* **361:** 613–619.

Kuhelj, R., Dolinar, M., Pungercar, J., and Turk, V. 1995. The preparation of catalytically active human cathepsin B from its precursor expressed in *Escherichia coli* in the form of inclusion bodies. *Eur. J. Biochem.* **229:** 533–539.

Kukor, Z., Mayerle, J., Krüger, B., Tóth, M., Steed, P.M., Halangk, W., Lerch, M.M., and Sahin-Tóth, M. 2002. Presence of cathepsin B in the human pancreatic secretory pathway and its role in trypsinogen activation during hereditary pancreatitis. *J. Biol. Chem.* **277:** 21389–21396.

Lenarcic, B., Gabrijelcic, D., Rozman, B., Drobnic-Kosorok, M., and Turk, V. 1988. Human cathepsin B and cysteine proteinase inhibitors (CPIs) in inflammatory and metabolic joint diseases. *Biol. Chem. Hoppe Seyler* **369:** 257–261.

Majeux, N., Scarsi, M., Apostolakis, J., Ehrhardt, C., and Caflisch, A. 1999. Exhaustive docking of molecular fragments with electrostatic solvation. *Proteins* **37:** 88–105.

Matsumoto, K., Mizoue, K., Kitamura, K., Tse, W.C., Huber, C.P., and Ishida, T. 1999. Structural basis of inhibition of cysteine proteases by E-64 and its derivatives. *Biopolymers* **51:** 99–107.

Matsunaga, Y., Saibara, T., Kido, H., and Katunuma, N. 1993. Participation of cathepsin B in processing of antigen presentation to MHC class II. *FEBS Lett.* **324:** 325–330.

McKay, M.J., Offermann, M.K., Barrett, A.J., and Bond, J.S. 1983. Action of human liver cathepsin B on the oxidized insulin B chain. *Biochem. J.* **213:** 467–471.

Michaud, S. and Gour, B.J. 1998. Cathepsin B inhibitors as potential anti-metastatic agents. *Expert Opin. Ther. Pat.* **8:** 645–672.

Mohamed, M.M. and Sloane, B.F. 2006. Cysteine cathepsins: Multifunctional enzymes in cancer. *Nat. Rev. Cancer* **6:** 764–775.

Momany, F.A. and Rone, R. 1992. Validation of the general purpose QUANTA®3.2/CHARMm® force field. *J. Comput. Chem.* **13:** 888–900.

Mort, J.S. 2004. Cathepsin B. In *Handbook of proteolytic enzymes*, 2nd ed. (eds. A.J. Barrett and N.D. Rawlings, J.F. Woessner, Jr.), pp. 1079–1086. Elsevier, London, UK.

Mort, J.S., Magny, M.C., and Lee, E.R. 1998. Cathepsin B: An alternative protease for the generation of an aggrecan ''metalloproteinase'' cleavage neoepitope. *Biochem. J.* **335:** 491–494.

Müntener, K., Zwicky, R., Csucs, G., and Baici, A. 2003. The alternative use of exons 2 and 3 in cathepsin B mRNA controls enzyme trafficking and triggers nuclear fragmentation in human cells. *Histochem. Cell Biol.* **119:** 93–101.

Müntener, K., Zwicky, R., Csucs, G., Rohrer, J., and Baici, A. 2004. Exon skipping of cathepsin B: Mitochondrial targeting of a lysosomal peptidase provokes cell death. *J. Biol. Chem.* **279:** 41012–41017.

Murata, M., Miyashita, S., Yokoo, C., Tamai, M., Hanada, K., Hatayama, K., Towatari, T., Nikawa, T., and Katunuma, N. 1991. Novel epoxysuccinyl peptides. Selective inhibitors of cathepsin B, in vitro. *FEBS Lett.* **280:** 307–310.

Musil, D., Zucic, D., Turk, D., Engh, R.A., Mayr, I., Huber, R., Popovic, T., Turk, V., Towatari, T., Katunuma, N., et al. 1991. The refined 2.15 Å X-ray crystal structure of human liver cathepsin B: The structural basis for its specificity. *EMBO J.* **10:** 2321–2330.

Nägler, D.K., Storer, A.C., Portaro, F.C.V., Carmona, E., Juliano, L., and Menard, R. 1997. Major increase in endopeptidase activity of human cathepsin B upon removal of occluding loop contacts. *Biochemistry* **36:** 12608–12615.

Nycander, M., Estrada, S., Mort, J.S., Abrahamson, M., and Björk, I. 1998. Two-step mechanism of inhibition of cathepsin B by cystatin C due to displacement of the proteinase occluding loop. *FEBS Lett.* **422:** 61–64.

Okamura-Oho, Y., Zhang, S.Q., Callahan, J.W., Murata, M., Oshima, A., and Suzuki, Y. 1997. Maturation and degradation of β-galactosidase in the post-Golgi compartment are regulated by cathepsin B and a non-cysteine protease. *FEBS Lett.* **419:** 231–234.

Otto, H.H. and Schirmeister, T. 1997. Cysteine proteases and their inhibitors. *Chem. Rev.* **97:** 133–171.

Palmier, M.O. and Van Doren, S.R. 2007. Rapid determination of enzyme kinetics from fluorescence: Overcoming the inner filter effect. *Anal. Biochem.* **371:** 43–51.

Pavlova, A., Krupa, J.C., Mort, J.S., Abrahamson, M., and Björk, I. 2000. Cystatin inhibition of cathepsin B requires dislocation of the proteinase occluding loop. Demonstration by release of loop anchoring through mutation of His110. *FEBS Lett.* **487:** 156–160.

Quraishi, O., Nägler, D.K., Fox, T., Sivaraman, J., Cygler, M., Mort, J.S., and Storer, A.C. 1999. The occluding loop in cathepsin B defines the pH dependence of inhibition by its propeptide. *Biochemistry* **38:** 5017–5023.

Rawlings, N.D., Tolle, D.P., and Barrett, A.J. 2004. MEROPS: The peptidase database (http://merops.sanger.ac.uk). *Nucleic Acids Res.* **32:** D160–D164.

Rofstad, E.K., Mathiesen, B., Kindem, K., and Galappathi, K. 2006. Acidic extracellular pH promotes experimental metastasis of human melanoma cells in athymic nude mice. *Cancer Res.* **66:** 6699–6707.

Rowan, A.D., Feng, R., Konishi, Y., and Mort, J.S. 1993. Demonstration by electrospray mass spectrometry that the peptidylpeptidase activity of cathepsin B is capable of rat cathepsin B C-terminal processing. *Biochem. J.* **294:** 923–927.

Schechter, I. and Berger, A. 1967. On the size of the active sites in proteases. I. Papain. *Biochem. Biophys. Res. Commun.* **27:** 157–162.

Schwabe, C. 1975. A fluorescence assay for proteolytic enzymes. *Anal. Biochem.* **53:** 484–490.

Selwyn, M.J. 1965. A simple test for inactivation of an enzyme during assay. *Biochim. Biophys. Acta* **105:** 193–195.

Shoichet, B.K. 2006. Screening in a spirit haunted world. *Drug Discov. Today* **11:** 607–615.

Takahashi, T., Dehdarani, A.H., Yonezawa, S., and Tang, J. 1986. Porcine spleen cathepsin B is an exopeptidase. *J. Biol. Chem.* **261:** 9375–9381.

Turk, D., Podobnik, M., Kuhelj, R., Dolinar, M., and Turk, V. 1996. Crystal structures of human procathepsin B at 3.2 and 3.3 Å resolution reveal an interaction motif between a papain-like cysteine protease and its propeptide. *FEBS Lett.* **384:** 211–214.

Yan, S.Q. and Sloane, B.F. 2003. Molecular regulation of human cathepsin B: Implication in pathologies. *Biol. Chem.* **384:** 845–854.

Zwicky, R., Müntener, K., Csucs, G., Goldring, M.B., and Baici, A. 2003. Exploring the role of 5′-alternative splicing and of the 3′-untranslated region of cathepsin B mRNA. *Biol. Chem.* **384:** 1007–1018.

Supplemental Table 1. Identification codes and source of 29 putative inhibitors of human cathepsin B. The ZINC-codes are those of the database 2005 [Irwin, J. J., and Shoichet, B. K. (2005) J. Chem. Inf. Model. 45, 177-182]. [2-(2,4-dioxothiazolidin-3-yl) ethylcarbamoylmethyl 2-(furan-2-carbonylamino) acetate (DOFA) is shown in boldface.

Source	ZINC 2005-codes
ChemDiv (San Diego, USA)	33816, 978038, 2487954, 2560859
Ambinter (Paris, France)	1271923, 1414169
ChemBridge (San Diego, USA)	958753, 2904166, 2973678, 2990182
Pharmerks (Moscow, Russia)	989395, 1755678, 1837733, 1871954
Life Chemicals (Burlington, Canada)	1797383
Enamine (Kiev, Ukraine)	**2616818**, 2667966, 3247330, 3333255, 3340535, 3417832, 3439551, 3451184
IBScreen (Moscow, Russia)	1419203, 2128374, 2131752
National Cancer Institute, U.S.A.	1581881, 1628238, 1682930

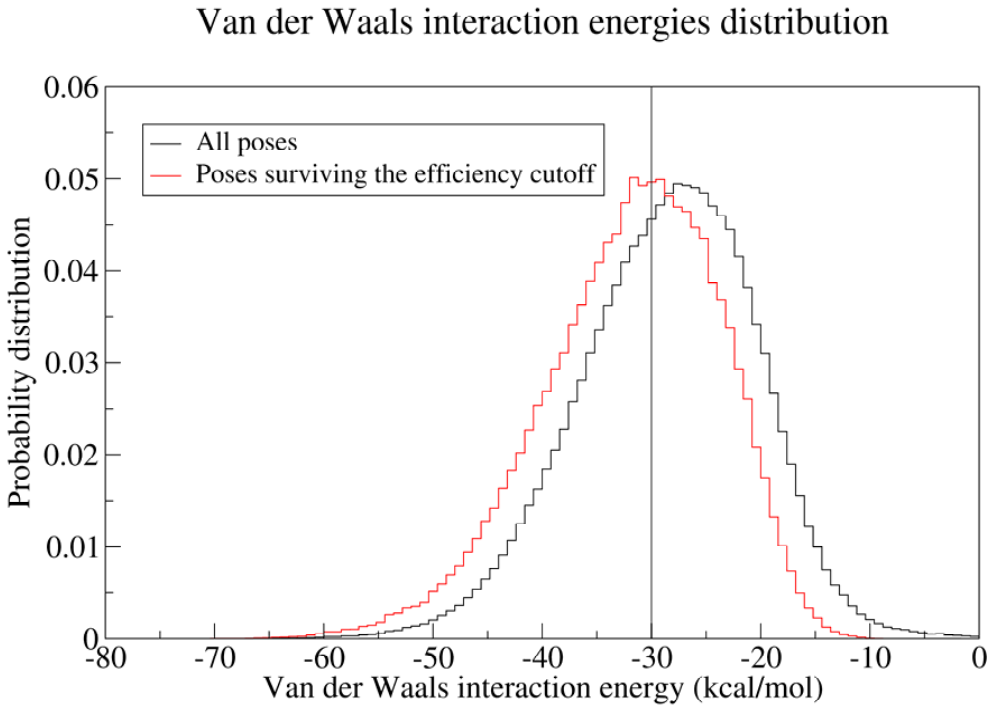

Supplemental Figure 1. **Van der Waals interaction energies distribution.** The histogram represents the distribution of van der Waals interaction energies before and after the efficiency cutoff. The vertical line marks the cutoff on van der Waals energy.

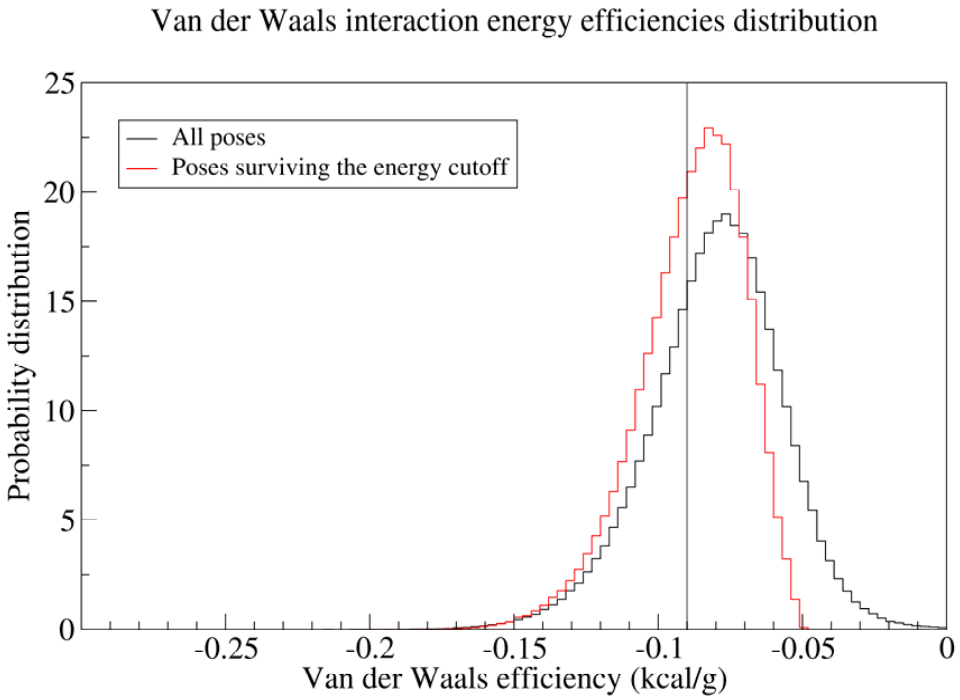

Supplemental Figure 2. **Van der Waals interaction energy efficiencies distribution.** The histogram represents the distribution of van der Waals interaction energy efficiencies before and after the energy cutoff. The vertical line represents the cutoff of van der Waals efficiency.

3-Fluoro-2,4-dioxa-3-phosphadecalins as inhibitors of acetylcholinesterase. A reappraisal of kinetic mechanisms and diagnostic methods

Chemistry and Biodiversity, 2009, 6:261−282

Abstract

Die systematische Untersuchung der Acetylcholin-mimetischen 2,4-dioxa-3-phosphadecalinen als irreversible Inhibitoren der Acetylcholinesterase eröffnete bisher übersehene Eigenschaften was die kinetischen Interaktionsmechanismen betrifft. Als eine Unterstützung für vergangene wie auch zukünftige Arbeiten in diesem Feld, beschreiben wir die Kinetik von acht Reaktionschemata, welche bei irreversiblen Enzymmodifikationen gefunden werden können und in Verbindung damit, zwei Mechanismen des reversiblen langsam-bindenden Inhibitionstypus. Für alle Mechanismen sind die relevanten kinetischen Gleichungen und die dazugehörigen graphischen Darstellungen gegeben, wie auch konkrete Beispiele, die ihren praktischen Gebrauch illustrieren. Da die irreversible Inhibition ein zeitabhängiges Phänomen darstellt, ist die kinetische Analyse durch das Anpassen der entsprechenden integrierten Geschwindigkeitsgleichung an eine Kurve des Reaktionsverlaufs durch nicht-lineare Regression stark vereinfacht. Diese erste Überprüfung ergibt kinetische Parameter, welche unabdingbare Werkzeuge für die Diagnose von kinetischen Mechanismen und die Berechung der Inhibitionskonstanten darstellen. Numerische Integration eines Sets von Differentialgleichungen ist zudem ein nützliches Werkzeug in kritischen Situationen, wie etwa bei unstabilen und/oder temporär irreversiblen Modifiern.

CHEMISTRY & BIODIVERSITY – Vol. 6 (2009) 261

3-Fluoro-2,4-dioxa-3-phosphadecalins as Inhibitors of Acetylcholinesterase. A Reappraisal of Kinetic Mechanisms and Diagnostic Methods

by **Antonio Baici***[a]), **Patricia Schenker**[a]), **Michael Wächter**[b]), and **Peter Rüedi***[b])

[a]) Biochemisches Institut der Universität Zürich, Winterthurerstrasse 190, CH-8057 Zürich
[b]) Organisch-chemisches Institut der Universität Zürich, Winterthurerstrasse 190, CH-8057 Zürich

A systematic survey of the acetylcholine-mimetic 2,4-dioxa-3-phosphadecalins as irreversible inhibitors of acetylcholinesterase revealed hitherto overlooked properties as far as the kinetic mechanisms of interaction are concerned. As a support to past and future work in this field, we describe the kinetics of eight reaction schemes that may be found in irreversible enzyme modification and compare them with two mechanism of reversible, slow-binding inhibition. The relevant kinetic equations and their associated graphical representations are given for all mechanisms, and concrete examples illustrate their practical use. Since irreversible inhibition is a time-dependent phenomenon, kinetic analysis is greatly facilitated by fitting the appropriate integrated rate equations to reaction-progress curves by nonlinear regression. This primary scrutiny provides kinetic parameters that are indispensable tools for diagnosing the kinetic mechanism and for calculating inhibition constants. Numerical integration of sets of differential equations is an additional useful investigation tool in critical situations, *e.g.*, when inhibitors are unstable and/or act as irreversible modifiers only temporarily.

1. Introduction. – In an earlier article [1], we have reported on the synthesis and characterization of the racemic *P(3)*-axially and *P(3)*-equatorially substituted *cis*- and *trans*-configured 2,4-dioxa-9-aza-, 2,4-dioxa-8-aza-, and 2,4-dioxa-7-aza-3-phosphabicyclo[4.4.0]decane 3-oxides (**I**–**III**, resp.; *Fig. 1*).

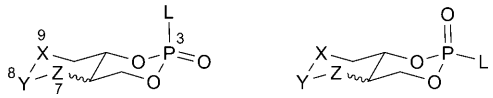

I X = NR, $\overset{\oplus}{N}R_2$, Y = Z = CH_2
II X = CH_2, Y = NR, $\overset{\oplus}{N}R_2$, Z = CH_2
III X = Y = CH_2, Z = NR, $\overset{\oplus}{N}R_2$
IV X = Y = Z = CH_2

L = electron-withdrawing group (F, Cl, Br, N_3, OR, NR_2, SR)

Fig. 1. *The 2,4-dioxa-3-phosphadecalins of types* **I**–**IV**

Being configuratively fixed and conformationally constrained P-analogues of acetylcholine (7-aza and 9-aza isomers) or γ-homoacetylcholine (8-aza isomers) (*Scheme 1*), these heterocycles represent acetylcholine mimetics, and they are

considered to be suitable for the investigation of molecular interactions with acetylcholinesterase (AChE), such as the recognition conformation of acetylcholine (ACh) and the stereochemistry of modification reactions[1]) of serine hydrolases. The related 3-fluoro- and 3-(2,4-dinitrophenoxy)-2,4-dioxa-3-phosphadecalins (type **IV**; *Fig. 1* and *Scheme 1*) have been successfully used as probes for the determination of the stereochemical course of the inhibition of δ-chymotrypsin [2] and the proof for the covalently phosphorylated enzyme [3] by ^{31}P-NMR spectroscopy. Enzyme-kinetic studies on the basis of a simplified approach according to *Scheme 2*[2]) had revealed that many of the prepared organophosphates of type **I**–**IV** (*Fig. 1*) are inhibitors of AChE [8–12] (*Scheme 2*), and preliminary results have been summarized [13]. However, during the past years, we have encountered significant inconsistencies concerning the reproducibility of the kinetic data of the phosphadecalins. Meanwhile, we have synthesized all the optically active (ee > 99%) organophosphates of type **I**–**IV** (L = F; *Scheme 1*), and the mentioned problems prompted us to start a thorough reinvestigation to find and apply an appropriate enzyme-kinetic system that is generally applicable to our compounds, providing reliable results.

2. Reappraisal of Kinetic Mechanisms and Diagnostic Methods. – 2.1. *General.* Although apparently a simple theme, the reaction of an enzyme with a substrate and/or an inhibitor to yield products or a modified enzyme species, is a highly complex cycle with multiple equilibria and accordingly complex rate parameters. As a matter of fact, there exists no analytical solution for the exact description of the general case [15][16]. Despite this inherent complexity, the kinetics of irreversible enzyme modification has been the subject of early studies, in which discontinuous methods were used for measuring residual enzyme activity after preincubating the enzyme of interest with modifiers [17–19]. More recently, continuous methods gained popularity because of the large information contained in progress curves obtained by monitoring the appearance of product following the hydrolysis of a chromogenic or fluorogenic substrate [20–23]. However, modifier instability and temporary inhibition constitute serious drawbacks for the practical use of many compounds, and represent a dilemma

---

[1]) The term 'modification' comprises all types of chemical interactions with enzymes and is not limited to inhibition reactions. Hence, it is more appropriate in the present re-evaluation that constitutes a general approach.

[2]) In most enzyme-kinetic studies on organophosphorus inhibitors of esterases, only the overall process is considered (*Scheme 2*). We relied on the basic procedure introduced by *Aldridge* [4] and later refined by *Main* and *Dauterman* [5], and *Hart* and *O'Brien* [6]. As our primary goal was the search for strong inhibitors with respect to their applicability for ^{31}P-NMR studies [2][3], we used these simplified, straightforward protocols that were applied at that time by several research groups (*e.g.*, [7]). For detailed experimental descriptions, representative calculations, and results, see [2][8–13]. Racemic 3-phosphadecalins with the following leaving groups have been prepared and tested (see *Scheme 1*): L = F [1][8][11–13] (types **I**–**IV**), Cl [1][8–10] (types **I**, **II**, and **IV**), Br, N_3 [8] (type **IV**), 4-nitrophenoxy [1][9][10] (types **I** and **II**), 2,4-dinitrophenoxy [1][8–10] (types **I**, **II**, and **IV**), OR [8][9] (types **I**, **II**, and **IV**), NR_2 [8] (type **IV**), and SR [8] (type **IV**). Remarkably, the *N,N*-dimethylammonium compounds ($R^1 = R^2 = Me$, L = Cl, 4-nitrophenoxy, 2,4-dinitrophenoxy) that constitute the most close mimetics were weak reversible inhibitors [10] (types **I** and **II**). For a compilation of the applied procedures, experimental conditions, cross-comparisons, and a critical discussion of the respective results, see [14].

Scheme 1. *The Basic Concept of the Organophosphorus Acetylcholine Mimetics*

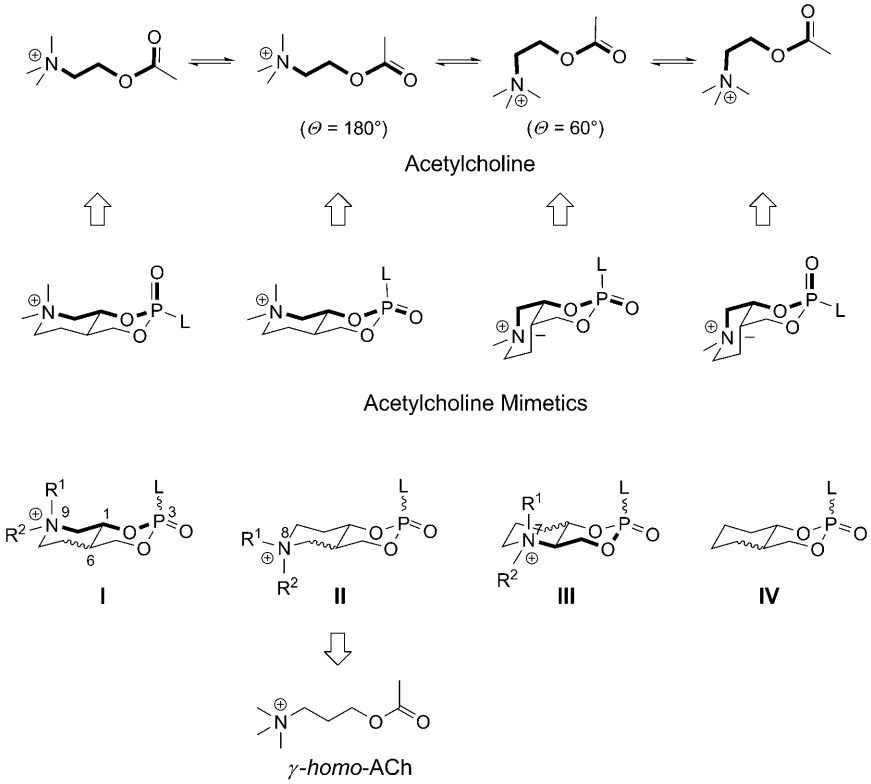

Each structural type, **I** – **IV**: *cis*-, *trans*-, axially, and equatorially P-substituted isomers
R = (*tert*-amines, free bases), H, Me, CH_2Ph; $R^1 = R^2$ or $R^1 \neq R^2$

Scheme 2. *The Simplified Kinetic Approach*

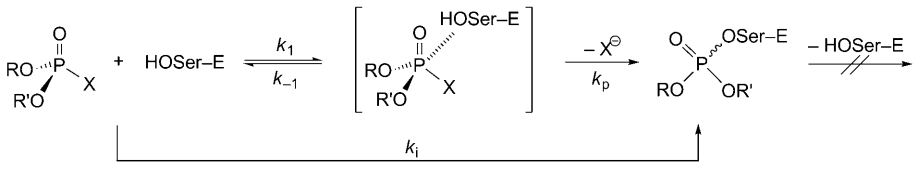

E = Enzyme: Serine hydrolase (acetylcholinesterase, chymotrypsin)
k_1,k_{-1}: Rate constants (also referred to as k_{on} and k_{off}, resp.)
$k_{-1}/k_1 = K_D$: Dissociation constant
k_p: Phosphorylation constant (also referred to as association constant, k_{ass})
$k_i = k_p/K_D$: Overall inhibitory potency ('bimolecular reaction constant')

for the kinetic interpretation of experimental data. In fact, when a continuous progress curve method for data acquisition is used, temporary inhibition and modifier instability can be mistaken for true reversibility of the reaction. In this article, we reconsider and discuss diagnostic criteria for distinguishing mechanisms of enzyme inhibition based on the analysis of progress curves. We will consider only inhibitors of the competitive type, *i.e.*, those that bind to free enzyme, not to the enzyme–substrate complex.

2.2. *Theoretical Considerations.* 2.2.1. *Reversible, Slow-Binding Inhibition*. For the purposes of the discussion that will follow on irreversible enzyme modification, it is useful to examine first the behavior of reversible, slow-acting inhibitors. *Scheme 3* shows two common mechanisms, **2A-R** and **1A-R**, of reversible, slow-binding inhibition. In mechanism **2A-R**, slow production of an enzyme–inhibitor complex ($E \cdot I$)[3]) is preceded by a rapid equilibration between E and I to form an adsorptive complex (EI). Mechanism **1A-R** is a degenerated form of mechanism **2A-R**, in which the concentration of EI is kinetically insignificant. Slow-binding, slow, tight-binding inhibition, and irreversible enzyme modification are time-dependent phenomena, *i.e.*, the final species do not form instantaneously, but in the range of minutes to hours. Apart from its physiological and pharmacological significance, this behavior offers a handy tool for measuring the kinetic parameters and for determining the respective inhibition mechanism. For such slow processes, the integrated rate equation, expressed as product concentration *vs.* time, takes the general form (*Eqn. 1* in *Table 1*). The term v_s represents the rate after attainment of the steady-state, and v_z (for zero time) corresponds to the rate at $t=0$. We purposely use the symbol v_z in the case of slow enzyme-modification reactions as a distinction from v_0, which is used to represent the rate in the absence of modifiers. Depending on the experimental conditions and mechanism, v_z can be greater or less than v_s, and it can be equal to or less than v_0. The first-order rate constant λ that describes the approach to the steady-state has a characteristic expression for each mechanism. The parameter d (displacement) is introduced in *Eqn. 1* (*Table 1*), and other forms of this equation to take into account product present before the start of the reaction or any spectroscopic signal proportional

Scheme 3. *Reversible, Slow-Binding Enzyme Inhibition.* These are the reversible counterparts (**R** indicates reversibility) of mechanisms **2A** (*Scheme 4*) and **1A** (*Scheme 5*), respectively.

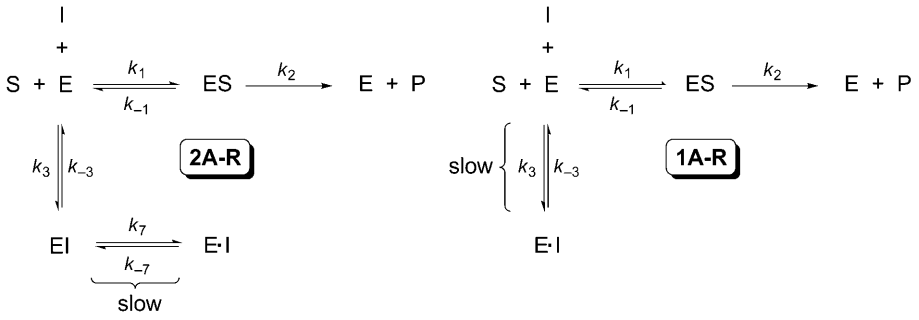

[3]) For a list of the symbols, see the *Appendix*.

Table 1. *Equations for Mechanisms* **2A-R** *and* **1A-R** (*cf. Scheme 3*). The expressions v_z and v_s apply to assays in which the reaction is started by adding the enzyme to a solution containing substrate and inhibitor.

Mechanism **2A-R**		Mechanism **1A-R**	
$[P] = v_s t + \frac{(v_z - v_s)(1 - e^{-\lambda t})}{\lambda} + d$	(1)	[P] as *Eqn. 1*	
$\lambda = k_{-7} + \frac{k_7[I]}{K_i\left(1 + \frac{[S]}{K_m}\right) + [I]}$ $K_i = \frac{k_{-3}}{k_3}$	(2)	$\lambda = k_{-3} + \frac{k_3[I]}{1 + \frac{[S]}{K_m}}$	(3)
$v_z = \frac{V[S]}{K_m\left(1 + \frac{[I]}{K_i}\right) + [S]}$	(4)	$v_z = v_0 = \frac{V[S]}{K_m + [S]}$	(5)
$v_s = \frac{V[S]}{K_m\left(1 + \frac{[I]}{K_i\left(\frac{k_{-7}}{k_7 + k_{-7}}\right)}\right) + [S]}$	(6)	$v_s = \frac{V[S]}{K_m\left(1 + \frac{[I]}{K_i}\right) + [S]}$	(7)

to it, which may be non-zero at the beginning of the reaction. *Eqn. 1* was originally derived for describing the concept of enzyme hysteresis [24], and was later used for characterizing slow-binding inhibition [25][26]. It applies to reactions in which enzymes respond slowly to a rapid change in the concentration of any modifier.

2.2.2. *Enzyme Inactivation; Irreversible Inhibition*[4]). In most cases, the kinetics of irreversible enzyme inhibition can be described by mechanism **2A** (*Scheme 4*). Mechanism **2A** consists in the formation of a fast-equilibrating adsorptive complex (EI), followed by a slow step in which the enzyme is irreversibly converted to a covalently modified enzyme (E–I), and thereby inactivated. The concentration of the reversible adsorptive intermediate may be kinetically insignificant, meaning that the dissociation constant $K_i = k_{-3}/k_3$ may be high with respect to the concentration of inhibitor used in the experiments; in this case, mechanism **2A** degenerates to mechanism **1A** (*Scheme 5*). While there is no reason for considering these two mechanisms as being chemically different (as is also for mechanisms **2A-R** and **1A-R**; *Scheme 3*), a distinction is made merely for practical purposes and mathematical convenience.

---

4) The term '*inactivation*' specifically indicates that a modifier covalently converts the enzyme to a species devoid of catalytic activity. The expression is preferentially used by the specialists in place of '*irreversible inhibition*' to distinguish reversibility and irreversibility at a glance. Although less accurate, the classical term '*irreversible inhibitor*', is retained in this article due to practical reasons.

Scheme 4. *Mechanisms for Two-Step Irreversible Enzyme Modification.* In the four variants of this mechanism (the number **2** denotes a two-step inhibition process), covalent enzyme modification (E–I) is preceded by the reversible formation of an adsorptive complex EI. Mechanism **2B** describes an unstable modifier, which undergoes spontaneous, nonenzymatic decomposition. Mechanism **2C** shows temporary inhibition, in which the inhibited enzyme decays to free enzyme, which is recycled, and an inert species I*. Mechanism **2D** illustrates the case of a chemically unstable modifier, which, at the same time, exerts temporary inhibition. I′ and I* do no longer affect enzyme activity and are withdrawn from the system.

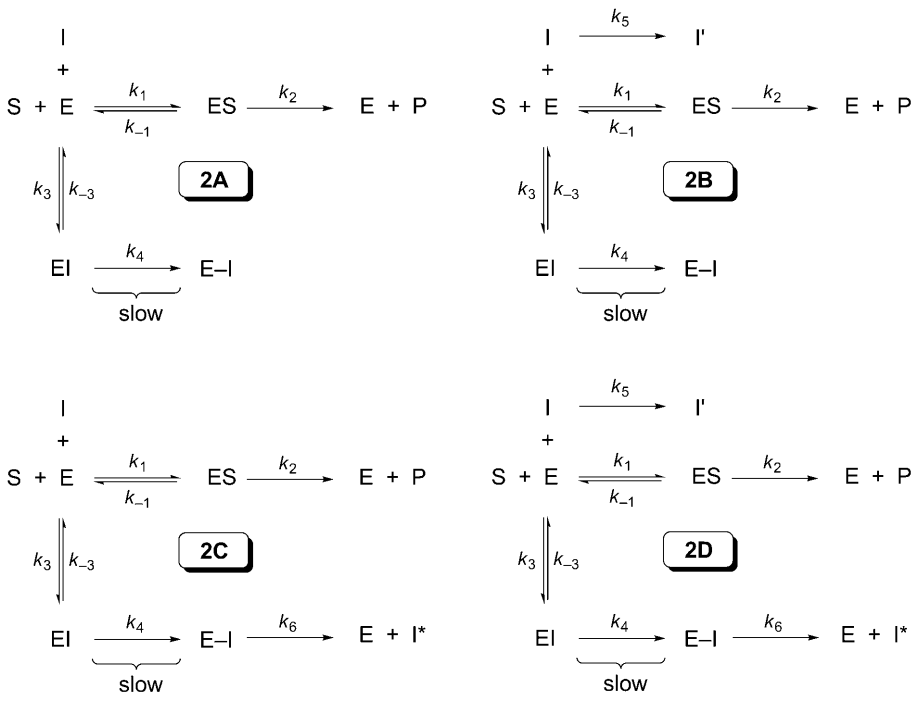

Often, molecules designed as irreversible modifiers of enzyme activity undergo spontaneous, nonenzymatic decomposition, usually by hydrolysis to an inert species (I′; mechanisms **2B** (*Scheme 4*) and **1B** (*Scheme 5*)). Other molecules act as temporary inhibitors, meaning that free enzyme and an enzymatically cleaved form of the modifier (I*) are generated (mechanisms **2C** (*Scheme 4*) and **1C** (*Scheme 5*)). In the worst case, a compound can be unstable and temporary as well (mechanisms **2D** (*Scheme 4*) and **1D** (*Scheme 5*)). In the same way as reversible inhibitors, enzyme inhibitors can be competitive, uncompetitive, or mixed-type. The latter is a blend of competitive and uncompetitive character [20]. In the case of genuinely irreversible processes, the steady-state rate v_s in *Eqn. 1* (*Table 1*) is set to zero, and the rate is expressed by *Eqn. 8* (*Table 2*).

For reasons of convenience, expressions which are found in the literature (*e.g.*, [16]) are summarized for reversible mechanisms (*Table 1*), for irreversible mechanisms in two steps (*Table 2*), and for irreversible mechanisms in one step (*Table 3*). To the best of our knowledge, analytical expressions have not been published for the temporary

Scheme 5. *Mechanisms for One-Step Irreversible Enzyme Modification.* In these mechanisms (the number **1** denotes one-step inhibition), enzyme and modifier form covalently inhibited E–I in a bimolecular reaction. The unstable inhibitor (**1B**), temporary inhibition (**1C**), and a blend of these two variants of the mechanism (**1D**) are analogous to the corresponding panels in *Scheme 4.*

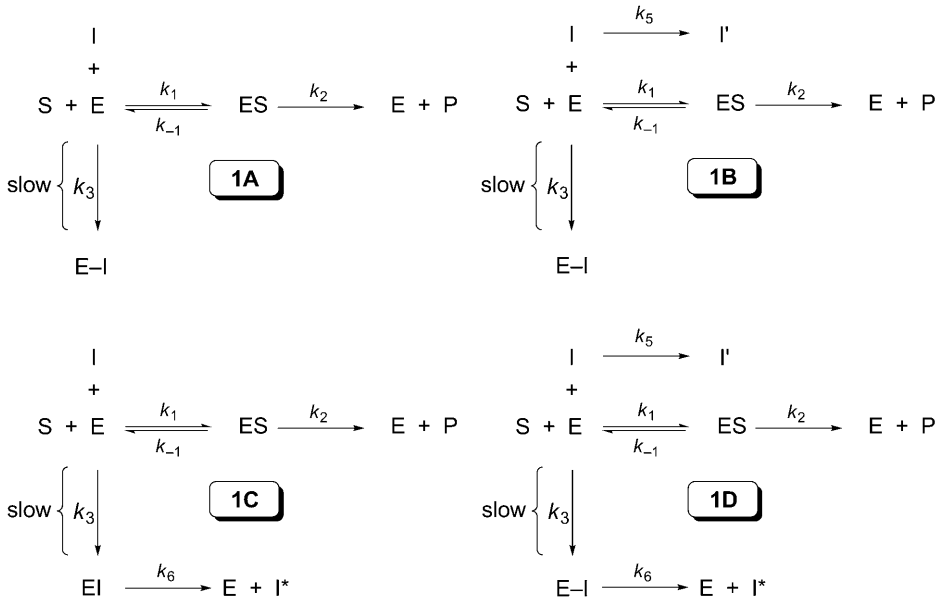

Table 2. *Equations for Mechanisms* **2A** *and* **2C** (*cf. Scheme 4*). The expressions v_z and v_∞ apply to assays in which the reaction is started by adding the enzyme to a solution containing substrate and inhibitor.

Mechanism **2A**		Mechanism **2C**	
$[P] = \frac{v_z}{\lambda}(1 - e^{-\lambda t}) + d$	(8)	$[P] = v_\infty t + \frac{v_z - v_\infty}{\lambda}(1 - e^{-\lambda t}) + d$	(9)
$\lambda = \frac{k_4[I]}{K_i\left(1 + \frac{[S]}{K_m}\right) + [I]}$	(10)	$\lambda = k_6 + \frac{k_4[I]}{K_i\left(1 + \frac{[S]}{K_m}\right) + [I]}$	(11)
$K_i = \frac{k_{-3}}{k_3}; \quad k_i = \frac{k_4}{K_i}$		$K_i = \frac{k_{-3}}{k_3}; \quad k_i = \frac{k_4}{K_i}$	
$v_z = \frac{V[S]}{K_m\left(1 + \frac{[I]}{K_i}\right) + [S]}$	(4)	v_z as for mechanism **2A**	
$v_\infty = 0$		$v_\infty = \frac{V[S]}{K_m\left(1 + \frac{[I]}{K_i}\left(1 + \frac{k_4}{k_6}\right)\right) + [S]}$	(12)

mechanisms **2C** (*Scheme 4* and *Table 2*) and **1C** (*Scheme 5* and *Table 3*) with explicit expressions in the style used in this article. The symbol v_∞ in these *Tables* is the counterpart of v_s in *Table 1*. The infinity subscript solely indicates that this rate is calculated at the end of the exponential phase, a condition mathematically obtained by setting $t = \infty$ in the expression $e^{-\lambda t}$.

Table 3. *Equations for Mechanisms* **1A** *and* **1C** (*cf. Scheme 5*). The expressions of v_z and v_∞ apply to assays in which the reaction is started by adding the enzyme to a solution containing substrate and inhibitor.

Mechanism **1A**		Mechanism **1C**	
$[P] = \frac{v_z}{\lambda}(1 - e^{-\lambda t}) + d$	(8)	$[P] = v_\infty t + \frac{v_z - v_\infty}{\lambda}(1 - e^{-\lambda t}) + d$	(9)
$\lambda = \frac{k_3[I]}{1 + \frac{[S]}{K_m}}$	(13)	$\lambda = k_6 + \frac{k_3[I]}{1 + \frac{[S]}{K_m}}$	(14)
$v_z = v_0 = \frac{V[S]}{K_m + [S]}$	(5)	v_z as for mechanism **1A**	
$v_\infty = 0$		$v_\infty = \frac{V[S]}{K_m\left(1 + \frac{k_3}{k_6}[I]\right) + [S]}$	(15)

A complete treatment of mechanisms **2B** (*Scheme 4*) and **1B** (*Scheme 5*) for unstable inhibitors was published by *Topham* in a comprehensive theoretical treatment that also included partial inhibitors as well as activators [23]. This valuable article, in which an impeccable mathematical language was used, may possibly be difficult for end users less familiar with this topic. Therefore, this treatment is summarized below for mechanism **1B** to show conceptual differences with integrated rate equations for systems **2A**, **2C**, **1A**, and **1C**, and to explain how to deal in practice with unstable modifiers. The complex integrated rate equation for mechanism **2B** will not be treated here because its solution is only possible under special circumstances [23]. In the case of either mechanism **2D** or **1D**, it is questionable whether the compounds under investigation should still be called inhibitors. Although integrated rate equations for these mechanisms can be derived, their concrete application to real cases is mathematically laborious, and the results are mere of academic interest.

2.2.3. *Discrimination of Mechanisms.* To provide a convenient reference for diagnostic purposes, progress curves for the mechanisms shown in this article were simulated by numerical integration of the appropriate sets of differential equations. All calculated and experimental curves shown below refer to reactions started by adding enzyme to a solution containing substrate and inhibitor. The differential diagnosis of the mechanisms is accomplished by inspection of the shapes of the progress curves, and by analysis of the dependencies of λ and velocities on inhibitor concentration.

Progress curves for mechanisms **2A-R** and **1A-R**, as well as the dependencies of the parameters λ, v_z, and v_s on [I], are shown in *Fig. 2*. Distinguishing mechanism **2A-R**

from its counterpart **1A-R** is straightforward, since the dependency of λ on [I] is hyperbolic for mechanism **2A-R** and linear for mechanism **1A-R**. Furthermore, v_z decreases hyperbolically with [I], or is independent of [I] for mechanisms **2A-R** and **1A-R**, respectively. Individual kinetic constants can be calculated from the plots of λ *vs.* [I], as shown in *Fig. 2*. From the fits of v_z and v_s, K_i, as well as the overall inhibition constant $(K_i k_{-7})/(k_7 + k_{-7})$, for mechanism **2A-R** can be calculated and used to check the internal consistency with results from the λ *vs.* [I] plot.

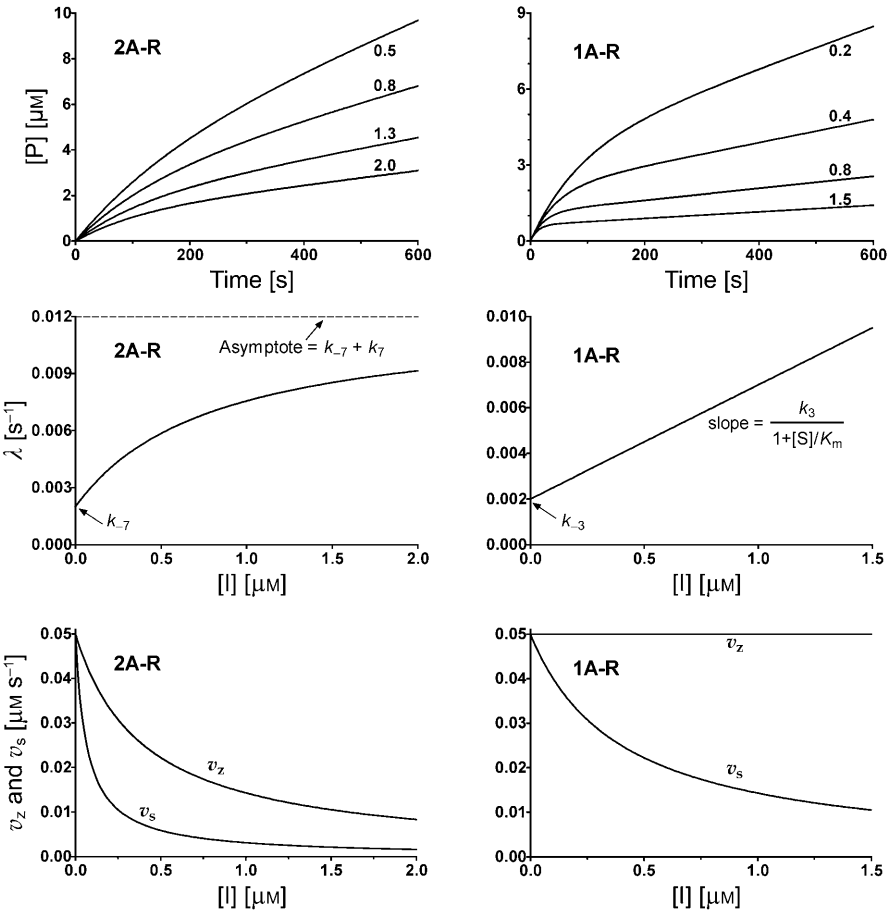

Fig. 2. *Progress curves and diagnostic parameters for mechanisms* **2A-R** *and* **1A-R** (*cf. Scheme 3*). Numbers next to the curves in the top panels indicate inhibitor concentrations (μM). Curves were generated with the following parameters common to both mechanisms: $k_2 = 20\ s^{-1}$, $[E]_t = 5$ nM, $[S] = K_m = 100$ μM; for mechanism **2A-R**: $k_3 = 0.5\ \mu M^{-1}\ s^{-1}$, $k_{-3} = 0.2\ s^{-1}$, $k_7 = 0.01\ s^{-1}$, $k_{-7} = 0.002\ s^{-1}$; for mechanism **1A-R**: $k_3 = 0.1\ \mu M^{-1}\ s^{-1}$, $k_{-3} = 0.002\ s^{-1}$.

Mechanism **2A** for irreversible inhibition can unmistakably be distinguished from its reversible counterpart **2A-R**, if the progress curves can be measured for a sufficiently long time to allow complete inhibition. The irreversible mechanism is

characterized by an end value of progress curves parallel to the time axis, indicating that there is no steady-state with a positive slope (*Fig. 3*). Also, the ordinate intercept of λ *vs.* [I] is zero in this case, while it is non-zero for mechanism **2A-R**. A distinction of mechanism **2C** from **2A-R** is impossible, when only progress curves and the dependencies of parameters on [I] are considered. In fact, the positive slope described by v_∞ can be mistaken for the steady-state of a reversible system. Instead, this slope is determined by free enzyme that is recycled in the reaction following the breakdown of E–I. However, a reliable discrimination is possible by preincubating enzyme and inhibitor, and starting the reaction by adding substrate: for a reversible mechanism, the steady-state slope will be independent of the preincubation time, while, for mechanism **2C**, the slope will increase by increasing the preincubation time. This corresponds to the decreasing inhibitor concentration available to the enzyme.

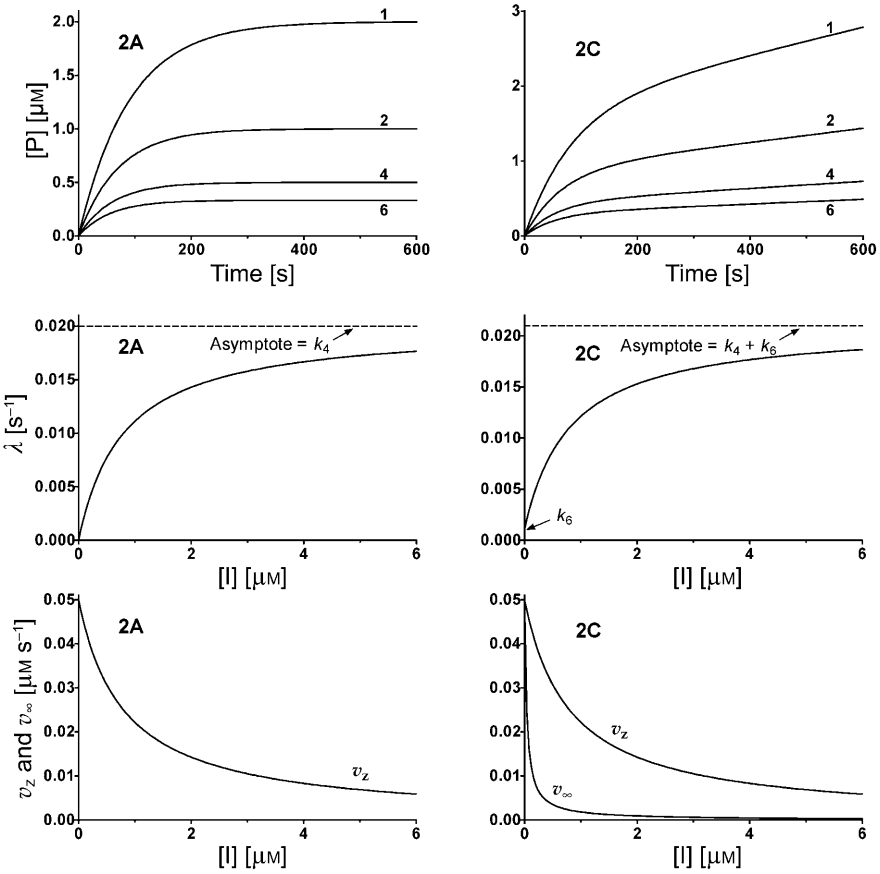

Fig. 3. *Progress curves and diagnostic parameters for mechanisms* **2A** *and* **2C** (*Scheme 4*). Numbers next to the curves in the top panels indicate inhibitor concentrations (μM). Curves were generated with the following parameters common to both mechanisms: $k_2 = 20\ s^{-1}$, $[E]_t = 5$ nM, $[S] = K_m = 100$ μM, $k_3 = 0.5\ \mu M^{-1}\ s^{-1}$, $k_{-3} = 0.2\ s^{-1}$, $k_4 = 0.02\ s^{-1}$; for mechanism **2C**: $k_6 = 0.001\ s^{-1}$.

Progress curves and parameter dependencies for mechanisms **1A** and **1C** are shown in *Fig. 4*. Diagnostic features of system **1A** are the reaction profiles ending up with slope zero and the linear dependency of λ on [I] with zero intercept on the ordinate. The non-zero intersection on the ordinate for mechanism **1C**, which corresponds to k_6, may not be accessible to unambiguous measurement, and its successful determination depends on data quality. A statistical test to evaluate a significant non-zero intercept will be very useful in this case. Also for mechanism **1C**, a definite distinction from mechanism **1A-R** is not possible from inspection of the graphics, but the preincubation method discussed above is reliable again.

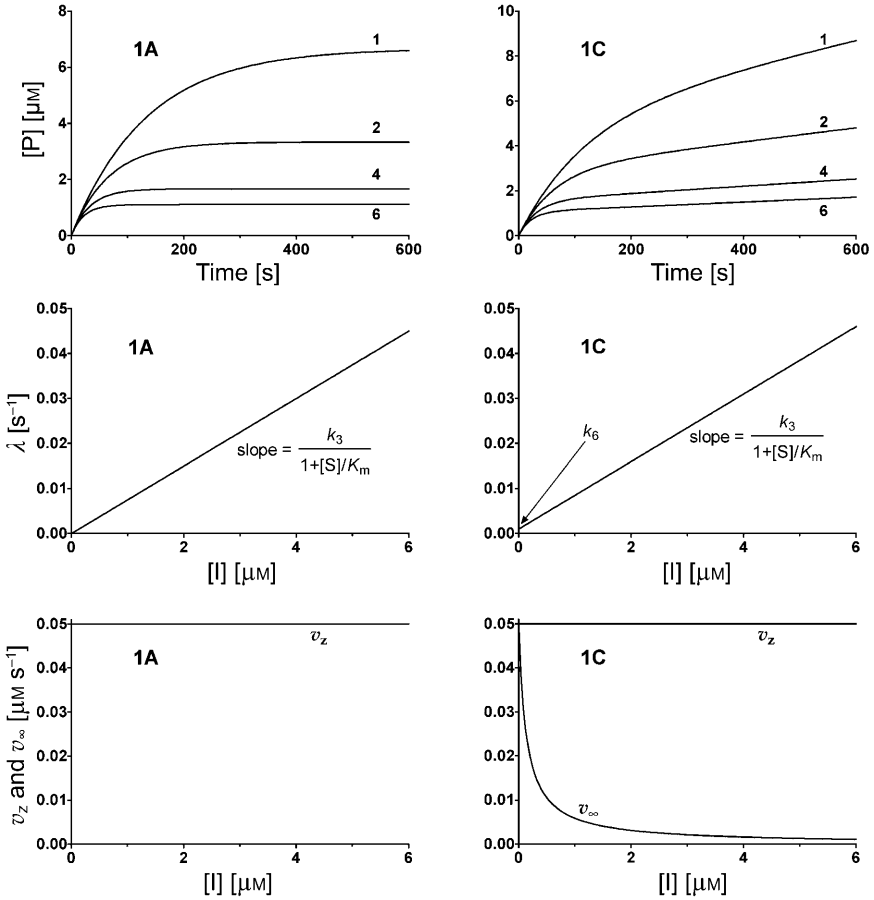

Fig. 4. *Progress curves and diagnostic parameters for mechanisms* **1A** *and* **1C** (*Scheme 5*). Numbers next to the curves in the top panels indicate inhibitor concentrations (μM). Curves were generated with the following parameters common to both mechanisms: $k_2 = 20\ s^{-1}$, $[E]_t = 5$ nM, $[S] = K_m = 100$ μM, $k_3 = 0.015\ \mu M^{-1}\ s^{-1}$; for mechanism **1C**: $k_6 = 0.001\ s^{-1}$.

2.2.4. *Inhibition by an Unstable Compound, Mechanism* **1B**. An analytical expression of λ does not exist for this model, because the concentration of the

inhibitor varies with time. However, an analytical expression for the integrated rate equation can be obtained upon *Maclaurin* series expansion [23]:

$$[\mathrm{P}] = \frac{v_z}{k_5} e^{-\left\{\frac{k_3 K_m [\mathrm{I}]_t}{k_5 (K_m + [\mathrm{S}])}\right\}} \left\{ k_5 t + \sum_{i=1}^{\infty} \left\{ \frac{k_3 K_m [\mathrm{I}]_t}{k_5 (K_m + [\mathrm{S}])} \right\}^i \frac{\left[1 - (e^{-k_5 t})^i\right]}{i \cdot i!} \right\} \qquad (16)$$

In *Eqn. 16*, $v_z = v_0$ (the rate in the absence of modifier), K_m can be evaluated from measurements performed with substrate alone, and $[\mathrm{I}]_t$ is the total inhibitor concentration introduced initially. Therefore, the rate constants k_3 and k_5 can be obtained by fitting this equation to progress curves by nonlinear regression. How many terms, denoted by the index *i* in *Eqn. 16*, should be used in the regression analysis depends on the value of k_5: a small value will require more terms than a large one. For instance, with $k_5 = 0.005\ \mathrm{s}^{-1}$, the third term is sufficient to fit a progress curve, while with $k_5 = 0.001\ \mathrm{s}^{-1}$, *Maclaurin* expansion till the 10th term is necessary. In turn, the last option can be used routinely.

Simulated progress curves for an unstable inhibitor obeying mechanism **1B** are shown in *Fig. 5* (*left panel*). These do not consist of a single exponential followed by a straight line parallel to the time axis as shown in the curve labeled $k_5 = 0$, which corresponds to a stable inhibitor. Instead, an increase of k_5 means an increase of the rate of degradation of the inhibitor to the inert species I′, as shown in *Fig. 5* (*right panel*). Thus, progress curves are similar to those obtained in the presence of a reversible inhibitor, and, for high values of k_5, I is degraded rapidly causing the progress curve to be linear. The straight line following the exponential phases in *Fig. 5* (*e.g.*, in the curve with $k_5 = 0.01\ \mathrm{s}^{-1}$) does not correspond to a steady-state but reflects the continuous decrease in the concentration of available inhibitor according to *Eqn. 16*. Attempting to fit either *Eqns. 8* or *9* to data obtained with unstable compounds results in inconsistent fittings with statistically meaningless results. This is due to the fact that

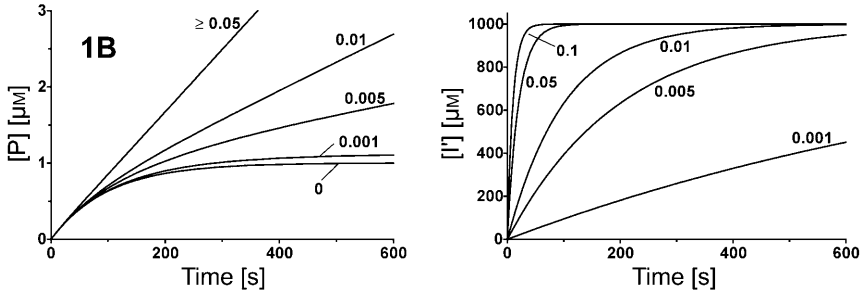

Fig. 5. *Progress curves for an unstable inhibitor, mechanism* **1B** (*Scheme 5*). *Left:* Progress curves. *Right:* concentration of the chemically inert inhibitor, I′. Curves were simulated by numerical integration with *Matlab–Simulink* software (www.mathworks.com) using the following parameters: $k_2 = 0.2\ \mathrm{s}^{-1}$, $k_3 = 10\ \mathrm{M}^{-1}\ \mathrm{s}^{-1}$, $K_m = 1$ mM, [S] = 1 mM, $[\mathrm{E}]_t = 100$ nM, $[\mathrm{I}]_t = 1$ mM, k_5 from 0 to $0.1\ \mathrm{s}^{-1}$ as shown (numbers next to the curves). For $k_5 = 0$, there is no production of I′, and the progress curve corresponds to that of mechanism **1A** (*Fig. 4* and *Scheme 5*).

the condition of constant [I] during the measurement time, necessary for integrating the rate equation, is violated. This represents a valuable diagnostic tool for differentiating **1B** from other mechanisms. Progress curves for an unstable inhibitor obeying mechanism **1B** are very similar to those of mechanisms **1A-R** and **1C**. Discrimination is possible by preincubating the inhibitor in assay buffer for 2–3 periods of time. Then, substrate is added followed by enzyme: for both mechanisms **1A-R** and **1C**, the reaction profiles will be independent on preincubation time, but rate will increase with the preincubation time in the case of mechanism **1B**, reflecting disappearance of inhibitor through hydrolysis. If all inhibitor undergoes hydrolysis during preincubation the rate returns to control values (slope of the curve as shown for $k_5 \geq 0.05\ s^{-1}$ in *Fig. 5* (*left panel*). For very low values of k_5, the instability of the inhibitor may not be appreciable in a dynamic assay over a relatively short time (*e.g.*, curve for $k_5 = 0.001\ s^{-1}$).

To summarize, the concept highlights the importance of progress curves as a means for discriminating among mechanisms and for calculating the second-order inhibition constants. The progress-curve method offers many practical and statistical advantages over previous methods [4–7]. After choosing an appropriate substrate that allows continuous detection of reaction progress, and knowing the kinetic parameters V and K_m for this substrate, data collection consists in continuously recording the appearance of product at a fixed substrate and enzyme concentration for several concentrations of the inhibitor. The competitive or other character of the inhibitor can be ascertained by collecting data at various substrate concentrations. *Eqns. 8* or *9* are fitted to each experimental curve by nonlinear regression to calculate λ, v_z, and v_∞ as appropriate, which are then plotted against the inhibitor concentration for establishing the mechanism and calculating the relevant kinetic parameters. A hyperbola or a straight line passing through the origin of the axes is diagnostic for mechanisms **2A** and **1A**, respectively. As a caveat, irreversible enzyme inhibition and reversible slow, tight-binding inhibition can hardly be distinguished from one another by this method. However, in slow, tight-binding inhibition saturation will occur at total inhibitor concentrations of the same order of magnitude as the total enzyme concentration $[E]_t$ used in the assays, while in irreversible inhibition this will usually occur at $[I]_t \gg [E]_t$.

3. Representative Examples. – The application of the concept presented above furnished reproducible and consistent kinetic data of our 2,4-dioxa-3-phosphadecalins of the types **I**–**IV** (*Fig. 1* and *Scheme 1*). In the following, selected representative results that clearly illustrate the convenient practice of the protocol are presented (structures in *Fig. 6*, and kinetic constants in *Table 4*). The inhibition experiments of AchE with the organophosphorus compounds were performed by means of the *Ellman* assay [27] at pH 7.00 ± 0.02 in the presence of substrate (acetylthiocholine) and the chromogenic '5,5′-dithiobis(2-nitrobenzoic acid-3,3′-6)'. The progress curves were monitored at 410–414 nm (yellow dianion of 5-thio-2-nitrobenzoic acid, $\lambda_{max} =$ 412 nm).

The comparison between **DFP** and a fully irreversible inhibitor, (−)-*trans*-**IVax**, is shown in *Fig. 7*. There are no diagnostic problems for these two inhibitors, for which the linear dependence of λ upon [I], with the intersection point on the ordinate statistically indistinguishable from zero, and the independence of v_z upon [I] clearly point to

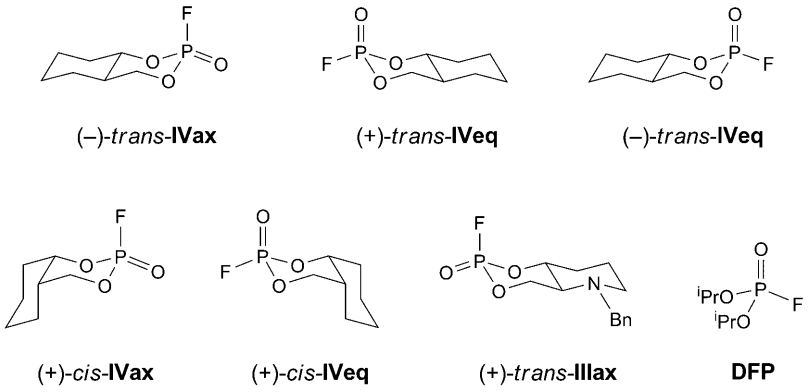

Fig. 6. *The representative 2,4-dioxa-3-fluoro-3-phosphadecalins* (DFP as reference)

Table 4. *Kinetic Data of the Inhibition of AChE with Selected 3-Fluoro-2,4-dioxa-3-phosphadecalins and Assigned Mechanisms,* **DFP** ((i-PrO)$_2$POF) *as Reference.* Numbers indicate best-fit parameters ± standard errors from nonlinear regression, with the exception of (+)-*cis*-**IVeq**, for which the parameters represent values optimized by numerical integration of a set of differential equations corresponding to mechanism **1D** obtained with *Matlab–Simulink* software (www.mathworks.com).

Compound	Kinetic Parameters	Mechanism
(−)-*trans*-**IVax**	$k_3 = 968 \pm 43$ м$^{-1}$ s^{-1}	**1A**
(+)-*trans*-**IVeq**	$K_i = 20.8 \pm 1.3$ μм	**2C**
	$k_4 = 0.037 \pm 0.004$ s^{-1}	
	$k_i = 1280 \pm 150$ м$^{-1}$ s^{-1}	
	$k_6 = 0.014 \pm 0.002$ s^{-1}	
(−)-*trans*-**IVeq**	$K_i = 463 \pm 47$ μм	**2C**
	$k_4 = 0.017 \pm 0.004$ s^{-1}	
	$k_i = 37 \pm 9$ м$^{-1}$ s^{-1}	
	$k_6 = 0.0013 \pm 0.0007$ s^{-1}	
(+)-*cis*-**IVax**	$K_i = 85 \pm 3$ μм	**2A**
	$k_4 = 0.026 \pm 0.001$ s^{-1}	
	$k_i = 306 \pm 16$ м$^{-1}$ s^{-1}	
(+)-*cis*-**IVeq**	$k_3 = 2260$ м$^{-1}$ s^{-1}	**1D**
	$k_5 = 0.026$ s^{-1}	
	$k_6 = 0.00004$ s^{-1}	
(+)-*trans*-**IIIax**	$k_3 = 39 \pm 3$ м$^{-1}$ s^{-1}	**1C**
	$k_6 = 0.00084 \pm 0.00024$ s^{-1}	
DFP	$k_3 = 181 \pm 28$ м$^{-1}$ s^{-1}	**1A**

mechanism **1A** for both of them. With a 5.3 times larger second-order inhibition constant k_3, (−)-*trans*-**IVax** is a significantly better inhibitor than **DFP**.

In *Fig. 8*, two examples of irreversible inhibition occurring in two steps are shown. The progress curves with asymptotes running parallel to the time axis, and the hyperbolic dependence of v_z and λ upon [I], with the trace of λ passing through the origin of the axes, leave no doubts about mechanism **2A** for (+)-*cis*-**IVax**. Instead, (+)-

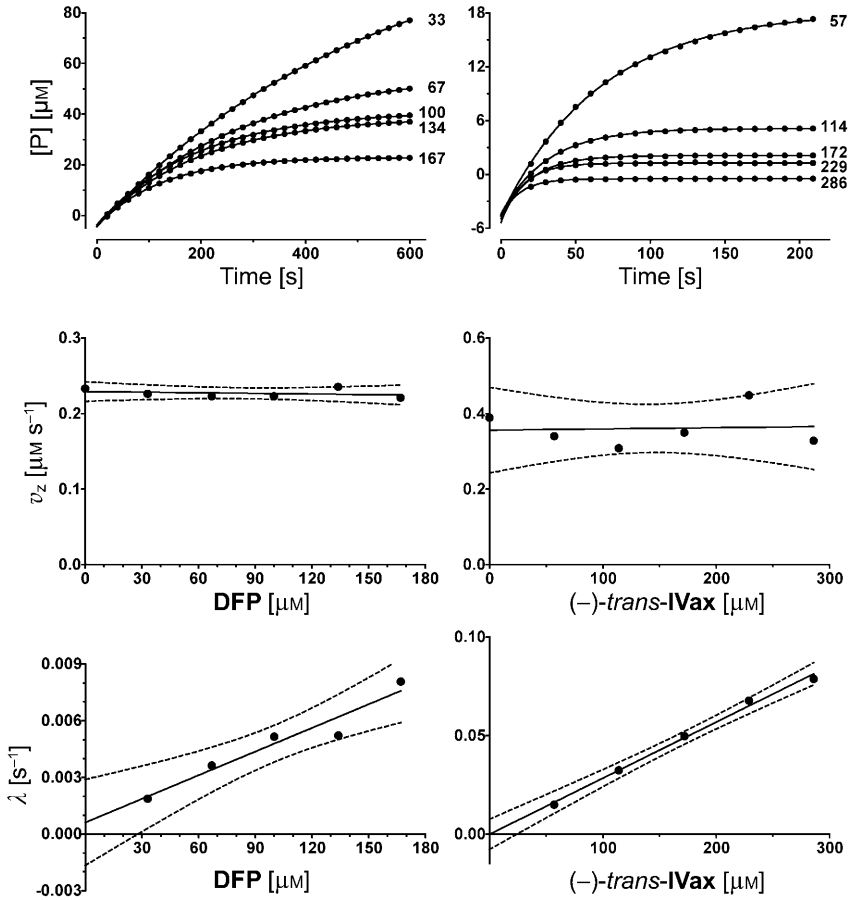

Fig. 7. *Inhibition of AChE by* **DFP** (*left panels*) *and (–)*-trans-**IVax** (*right panels*). In the two *top panels*, only every 20th experimental point is shown for clarity, and solid lines are best-fits according to *Eqn. 8*. Dashed lines around experimental points in the central and bottom panels indicate 95% confidence intervals. Both inhibitors are described by mechanism **1A** with equations shown in *Table 3*, reactions paths in *Scheme 5*, and theoretical curves in *Fig. 4*.

trans-**IVeq** is characterized by progress curves that would suggest a reversible, slow-binding mechanism. However, the chemical nature of the inhibitor and independent evidence from ^{31}P-NMR measurements indicate temporary irreversible inhibition following formation of E–I in a two-step process. E–I is degraded to free enzyme and an inert inhibitor derivative with rate constant $k_6 = 0.014$ s^{-1}, which corresponds to a half-life of 49.5 s, *i.e.*, the covalent E–I compound is almost completely degraded in *ca.* 6 min (7 times the half-life).

The examples in *Fig. 9* illustrate two critical cases that occur when an irreversible inhibitor binds slowly to the enzyme (second-order inhibition constants around 40 M^{-1} s^{-1} in these two examples) and is temporary as well. Since E–I formation is quite a slow process, progress curves can only be measured for a limited time, *i.e.*, until no more

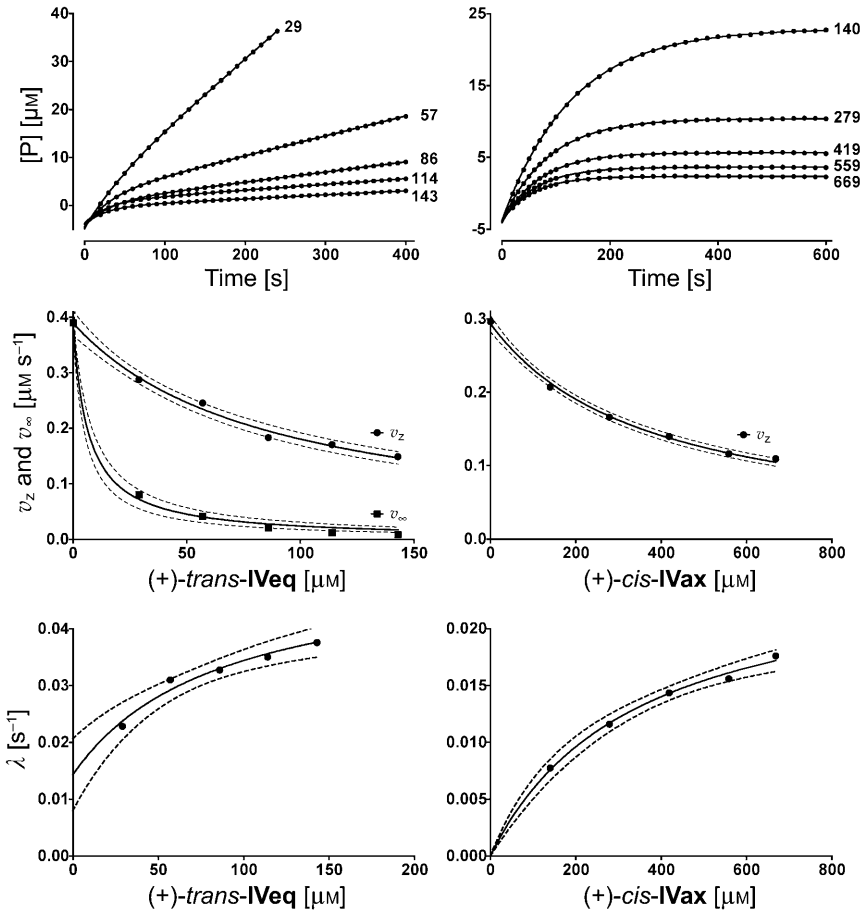

Fig. 8. *Inhibition of AChE by (+)*-trans-**IVeq** (*left panels*) *and (+)*-cis-**IVax** (*right panels*). In the two *top panels*, only every 20th experimental point is shown for clarity, and solid lines are best-fits according to *Eqn. 9* (*left*) or *Eqn. 8* (*right*). Dashed lines around experimental points in the central and bottom panels indicate 95% confidence intervals. (+)-*trans*-**IVeq** is described by mechanism **2C** and (+)-*cis*-**IVax** by mechanism **2A** (*Eqns.* in *Table 2*, reaction paths in *Scheme 4*, and theoretical curves in *Fig. 3*).

than 10–15% of the substrate employed in the assay is used up. As shown, the curves obtained are not very useful because they are incomplete. Of course, reactions can be monitored for longer times, but, in this case, we are faced with two problems. First, excessive substrate consumption violates the necessary condition that the substrate concentration does not appreciably change during the measuring time: the resulting curvature of the progress curves is added to that of irreversible, temporary inhibition. Second, absorbance readings increase excessively causing deviations from the *Lambert–Beer* law. Therefore, a reliable interpretation would be difficult or impossible. Such inhibitors have, of course, little practical interests, but, nevertheless, their kinetics can be interpreted at least qualitatively. Thus, the diagnostic plots for (+)-

trans-**IIIax** (*right panels* in *Fig. 9*) suggest **1C** as the most probable mechanism, although v_z is not perfectly independent of [I]. For (−)-*trans*-**IVeq**, the *left panels* in *Fig. 9* show fits with mechanism **2C** simply because statistical criteria from nonlinear regression of the progress curves suggest a better fit with mechanism **2C** rather than **1C**. With a little portion of common sense, one must, however, admit that there is not much difference between the left and right panels in *Fig. 9*, and that (−)-*trans*-**IVeq** can also be described by mechanism **1C**. Considering mechanism **1C**, the calculated second-order inhibition constant is $k_3 = 30\ \text{M}^{-1}\ \text{s}^{-1}$, and with mechanism **2C**, this is $k_i = 37\ \text{M}^{-1}\ \text{s}^{-1}$, thus a minimal discrepancy considering the technical complexity. This last example shows the limits of the present analysis in decision making, but, fortunately, this is a feature confined to molecules of scarce practical interest.

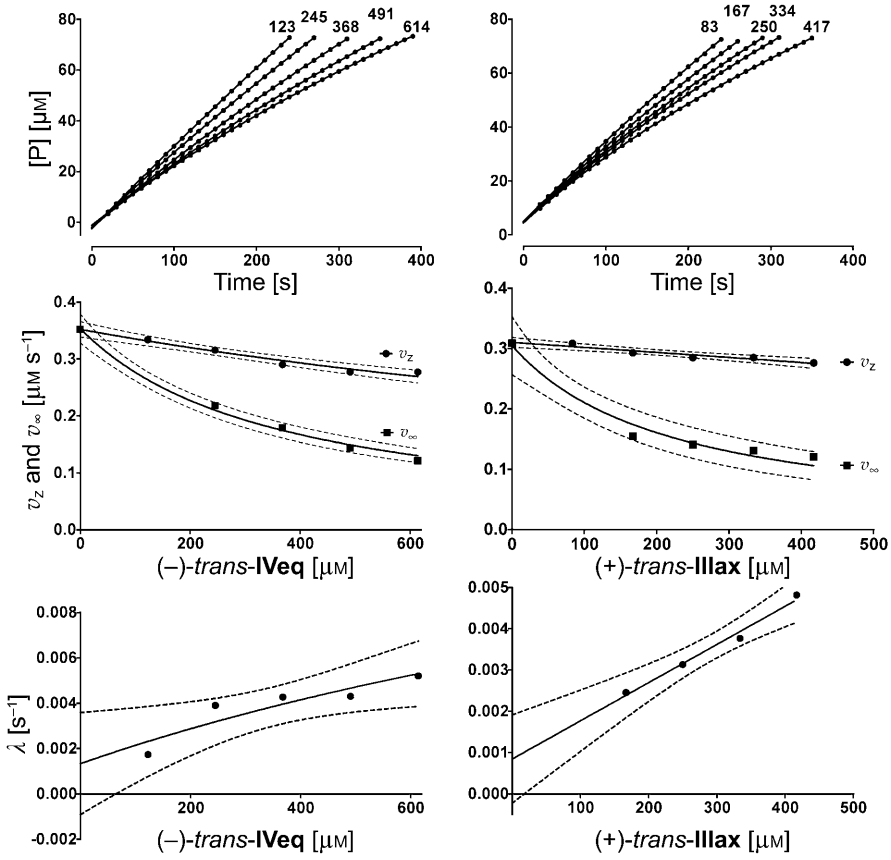

Fig. 9. *Inhibition of AChE by (−)*-trans-**IVeq** (*left panels*) *and (+)*-trans-**IIIax** (*right panels*). In the two *top panels*, only every 20th experimental point is shown for clarity, and solid lines are best-fits according to *Eqn. 9*. Dashed lines around experimental points in the central and bottom panels indicate 95% confidence intervals. (−)-*trans*-**IVeq** is described by mechanism **2C** (*Eqns.* in *Table 2*, reaction paths in *Scheme 4*, and theoretical curves in *Fig. 3*) and (+)-*trans*-**IIIax** by mechanism **1C** (*Eqns.* in *Table 3*, reaction paths in *Scheme 5*, and theoretical curves in *Fig. 4*).

Finally, in *Fig. 10*, a puzzling case is analyzed for compound (+)-*cis*-**IVeq**. Progress curves (*top left panel*) may suggest complete irreversible inhibition according to mechanism **1A**. However, analysis of residuals reveals slight but significantly positive slopes following the exponential phase, which point to either a reversible (**1A-R**) or an irreversible temporary mechanism (**1C**). Another feature is the inconsistent dependency of λ upon inhibitor concentration after primary analysis with *Eqns. 1*, *8*, or *9*. This is now the point where even the best enzyme-kinetic expertise needs help from chemistry. The *right panels* in *Fig. 10* show the instability of (+)-*cis*-**IVeq** as analyzed by ^{31}P-NMR spectroscopy. The signal corresponding to the original molecule ($\delta = -13.34$ ppm) progressively disappears (*lower right panel*), because the molecule is transformed in parallel to the *P(3)*-epimer ((−)-*cis*-**IVax**, $\delta = -12.95$ ppm) and to a hydrolysis product ($\delta = -1.98$ ppm)[5]). Thus, this is an example of unstable inhibitor, and the best-fit curves to experimental data in the *top left panel* of *Fig. 10* were obtained by fitting *Eqn. 16* using a *Maclaurin* expansion to the 10th term under the provisional assumption of mechanism **1B**. However, this equation is valid when the unstable inhibitor is transformed into inert molecules only, whereas the *P(3)*-epimer of (+)-*cis*-**IVeq** also acts as an inhibitor albeit at a much lower rate [14]. Furthermore, we have

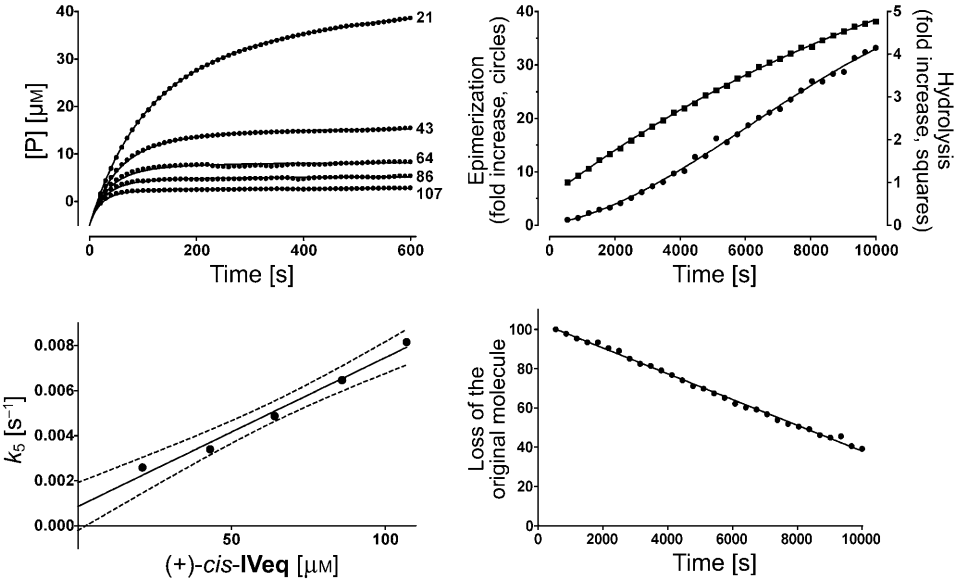

Fig. 10. *Inhibition of AChE by (+)*-cis-**IVeq**. In the top left panel, only every 20th experimental point is shown for clarity, and solid lines are best-fits according to *Eqn. 16*. The decay constant k_5 is not actually constant, but depends on inhibitor concentration (see text for interpretation). The *lower right panel* shows the instability of the molecule as measured by the disappearance with time of its ^{31}P-NMR signal (δ −13.34 ppm), and the *top right panel* the appearance of the epimer (δ −12.95 ppm), as well as of a hydrolysis product, also monitored as ^{31}P-NMR signal (δ −1.98 ppm). The mechanism for this inhibitor is **1D** (*Scheme 5*).

[5]) For further details, see *Exper. Part* and [14].

evidence that E–I also slowly decays, liberating free enzyme and generating another degradation product of the inhibitor. These factors explain why the instability constant k_5 obtained by nonlinear regression is not really constant, but varies with total inhibitor concentration (*Fig. 10*, *lower left panel*) if analysis is performed with *Eqn. 16*, which holds for mechanism **1B**, while the true mechanism is **1D**. Since the contribution of the epimer to total inhibition during the measuring time was found to be minimal, a satisfactory solution of this puzzle comes finally from a combination of nonlinear regression and numerical integration analysis giving the kinetic constants shown in *Table 4*.

4. Conclusions. – The compounds are remarkable irreversible inhibitors (inactivators[4])) of AChE, and several of them are significantly stronger than diisopropyl fluorophosphate (**DFP**) that is generally used as a very potent standard reference (*Table 4*). Moreover, the stereoselectivity of the inhibition reaction is demonstrated for the enantiomers (+)- and (−)-*trans*-**IVeq**. However, since this report places main emphasis on the methodological aspects, we confine ourselves to just presenting distinct examples that demonstrate the easy applicability of our approach. Meanwhile, we have prepared the complete set of the optically active (ee > 99%) 2,4-dioxa-3-fluoro-3-phosphadecalins (type **IV**) [14], and the N-heterocyclic 9-aza- (type **I**) [28], 8-aza- (type **II**) [29], and 7-aza-congeners (type **III**) [30]. Full kinetic data with detailed analyses and interpretations of the inhibition behavior will be presented in following reports [14][28–30].

The authors are indebted to the *Swiss National Science Foundation* and the *Albert-Böni Foundation* (*A. B.*) for their generous financial support.

Experimental Part

1. *General.* The preparation and the full characterization of the 3-substituted 3-phosphadecalins of the types **I**–**IV** are described in [1][14][28–30]. Acetylcholinesterase (AChE) from *Electrophorus electricus* (electric eel), *Sigma C-2888*, type *V-S*, lyophilized powder ≥1000 units/mg protein (lots 39H7402, 103K7651, 129F8080, 228F8040); acetylthiocholine (ATC), *Fluka 01480 BioChemika*; 5,5′-dithiobis(2-nitrobenzoic acid-3,3′-6) (DTNB; *Ellman*'s reagent [27]), *Fluka 43760 BioChemika*; diisopropyl fluorophosphate (DFP), *Fluka 38399*, *pract.*; H_2O, *Fluka 95304* (HPLC quality); MeCN, *Fluka 00695 puriss.* abs. (over molecular sieves); NaCl, *Fluka 71378 BioChemika MicroSelect*; $NaH_2PO_4 \cdot H_2O$, *Merck 6346 p.a.*; $Na_2HPO_4 \cdot 2\,H_2O$, *Merck 6580 p.a.*; *Pluronic F-68*, *Sigma P-1300* (lot 88H1000); *Tris* buffer, *Fluka 93349 BioChemika MicroSelect*. Volumes ≤1 ml were measured accurately with microliter pipettes *Socorex S+* (100–1000 µl) and *Socorex Autoclavable Calibra 822* (10–100 µl, 1–10 µl), and volumes <1 ml by diluting in volumetric flasks. pH Determinations: *Knick Portamess 762 Calimatic*, electrode: *Mettler InLab 423 S7*; calibration: *Mettler* standard buffers pH 4.01 and pH 7.00; electrolyte: *Mettler* standard, 3M KCl sat. with AgCl; measurements at 22°, accuracy ± 0.02 pH units. Enzyme kinetic progress curves and photometric titration of the active sites of AChE: *Hewlett-Packard 8452A* diode array spectrophotometer with *HP 89532A* UV/VIS Software (Rev. A.00.00). Curve-fitting and data analyses were performed with OriginPro 7.5G SR3 v.7.5853 (www.originlab.com) and *GraphPad Prism* version 5.00 for Windows, *GraphPad* Software, San Diego California USA (www.graphpad.com).

2. *Enzyme Kinetics.* 2.1. *Phosphate Buffer pH 7.00.* Soln. *A:* $Na_2HPO_4 \cdot 2\,H_2O$ (4.45 g), NaCl (1.46 g), and *Pluronic F-68* (25 mg) were dissolved in H_2O (250 ml). Soln. *B:* $NaH_2PO_4 \cdot H_2O$ (6.90 g), NaCl (2.92 g), and *Pluronic F-68* (25 mg) were dissolved in H_2O (500 ml). The solns. were adjusted to pH 7.00 ± 0.02 by mixing. Prior to use, the buffer was filtered (*TRP* syringe filter, max. 0.5 MPa, PES membrane 0.22 µ, gamma sterilized, free of pyrogens).

2.2. *AChE Solns.* AChE (1 mg) was dissolved in the phosphate buffer pH 7.00 (1 ml), thoroughly mixed, and stored at 5° (stock soln.). To the phosphate buffer (5 ml), AChE stock soln. (5 µl) was added and thoroughly mixed. The soln. (1 ml) was diluted to 10 ml with phosphate buffer. Such a soln. could be used for the determination of K_m and one assay series.

2.3. *ATC Soln.* ATC (22.6 mg) was dissolved in phosphate buffer (1 ml (→78 mM)) and thoroughly mixed. The solns. were freshly prepared prior to use and stored at 0° (ice bath).

2.4. *DTNB Soln.* DTNB (15 mg) was dissolved in phosphate buffer (2 ml (→19 mM)) and well mixed prior to use.

2.5. *Inhibitor Soln.* (representative example). The respective 3-substituted 3-phosphadecalin (3.5 mg) was dissolved in abs. MeCN (200 µl). From this stock soln., a dilution series was prepared to yield five different concentrations. The total volume of each assay was 25 µl.

2.6. *Determination of* K_m. Prior to each assay series, the *Michaelis* constant (K_m) was determined under the assay conditions (instead of an inhibitor, MeCN (25 µl) was added). The linear increase of the absorption was monitored at 410–414 nm at five different concentrations of the substrate (ATC; [S] = [ATC] from 100–500 µM). The *Michaelis–Menten* equation was fitted to the steady-state rates to calculate K_m by nonlinear regression, which was always in the range of 160 µM.

2.7. *Assay.* In a polystyrene cell ($d = 10$ cm), phosphate buffer pH 7.00 (2 ml), DTNB soln. (100 µl), and ATC soln. (20 µl) were mixed and thermostatted at 25°. The inhibitor soln. (25 µl, known [I]) was added. At $t = 0$, the AChE soln. (1 ml) was added, and the mixture gently mixed for 20 s. After 20 s, the monitoring of the absorption automatically started, and 600 data points were collected for 10 min at various concentrations of the inhibitors. As in the K_m determinations, the total volume was 3.15 µl, the concentration of the substrate [S] = 502 µM. Per inhibitor, at least five measurements with different inhibitor concentrations were performed, the smallest one being *ca.* 1/5–1/10 of the largest one.

2.8. *Titration of the Active Sites of AChE.* The concentrations of the active sites in the AChE samples were determined photometrically by titration with *N,N*-dimethyl-*O*-(2-nitrophenyl)carbamate according to [31] at 25°. In this reaction, the enzyme hydrolyzes an equimolar amount of 2-nitrophenolate that is monitored at 415 nm. The concentration is determined by means of a calibration line that was established with 2-nitrophenolate under identical reaction conditions. *Phosphate Buffer pH 7.70.* Soln. *A:* $NaH_2PO_4 \cdot H_2O$ (39.3 mg), NaCl (58.4 mg), and *Pluronic F-68* (1 mg) were dissolved in H_2O (10 ml). Soln. *B:* $Na_2HPO_4 \cdot 2\,H_2O$ (1.25 g), NaCl (584 mg), and *Pluronic F-68* (10 mg) were dissolved in H_2O (100 ml). The solns. were adjusted to pH 7.70 ± 0.02 by mixing. *AChE Solutions.* AChE (1 mg) was dissolved in the phosphate buffer pH 7.70 (250 µl). *Titration* (representative example for AChE lot 129F8080). To phosphate buffer pH 7.70 (2 ml) in a polystyrene cell ($d = 10$ cm), a soln. (50 µl) of *N,N*-dimethyl-*O*-(2-nitrophenyl)carbamate (7.57 mg/ml in abs. MeCN) was added, and the absorption was measured at 415 nm for 5 min. Then, the soln. (50 µl) of AChE was added, and the progress curve was monitored for 15 min. The procedure was repeated twice to confirm its reproducibility. Data analysis showed the concentration of active sites to be $1.75 \cdot 10^{-8}$ mol/mg.

2.9. *Data Analysis and Assignment of the Inhibition Mechanisms. Eqns. 8* or *9* were fitted to progress curves by nonlinear regression using *GraphPad Prism* version 5.00 for Windows, *GraphPad* Software, San Diego, California USA (www.graphpad.com). The runs test and analysis of residuals were performed to monitor significant deviations from the model. λ, v_z, and v_∞ (where appropriate) obtained as the parameters of this primary analysis were plotted *vs.* the inhibitor concentration. The dependence of λ on [I] was analyzed with models **2A**, **2C**, **1A**, and **1C** (*Eqns.* in *Tables 2* and *3*), and model discrimination was performed by analysis of variance of the difference between the sum of squares (extra sum-of-squares test), and calculation of *F* ratios and *p* values. The dependence of v_z and v_∞ on [I] was analyzed using the appropriate *Eqns.* in *Tables 2* and *3*. When primary fittings to progress curves using *Eqns. 8* and *9* were inconsistent, and there was no clear dependency of λ upon [I], mechanism **1B** was considered and *Eqn. 16* was fitted to data. ^{31}P-NMR Analyses confirmed in these cases instability of the inhibitors under the assay conditions resulting in hydrolysis and/or epimerization of the molecule. Data shown in *Table 4* report the mechanism and the best-fit inhibition constants with associated standard error from regression analysis.

3. *^{31}P-NMR Experiments. Stability of (+)*-cis-**IVeq**. 3.1. *General.* The ^{31}P{^{1}H}-NMR spectra were recorded at 161.98 MHz on a *Bruker AV2-400* spectrometer at 300 K (δ in ppm, *J* in Hz).

3.2. *Solvents.* Soln. *A:* $Na_2HPO_4 \cdot 2\,H_2O$ (445 mg), NaCl (146 mg), and *Pluronic F-68* (2.5 mg) were dissolved in D_2O (25 ml). Soln. *B:* $NaH_2PO_4 \cdot H_2O$ (690 mg), NaCl (292 mg), and *Pluronic F-68* (2.5 mg) were dissolved in D_2O (50 ml). The solns. were adjusted to pH*[6]) 7.00 ± 0.02 by mixing.

3.3. *Data.* (+)-*cis*-**IVeq**: δ −13.34 (*d*, ^1J(P,F) = 986); (−)-*cis*-**IVax**: δ −12.95 (*d*, ^1J(P,F) = 1003). The hydrolysis product (2,4-dioxa-3-hydroxy-3-phosphabicyclo[4.4.0]decane 3-oxide) appeared at δ −1.98 ppm (*s*), and inorg. phosphate was detected at δ 2.11 (*s*)[5]).

Appendix. – *Symbols and Nomenclature Conventions Used in This Article:* d = Displacement of a progress curve from the zero value; E = free enzyme; EI = adsorptive enzyme–inhibitor or enzyme–inactivator[4]) complex; E·I = reversible enzyme–inhibitor complex (competitive with substrate); E–I = irreversibly, covalently modified enzyme (competitive with substrate); ES = enzyme–substrate complex; I = inhibitor (reversible inhibitor or irreversible modifier (inactivator[4]))); I′ = chemically transformed I (*e.g.*, by hydrolysis), which does no longer bind to the enzyme; I* = enzymatically transformed I, which does no longer bind to the enzyme; k_1, k_3 = second-order rate constants; k_{-1}, k_2, k_{-3}, k_4, k_5, k_6, k_7, k_{-7} = first-order rate constants; $K_i = k_{-3}/k_3$ = dissociation constant; $k_i = k_4/K_i$ = second-order inhibition constant; P = product(s); S = substrate; v_s = reaction rate at steady-state; v_z = reaction rate at time zero (t = 0); v_0 = reaction rate in the absence of modifiers; λ = first-order rate constant of the exponential phase for the formation of E–I or EI; [X] = concentration of the free species X in mol dm^{-3}; $[X]_t$ = total concentrations of species X; $[X]_z$ = concentrations of species X at $t = 0$.

REFERENCES

[1] S. Furegati, W. Ganci, F. Gorla, U. Ringeisen, P. Rüedi, *Helv. Chim. Acta* **2004**, *87*, 2629.
[2] W. Ganci, E. J. M. Meier, F. Merckling, G. Przibille, U. Ringeisen, P. Rüedi, *Helv. Chim. Acta* **1997**, *80*, 421; S. Furegati, W. Ganci, G. Przibille, P. Rüedi, *Helv. Chim. Acta* **1998**, *81*, 1127.
[3] M. J. Stöckli, P. Rüedi, *Helv. Chim. Acta* **2001**, *84*, 106; M. J. Stöckli, P. Rüedi, *Helv. Chim. Acta* **2007**, *90*, 2058.
[4] W. N. Aldridge, *Biochem. J.* **1950**, *46*, 451.
[5] A. R. Main, W. C. Dauterman, *Nature* **1963**, *4880*, 551; A. R. Main, *Science* **1964**, *114*, 992.
[6] G. Hart, R. D. O'Brien, *Biochemistry* **1973**, *12*, 2940.
[7] H. A. Berman, K. Leonard, *J. Biol. Chem.* **1989**, *264*, 3942; H. A. Berman, M. M. Decker, *J. Biol. Chem.* **1989**, *264*, 3951; H. A. Berman, K. Leonard, *J. Biochem.* **1990**, *29*, 10640, and refs. cit. therein.
[8] F. A. Merckling, '^{31}P-NMR-spektroskopische Untersuchungen der Inhibierung von Acetylcholinesterase mit Organophosphaten', Ph.D. Thesis, University of Zurich, 1993.
[9] U. Ringeisen, 'Synthese und Charakterisierung von N-heterocyclischen Organophosphaten als Inhibitoren der Acetylcholinesterase', Ph.D. Thesis, University of Zurich, 1996.
[10] W. M. Ganci, 'Untersuchung der Wechselwirkungen von Serinhydrolasen mit Organophosphaten: Synthese kationischer N-Heterocyclen als Acetylcholin-Mimetika und ^{31}P-NMR-Spektroskopie von Enzym-Inhibitoraddukten', Ph.D. Thesis, University of Zurich, 1998.
[11] S. Furegati, 'Synthese von konformativ definierten Organophosphat-Acetylcholinmimetika zur Untersuchung der Inhibition von Acetylcholinesterase', Ph.D. Thesis, University of Zurich, 2002.
[12] F. Gorla, 'Internal Progress Report', University of Zurich, 1998.
[13] S. Furegati, F. Gorla, A. Linden, P. Rüedi, *Chem.-Biol. Interact.* **2005**, *157–158*, 415.
[14] M. Wächter, 'Herstellung optisch aktiver Organophosphate mit *cis*- und *trans*-Decalingerüst zur Untersuchung der Inhibition von Acetylcholinesterase', M.Sc. Thesis, University of Zurich, 2005; M. Wächter, P. Rüedi, *Chem. Biodiversity* **2009**, *6*, 283.
[15] S. E. Szedlacsek, R. G. Duggleby, *Methods Enzymol.* **1995**, *249*, 144.
[16] A. Baici, *Biol. Chem.* **1998**, *379*, 1007.
[17] L. H. Easson, E. Stedman, *Proc. R. Soc. London, Ser. B* **1936**, *121*, 142.

---

[6]) pH* is the nominal pH value of a soln. in D_2O read on a pH-meter calibrated with standard buffers in H_2O; pD ≈ pH + 0.4 [32].

[18] W. W. Ackerman, V. R. Potter, *Proc. Soc. Exp. Biol. Med.* **1949**, *72*, 1.
[19] R. Kitz, I. B. Wilson, *J. Biol. Chem.* **1962**, *237*, 3245.
[20] W. X. Tian, C. L. Tsou, *Biochemistry* **1982**, *21*, 1028; C. L. Tsou, *Adv. Enzymol. Relat. Areas Mol. Biol.* **1988**, *61*, 381.
[21] P. J. Gray, R. G. Duggleby, *Biochem. J.* **1989**, *257*, 419.
[22] K. F. Tipton, in 'Enzyme Inhibitors as Drugs', Ed. M. Sandler, McMillan, London, 1980, p. 1.
[23] C. M. Topham, *J. Theor. Biol.* **1990**, *145*, 547.
[24] C. Frieden, *J. Biol. Chem.* **1970**, *245*, 5788.
[25] S. Cha, *Biochem. Pharmacol.* **1975**, *24*, 2177.
[26] J. F. Morrison, *Trends Biochem. Sci.* **1982**, *7*, 102; J. F. Morrison, S. R. Stone, *Comments Mol. Cell. Biophys.* **1985**, *2*, 347.
[27] G. L. Ellman, K. D. Courtney, V. Andres Jr., R. M. Featherstone, *Biochem. Pharmacol.* **1961**, *7*, 88.
[28] P. G. Lorenzetto, A. Strehler, P. Rüedi, *Helv. Chim. Acta* **2006**, *89*, 3023; P. G. Lorenzetto, 'Synthese und Charakterisierung der enantiomerenreinen 9-Aza-3-phosphadecaline als Acetylcholin-Mimetika', Ph.D. Thesis, University of Zurich, 2009; P. G. Lorenzetto, A. Linden, M. Wächter, P. Rüedi, *Helv. Chim. Acta*, in preparation.
[29] C. Clerc, 'Synthese und Charakterisierung von enantiomerenreinen N-heterocyclischen Phosphadecalinen als Inhibitoren von Acetylcholinesterase', Ph.D. Thesis, University of Zurich, 2008; C. Clerc, P. Rüedi, *Helv. Chim. Acta*, in preparation.
[30] M. Wächter, 'Herstellung von optisch aktiven Organophosphaten mit *cis*- und *trans*-Decalingerüst zur Untersuchung der Inhibition von Acetylcholinesterase mittels Enzymkinetik und ^{31}P-NMR-Spektroskopie', Ph.D. Thesis, University of Zurich, submitted; M. Wächter, P. Rüedi, *Helv. Chim. Acta*, in preparation.
[31] M. L. Bender, M. L. Begué Cantón, R. L. Blakeley, L. J. Brubacher, J. Feder, C. R. Gunter, F. J. Kézdy, J. V. Killheffer Jr., T. H. Marshall, C. G. Miller, R. W. Roeske, J. K. Stoops, *J. Am. Chem. Soc.* **1966**, *88*, 5890.
[32] A. Krezel, W. Bal, *J. Inorg. Biochem.* **2003**, *98*, 161.

Received October 10, 2008

Simultaneous interaction of enzymes with two modifiers: reappraisal of kinetic models and new paradigms

Journal of Theoretical Biology, 2009, 261:318−329

Abstract

Die Aktivität eines Enzyms kann durch die gleichzeitige Einwirkung von zwei Modifiern, Aktivatoren oder Inhibitoren, moduliert werden. Die kinetischen Mechanismen für die Interaktion der individuellen Modifier mit dem Enzym können sich beträchtlich verändern, wenn zwei Modifier gleichzeitig binden. Wir beschreiben eine generelle Gleichung für diese Art von Interaktionen, welche das Verhalten von Aktivatoren und Inhibitoren eindeutig beschreiben kann, bei jegwelcher Kombination von klassischen kinetischen Mechanismen. Die Flexibilität dieses Modells ist beispielhaft erläutert durch die Kombination von Aktivatoren und/oder Inhibitoren, die kompetitiv, unkompetitiv oder vom gemischten Typ sein können und das Enzym in einer vorgeschriebenen oder zufälligen Weise binden und die Enzymaktivität bei Sättigungsbedingungen auf keine oder geringe Aktivität erniedrigen können. Das Modell zeigt, dass die Effekte von 'Zero-Interaction' und 'Synergy' zwischen gleichzeitig agierenden Enzymmodifiern häufige Ereignisse sind. Jedoch, im Unterschied zu früheren Theorien, 'Antagonism' zwischen Enzymmodifiern ein sehr seltener Effekt ist, der nur unter ganz bestimmten Umständen zu erwarten ist.

Journal of Theoretical Biology 261 (2009) 318–329

Contents lists available at ScienceDirect

Journal of Theoretical Biology

journal homepage: www.elsevier.com/locate/yjtbi

Simultaneous interaction of enzymes with two modifiers: Reappraisal of kinetic models and new paradigms

Patricia Schenker, Antonio Baici *

Department of Biochemistry, University of Zurich, Winterthurerstrasse 190 CH-8057 Zurich, Switzerland

ARTICLE INFO

Article history:
Received 13 May 2009
Received in revised form
13 July 2009
Accepted 24 July 2009
Available online 4 August 2009

Keywords:
Enzyme kinetics
Double inhibition
Activation
Synergy
Antagonism

ABSTRACT

Enzyme activity can be modulated by the concurrent action of two modifiers, either activators or inhibitors. The kinetic mechanisms for the interaction of the individual modifiers with the target enzyme can change considerably when two modifiers bind simultaneously. We illustrate a general equation for this kind of interactions, which can unambiguously describe the behavior of activators and inhibitors acting by any combination of classical kinetic mechanisms. The flexibility of this model is exemplified by combinations of activators and/or inhibitors, which can be competitive, uncompetitive or mixed-type, bind the target enzyme in either compulsory or random order, and are able to drive or not enzyme activity to zero at saturation. The model shows that the effects of zero-interaction and synergy between simultaneously acting enzyme modifiers are common events. Yet, in disagreement with previous theories, this model shows that antagonism between enzyme modifiers is a rare effect, which can be predicted only under very particular circumstances.

1. Introduction

The velocity of enzyme-catalyzed reactions can be regulated by modifiers, which may be activators or inhibitors. A large number of classical studies have been dedicated to the development of methods for gaining information on mechanisms of interaction and kinetic constants in systems consisting of an enzyme, one or more substrates, and a modifier. The simultaneous action of two or more modifiers on the same enzyme molecule received attention after observing that the combination of two modifiers may not result in simple additive effects. This was shown in a study of the 'succinic oxidase' system subjected to simultaneous inhibition by fluoride and phosphate (Slater and Bonner, 1952). Other contributions to multiple inhibition of both practical and theoretical character were published after this seminal paper and were concerned with specific mechanism.

Multiple enzyme modification by inhibitors and activators is relevant to biochemistry and pharmacology for several reasons. Two or more endogenous or exogenous inhibitors may interact with the same enzyme molecule and generate a multitude of combined effects that depend on the individual kinetic mechanisms of the inhibitors, as well as on substrate and inhibitor concentrations. An exogenous inhibitor may bind a target enzyme and contend or share binding with an endogenous inhibitor. An inhibitor may bind an enzyme in concert with an activator, or two activators can act at the same time. All possible individual inhibition and activation kinetic mechanisms give rise to a large and multi-faceted spectrum of interactions. Out of many situations that may occur in vitro, we mention just the example of an enzyme acting on a racemic substrate, of which only one of the optical isomers is a true substrate, while the other behaves as a competitive inhibitor. Hence, in the presence of a true inhibitor, the enzyme interacts in reality with two inhibitors (Mares-Guia and Shaw, 1965). Physiopathologically relevant examples can be found in the field of extracellular matrix degrading hydrolases. For instance, in the extracellular space, the leukocyte peptidases elastase, cathepsin G and myeloblastin interact unspecifically with glycosaminoglycans, components of the extracellular matrix, and this interaction may result in either inhibition or activation (Baici et al., 1993; Früh et al., 1996; Kostoulas et al., 1997). In the presence of endogenous or exogenous inhibitors, these interactions generate a spectrum of hitherto unpredictable effects spanning from synergy to antagonism. In the light of these observations, we undertook the study of multiple enzyme modification with the aim of giving a quantitative and mechanistic interpretation to the difficulties encountered with synthetic inhibitors against enzymes with these unusual properties (Baici, 1998).

Here we reconsider the simultaneous action of two modifiers on one enzyme molecule by treating the most general situation, from which particular cases can be derived. For properly understanding the significance of our present treatment, a comparison with previous literature and a critical assessment of general concepts is essential. This discussion will be presented in Appendix B. The literature on multiple inhibition, at least in the early phases of the development of the underlying theories, suffered from overlooking

* Corresponding author. Tel.: +41 44 6355542; fax: +41 44 6356805.
E-mail address: abaici@bioc.uzh.ch (A. Baici).

0022-5193/$ - see front matter © 2009 Elsevier Ltd. All rights reserved.
doi:10.1016/j.jtbi.2009.07.033

previously published work and caused occasional confusion, rediscoveries and misinterpretations. This analysis is in no way aimed at censuring authors but at linking theories with their legitimate sources to the best of our knowledge and, where appropriate, at amending mathematical mistakes.

We call attention to linear and hyperbolic mixed-type inhibition, a blend of competitive and uncompetitive character. The kinetic mechanism of such inhibitors may be much more widespread than commonly realized, and may be representative of a major class of modifiers such as allosteric effectors. Results from our laboratory on a designed ankyrin repeat protein as inhibitor of caspase-2 are an example (Schweizer et al., 2007). In a natural environment, e.g. when used as drugs, such artificially designed protein modifiers and any other synthetic compound will possibly interact with naturally occurring modifiers against the target enzyme. It is therefore helpful to set up criteria by which these interactions may be interpreted and predicted on the basis of mathematical models.

2. Theory of double enzyme modification

Double modifier systems have been described in the past with numerous different terminologies and symbols for kinetic parameters and coefficients. In the majority of publications, particular cases have been considered and the comparison of the associated theoretical treatments with those in other publications is not always straightforward, particularly when an extension has to be made to a general mechanism. In the literature on this subject the terms non-competitive and mixed-type inhibition have been used with various ambiguous meanings. In our own theory, in line with the recommendations of the International Union of Biochemistry, we will not use the term non-competitive inhibition, which is '… discouraged for all purposes' (International Union of Biochemistry, 1982). We will use instead the term mixed-type or simply mixed inhibition, which also includes the non-competitive inhibition as a special case where the competitive and the uncompetitive components contribute equally.

2.1. The general modifier mechanism

A generic classical modifier can be adequately described with the general modifier mechanism (Botts and Morales, 1953) with the notation shown in Scheme 1. Here, the symbol I denotes an inhibitor but this can be an activator as well. For inhibitors, the coefficient α defines the proportion of competitive and uncompetitive character and β is a factor that multiplies the catalytic constant. If $\beta<1$ hyperbolic inhibition is observed, $\beta>1$ describes activation and $\beta=1$, together with $1<\alpha<\infty$, occurs in the particular case of hyperbolic competitive inhibition.

The use of the symbol S for substrate does not imply that the scheme is restricted to single-substrate enzymes. In case of multisubstrate reactions, S represents the varied substrate, while the other(s) is/are kept at a constant concentration, and the same is valid for the product(s) P.

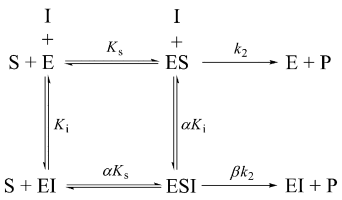

Scheme 1. The general modifier mechanism: E = enzyme, S = substrate, and I = inhibitor or other modifier.

The 'specific velocity plot' has been developed as a diagnostic tool for the analysis of modification mechanisms conforming to Scheme 1 (Baici, 1981). While the method applies equally to inhibitors and activators, the following specific velocity equation is shown here for an inhibitor, I:

$$\frac{v_0}{v_i}=\frac{[\mathrm{I}]\left(\frac{1}{\alpha K_\mathrm{i}}-\frac{1}{K_\mathrm{i}}\right)}{1+\beta\frac{[\mathrm{I}]}{\alpha K_\mathrm{i}}}\frac{\sigma}{1+\sigma}+\frac{1+\frac{1}{K_\mathrm{i}}}{1+\beta\frac{[\mathrm{I}]}{\alpha K_\mathrm{i}}}. \tag{1}$$

v_0 and v_i are the rates in the absence and in the presence of inhibitor, respectively, and $\sigma=[\mathrm{S}]/K_\mathrm{m}$. Eq. (1) was derived under the assumptions of quasi-equilibrium for the binding of I to E and ES, and steady-state for the fluxes around ES and ESI. Accordingly, in Eq. (1) K_m substitutes K_s shown in Scheme 1. An expert account on the validity of these assumptions has been published (Topham and Brocklehurst, 1992). In Eq. (1) and in all other equations in this paper, it is assumed that the concentration of modifiers is much larger than the enzyme concentration, i.e. the total and free modifier concentrations are approximately the same (no depletion of modifier by tight-binding). We will consistently use the terminology of Scheme 1 throughout this article and will extend it to the case of two modifiers acting on the same enzyme. In particular, we will retain the β-coefficients as multiplicative factors for the catalytic step constants.

2.2. The double modifier mechanism

Double interactions by two simultaneously acting modifiers, I and X, can be described with a three-dimensional path of reactions as shown in Scheme 2a, which is analogous to Scheme 1. In Scheme 2a, the reactant addition paths, such as I+EX→EIX and similar, have been omitted for simplicity.

The meaning of coefficients and parameters in Scheme 2a is explained in Table 1 and compared with the corresponding symbols in three previous theoretical treatments (see Appendix B). The coefficients α_S, α_I and α_X multiplying K_S, K_I and K_X, respectively, may appear eccentric at a first sight and could actually be omitted if it were not for some special cases of modifier binding. In fact, Scheme 2a describes the most general possibility of interactions but not all paths shown must necessarily exist and α_S, α_I and α_X can only take the values 1 (the path exists) or ∞ (the path does not exist). The individual notations for the α- and γ-coefficients are useful for the same reason, and they can take any positive value. This terminology helps avoid mathematical mistakes in the cases of essential activation and uncompetitive inhibition because our symbols are based on the use of multiplication coefficients for equilibrium constants rather than on the constants themselves, such as for instance $\alpha_{\mathrm{XS}}K_\mathrm{S}$, which could be written K'_S as well. To illustrate the usefulness of the terminology in Scheme 2a and b four examples are discussed in Appendix A, including essential activation. However, in the general case, all interconversions shown in Scheme 2a take place and parallel pathways in the thermodynamic boxes described by the edges of the cube must be taken into account. In this case it is convenient to proceed with less cumbersome symbols defined as combined coefficients

$$\mathrm{a}=\alpha_\mathrm{I}\alpha_{\mathrm{IS}}=\alpha_\mathrm{S}\alpha_{\mathrm{SI}},$$

$$\mathrm{b}=\alpha_\mathrm{X}\alpha_{\mathrm{XS}}=\alpha_\mathrm{S}\alpha_{\mathrm{SX}},$$

$$\mathrm{c}=\alpha_\mathrm{X}\alpha_{\mathrm{XI}}=\alpha_\mathrm{I}\alpha_{\mathrm{IX}}, \tag{2}$$

and the symbolism in Scheme 2a can be simplified as shown in Scheme 2b. Nonetheless, we emphasize that for ordered mechanisms equalities (2) should be interpreted as follows

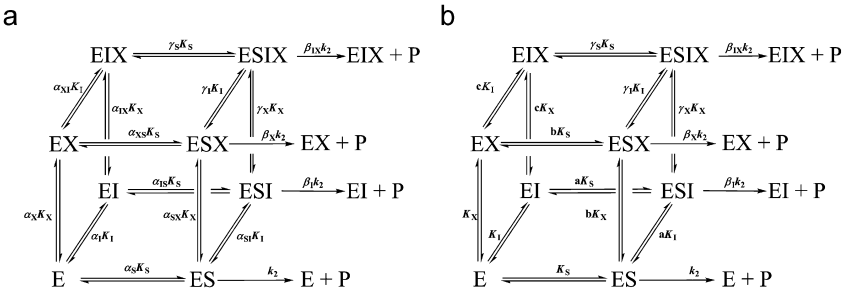

Scheme 2. (a) Extension of the general modifier mechanism to the simultaneous action of two modifiers, I and X and (b) the same mechanism written with the definitions in equalities (2).

Table 1
Definition of elementary reaction steps, equilibrium and interaction constants in Scheme 2a, and comparison with previously published terminology.

#	Elementary reactions	This work	Keleti and Fajszi (1971)	Segel (1975)	Webb (1963)
1	$E + S \rightleftharpoons ES$	$\alpha_S K_S = \frac{[E][S]}{[ES]}$	K_0	K_s	K_s
2	$E + I \rightleftharpoons EI$	$\alpha_I K_I = \frac{[E][I]}{[EI]}$	K_1	K_i	K_{i1}
3	$E + X \rightleftharpoons EX$	$\alpha_X K_X = \frac{[E][X]}{[EX]}$	K_2	K_x	K_{i2}
4	$ES + I \rightleftharpoons ESI$	$\alpha_{SI} K_I = \frac{[ES][I]}{[ESI]}$	K_{01}	αK_i	βK_{i1}
5	$ES + X \rightleftharpoons ESX$	$\alpha_{SX} K_X = \frac{[ES][X]}{[ESX]}$	K_{02}	βK_x	γK_{i2}
6	$EI + S \rightleftharpoons ESI$	$\alpha_{IS} K_S = \frac{[EI][S]}{[ESI]}$	K_{10}	αK_s	βK_s
7	$EX + S \rightleftharpoons EXS$	$\alpha_{XS} K_S = \frac{[EX][S]}{[ESX]}$	K_{20}	βK_s	γK_s
8	$EI + X \rightleftharpoons EIX$	$\alpha_{IX} K_X = \frac{[EI][X]}{[EIX]}$	K_{12}	γK_x	αK_{i2}
9	$EX + I \rightleftharpoons EIX$	$\alpha_{XI} K_I = \frac{[EX][I]}{[EIX]}$	K_{21}	γK_i	αK_{i1}
10	$ESI + X \rightleftharpoons ESIX$	$\gamma_X K_X = \frac{[ESI][X]}{[ESIX]}$	K_{012}	$\beta\gamma K_x$	$\alpha\gamma K_{i2}$
11	$ESX + I \rightleftharpoons ESIX$	$\gamma_I K_I = \frac{[ESX][I]}{[ESIX]}$	K_{021}	$\alpha\gamma K_i$	$\alpha\beta K_{i1}$
12	$EIX + S \rightleftharpoons ESIX$	$\gamma_S K_S = \frac{[EIX][S]}{[ESIX]}$	K_{120}	$\alpha\beta K_s$	$\beta\gamma K_s$

α_S, α_I and α_X can only take the values 1 (the path exists) or ∞ (the path does not exist).

depending on the existing path:

$$a = \alpha_I\alpha_{IS} \quad \text{or} \quad a = \alpha_S\alpha_{SI},$$

$$b = \alpha_X\alpha_{XS} \ \text{or} \ \ b = \alpha_S\alpha_{SX},$$

$$c = \alpha_X\alpha_{XI} \quad \text{or} \quad c = \alpha_I\alpha_{IX}. \tag{3}$$

For the three paths leading to ESIX in Scheme 2b, the interaction coefficients γ_S, γ_I and γ_X are left as they are in Scheme 2a. Without the explicit α_S, α_I and α_X coefficients in Scheme 2a, the symbols in Scheme 2b, although correct, may lead to ambiguities in the case of essential activation, uncompetitive inhibition and compulsory order of reactant binding as illustrated by examples in Appendix A. The general equation for double enzyme modification contains a further combined interaction constant, e, from equalities (4). This constant derives from microreversibility and does not explicitly appear in the reaction scheme of the system:

$$e = a\gamma_X = b\gamma_I = c\gamma_S. \tag{4}$$

Again, in special cases the value of e in (4) will correspond to either one of the terms. With these notions, considering quasi-equilibrium conditions for all steps but the catalytic paths and steady-state conditions for the four fluxes around the catalytic steps, the rate equation for the mechanism in Scheme 2a and its variant in Scheme 2b is given by

$$v_{IX} = v_0(1+\sigma)\frac{\frac{1}{\alpha_S} + \beta_I\frac{[I]}{aK_I} + \beta_X\frac{[X]}{bK_X} + \beta_{IX}\frac{[I][X]}{eK_IK_X}}{1 + \frac{[I]}{\alpha_IK_I} + \frac{[X]}{\alpha_XK_X} + \frac{[I][X]}{cK_IK_X} + \sigma\left(\frac{1}{\alpha_S} + \frac{[I]}{aK_I} + \frac{[X]}{bK_X} + \frac{[I][X]}{eK_IK_X}\right)}. \tag{5}$$

The terms in the right hand side of Eq. (5) are grouped to explicitly show four terms in the numerator, which correspond to the four catalytic steps, and eight terms in the denominator, which correspond to the enzyme-containing species, i.e. the corners of the cube, with the number 1 representing free enzyme. Particular cases can be derived from this general equation by deleting terms as needed as illustrated in the examples in Appendix A. The coefficient e characterizes the paths leading to the quaternary complex ESIX, in the respect of the underlying thermodynamic boxes, according to relationship (4).

The coefficient c in Scheme 2b and Eq. (5) is a measure of four types of interaction that may occur between the modifiers I and X on the free enzyme (Keleti and Fajszi, 1971):

facilitation $0 < c < 1$,

independence $c = 1$,

hindrance $1 < c < \infty$,

exclusion $c = \infty$. (6)

These interactions, which are defined on the assumption of a model such as Eq. (5), should not be mistaken for and used as synonyms of phenomenological effects that may be observed in double modifier systems and defined as synergy, antagonism or zero-interaction (discussed in Section 3). In particular, the coefficient c alone cannot be used as a criterion for predicting such effects. Criteria (6) can, however, be used to analyze experimental data and to discriminate between synergy and zero-interaction provided the mathematical model truthfully describes the system. The most important issue in this matter is whether or not the individual behavior of the modifiers I and X changes upon concomitantly binding to the enzyme, a property taken into account by the coefficients c and e in Scheme 2b and Eq. (5), respectively.

We consider now the possible combinations of two inhibitors I and X, which can individually be competitive, uncompetitive or mixed and additionally linear or hyperbolic. When acting together on the same enzyme molecule, the possibilities can be calculated considering an *r*-combination of a multiset *M* of size *r*, chosen from a set of *n* elements, $M(n+r-1, r)$. This is also called *r-combination with repetition allowed*. In this case, $r = 2$ (the two inhibitors I and X) and the set has six elements ($n = 6$), i.e. a hyperbolic inhibitor can be competitive, uncompetitive or mixed and the same holds for a linear inhibitor. The number of *r*-combinations is therefore given by

$$\left\langle \begin{matrix} n \\ r \end{matrix} \right\rangle = \binom{n+r-1}{r} = \left(\frac{(n+r-1)!}{r!(n-1)!}\right), \tag{7}$$

which gives a total of 21:

$$M(6+2-1,2) = \left(\frac{7!}{2!5!}\right) = 21. \tag{8}$$

The interaction coefficients c and e and the possibility that ESIX is catalytically active ($\beta_{IX} \neq 0$) give rise to six situations (Table 2). Thus, excluding occurrences of ordered binding, a total of $21 \times 6 = 126$ cases can be predicted for double inhibitions. In practice, however, many of these 126 cases will hardly occur because they are either non-sensical or very rare.

A non-sensical combination is for instance that of two linear competitive inhibitors with $c < \infty$, $e < \infty$ and $\beta_{IX} \neq 0$. Uncompetitive inhibition is a well-known feature of multisubstrate systems, in which inhibition by one of the products is genuinely uncompetitive (Segel, 1975, Chapter 9). Uncompetitive inhibition in multisubstrate systems is also possible for molecules structurally unrelated to the substrates of the reaction (King et al., 2009). Nevertheless, in single substrate enzyme-catalyzed reactions uncompetitive inhibition is more a theoretical than a real situation, which is yet necessary, together with competitive inhibition, to describe all gradations of mixed inhibition (Scheme 1). Uncompetitive inhibition is a very rare mechanism in nature because of its detrimental effects. Indeed, metabolites acting as uncompetitive inhibitors have conceivably been evolutionarily excluded by selection but this does not preclude the utilization of synthetic uncompetitive inhibitors as toxic agents, e.g. for pest control (Cornish-Bowden, 1986). Linear non-competitive inhibition, in its classical definition, is described by $\alpha = 1$ and $\beta = 0$ in Scheme 1. As commented by Cornish-Bowden, this type of inhibition is limited to protons, metal ions and small anions like chloride, and it is unlikely that molecules larger than these simple ions obey this mechanism. Furthermore, non-competitive inhibition has in many cases been mistaken for partial irreversible inactivation (Cornish-Bowden, 2004, p. 117). Thus, double inhibition systems containing linear non-competitive modifiers will have little chance to be observed in nature. Nevertheless, double inhibitions with the participation of an uncompetitive inhibitor are observed in multisubstrate systems, e.g. (Brandt et al., 1990; King et al., 2009).

Table 2
Interactions between two inhibitors in the double modifier mechanism (Scheme 2b) considering the linear or the hyperbolic character of double inhibition.

	Interaction	c	e
1	I and X exclude each other on E and on ES and $\beta_{IX} = 0$	∞	∞
2	I and X exclude each other only on ES and $\beta_{IX} = 0$	$(0, \infty)$	∞
3	I and X exclude each other only on E and $\beta_{IX} = 0$	∞	$(0, \infty)$
4	EIX does not exist but ESIX does exist and $0 < \beta_{IX} \leq 1$	∞	$(0, \infty)$
5	EIX and ESIX exist but $\beta_{IX} = 0$	$(0, \infty)$	$(0, \infty)$
6	EIX and ESIX exist, and $0 < \beta_{IX} \leq 1$	$(0, \infty)$	$(0, \infty)$

3. Synergy, antagonism and zero interaction

In pharmacology, synergy and antagonism between drugs is customarily described with isobolograms, a graphical procedure for characterizing their equieffective combinations. In the case of two substances A and B, isobolograms are obtained by representing the 'doses' or concentrations in an orthogonal coordinate system. Lines in this diagram, the isoboles, connect different dose combinations which produce the same effect. A first empirical description of this concept (Fraser, 1870–1871), was expanded by Loewe and Muischnek (1926), who also coined the term isobole. Berenbaum (1977, 1989) reviewed the rich literature on this subject, discussed nomenclature conflicts and provided a mathematical proof for the equation used to describe interactions between drugs. For two compounds A and B, a resulting effect *E* is characterized by the relationship

$$\frac{d_a}{D_a} + \frac{d_b}{D_b} = E, \tag{9}$$

where d_a and d_b are the doses (or concentrations as appropriate) of A and B used in combination, while D_a and D_b are the doses of A and B, which individually produce the same effect as the combination. The effect is defined as *synergy* if $E < 1$, *antagonism* if $E > 1$ and *zero-interaction* if $E = 1$, and we will consistently use these terms. The third effect, zero interaction, is also called *addition*, *additivism* or *summation*, synonyms which have, however, been used with several different meanings (Berenbaum, 1989). Examples of isoboles are illustrated in Fig. 1: zero-interaction in Fig. 1a, synergy in Fig. 1b and c, and antagonism in Fig. 1d (convex curve following straight zero-interaction lines).

Webb (1963, Chapter 10) suggested that the effects observed in multiple enzyme inhibitions may be represented by isobolograms in a way similar to that used in pharmacology and that interactions taking place between two inhibitors simultaneously acting on an enzyme may also be classified as synergism, antagonism and summation. In the treatment of double inhibitions by Keleti and Fajszi (1971), the rate equations were derived correctly for the general case (Scheme 7c in Appendix B) as well as for all special cases discussed therein. However, in making predictions about synergy and antagonism, the authors used the following relationships for all purposes, i.e. for any combination of mechanisms and interaction coefficients, in particular whether the two inhibitors were or were not mutually exclusive:

zero-interaction $v_{1,2} = \frac{v_1 v_2}{v_0}$, (10)

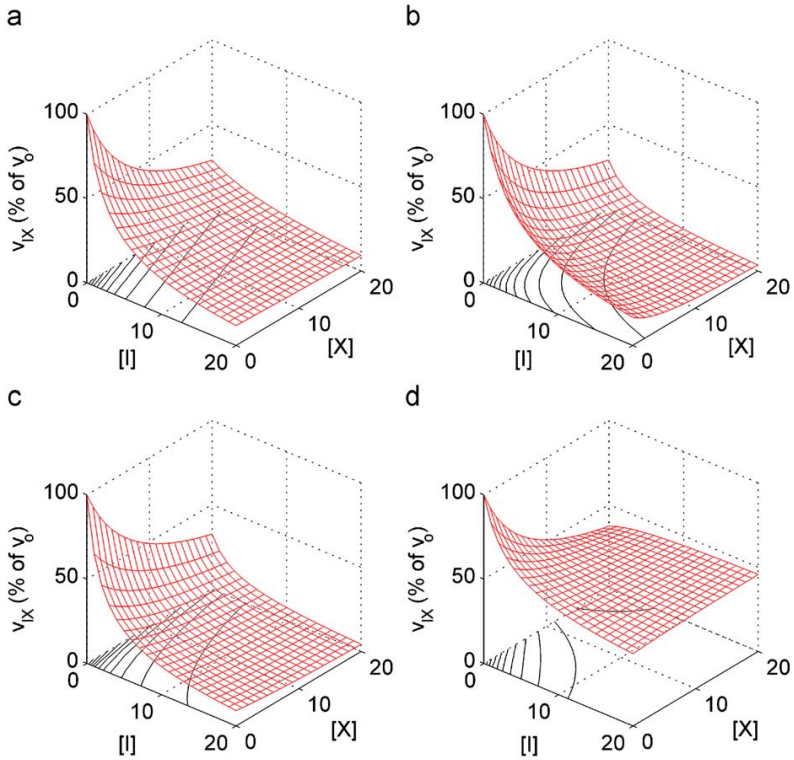

Fig. 1. Plots of the reaction rate as a function of the concentration of two modifiers. Concentrations and inhibition constants are in μM units, coefficients as defined in Scheme 2. (a) I and X are linear, mutually exclusive mixed-type inhibitors, $\alpha_I = \alpha_X = \alpha_S = 1$, a = 2, b = 4, c = ∞ (exclusion), e = ∞, $\sigma = 1$, $\beta_I = \beta_X = \beta_{IX} = 0$, $K_I = 2$, $K_X = 5$. (b) I is a linear competitive inhibitor and X is a linear mixed-type inhibitor, $\alpha_I = \alpha_X = \alpha_S = 1$, a = ∞, b = 4, c = 1 (independence), e = ∞, $\sigma = 1$, $\beta_I = \beta_X = \beta_{IX} = 0$, $K_I = 2$, $K_X = 5$. (c) I is a linear uncompetitive inhibitor and X a linear mixed-type inhibitor, $\alpha_I = \infty$, $\alpha_X = \alpha_S = 1$, a = 1, b = 4, c = 5 (hindrance), e = 8, $\sigma = 1$, $\beta_I = \beta_X = \beta_{IX} = 0$, $K_I = 1$, $K_X = 6$. (d) I is a hyperbolic competitive inhibitor and X is a hyperbolic mixed-type inhibitor, $\alpha_I = \alpha_X = \alpha_S = 1$, a = 5, b = 4, c = 5, e = 8, $\sigma = 1$, $\beta_I = 1$, $\beta_X = 0.3$, $\beta_{IX} = 0.8$, $K_I = 2$, $K_X = 5$. The straight, convex and concave lines in these plots represent the isoboles, i.e. the equieffective concentrations of the modifiers, I and X, obtained by projection of the three-dimensional graphs onto the [I]–[X] plane.

antagonism $$v_{1,2} > \frac{v_1 v_2}{v_0}, \tag{11}$$

synergy $$v_{1,2} < \frac{v_1 v_2}{v_0}. \tag{12}$$

In Eqs. (10)–(12), v_1, v_2 and $v_{1,2}$ correspond to the rates in the presence of modifier 1 alone, modifier 2 alone, and in the presence of both modifiers, respectively.

Indeed, Eq. (10) is valid only if $a = b = c = e = 1$ and $\beta_I = \beta_X = \beta_{IX} = 0$. If satisfied, this equation predicts zero-interaction. The prediction of antagonism with (11) and synergy with (12) is a minimal statement that says nothing but that there is a deviation from the behavior predicted by Eq. (10). We will show below that, while synergy is a genuine and common feature, antagonism is a rare property in double inhibition systems and that it occurs only with peculiar combinations of the interaction coefficients in Scheme 2b.

Chou and Talalay (1977) extended the relationship (10) to n mutually non-exclusive inhibitors, of which at least one must be non-competitive:

$$\frac{v_{1,2,3,\ldots,n}}{v_0} = \frac{v_1}{v_0} \times \frac{v_2}{v_0} \times \frac{v_3}{v_0} \cdots \frac{v_n}{v_0}. \tag{13}$$

v_1–v_n represent the rates in the presence of the individual modifiers and $v_{1,2,\ldots,n}$ the rate in the presence of all modifiers. With $n = 2$ Eq. (13) is the same as Eq. (10). Fajszi and Keleti (1974) used expressions (10)–(12) in a rearranged form in making predictions of effects arising from combinations of mechanisms and listed several special cases. Unfortunately, their estimates are true only in a few particular cases because expressions (10)–(12) cannot be indiscriminately used for any combination of inhibition mechanisms. For instance, the authors predicted antagonism between two mutually exclusive competitive inhibitors, whereas in this case only zero-interaction can result. Also, when two competitive inhibitors are mutually non-exclusive with hindrance ($1 < c < \infty$) Fajszi and Keleti predicted antagonism or zero-interaction depending on the substrate concentration. However, in this case only synergy will be observed independently of substrate concentration.

The theory named by Fajszi and Keleti (1974) 'the triple-faced enzyme–inhibitor relation' must be rejected in its original form because it is based on a wrong general assumption which leads to false predictions. In some instances (Leoncini et al., 1989; Lien et al., 1979a, 1979b), the term 'antagonism' has been misapplied as a synonym of mutual exclusion or hindrance, but this is likely to be a linguistic lapse. In fact, mutual exclusion ($c = e = \infty$, $\beta_{IX} = 0$) results by definition in zero-interaction.

The following Eq. (14) was originally proposed to describe the combined effects of a linear competitive and of a linear non-competitive inhibitor, which do not interact with each other (Lienhard, 1971):

$$\frac{1}{v_{1,2}} = \frac{1}{v_1} + \frac{1}{v_2} - \frac{1}{v_0}. \tag{14}$$

In a more general context, Fajszi (1974) used Eq. (14) as 'an immediate method' to ascertain whether both the EIX and ESIX complexes are absent in the general case (Scheme 2). This means, if the relationship (14) between the velocities does not apply, then the two inhibitors interact in some way or are of the hyperbolic type. Overlooking the previous publications by Keleti and Fajszi, Chou and Talalay (1977) provided an extension of (14) to n modifiers as

$$\frac{1}{v_{1,2,3,\ldots,n}} = \sum_{i=1}^{n} \frac{1}{v_i} - \frac{n-1}{v_0}, \tag{15}$$

but acknowledged without comment the contributions of Keleti and Fajszi in a subsequent paper (Chou and Talalay, 1981). It should be pointed out that neither Eq. (15) nor Eq. (13) fulfill the statement of being a 'simple generalized equation for the analysis of multiple inhibitions' (Chou and Talalay, 1977). In fact, these equations are valid only in particular cases and predict zero-interaction between linear, mutually exclusive inhibitors ($c = e = \infty$, $\beta_{IX} = 0$ in Scheme 2) independently of their individual mechanisms [Eq. (15)]. Synergy is observed in the case of non-exclusive linear inhibitors [Eq. (13)] when $a = b = c = e = 1$. If the result of (15) is not satisfied the only reliable prediction that can be made is that the EIX and ESIX do exist or at least one inhibitor is of the hyperbolic type. The prediction of antagonism when $1/v_{1,2} < 1/v_1 + 1/v_2 - 1/v_0$ (Chou and Talalay, 1977) is valid only if at least one of the inhibitors is hyperbolic and only for particular values of the interaction coefficients (Section 3.1). The same comments apply to the 'general coefficient' as a measure of synergy for all purposes (Mazat et al., 1981) because the highly unpredictable behavior of hyperbolic mixed inhibitors is not taken into account also in this case.

From the issues discussed above it becomes clear that a general expression relating the initial rate in presence of two modifiers, v_{IX}, to the individual rates of the modifiers, v_I and v_X, and to the rate in absence of modifiers, v_0, with the purpose of predicting synergistic and antagonistic effects, can theoretically be derived but results in a too complex expression for practical purposes. Additionally, it is mandatory to take into account mixed type inhibitors and the possible hyperbolic nature of one or both of the modifiers. As mentioned in the Introduction, we believe that hyperbolic mixed-type modifiers represent a class of inhibitors with crucial physiological roles that have been poorly characterized in the past. However, positive examples are antitumoral agents as inhibitors of cathepsin B (Bincoletto et al., 2005); antistatin as inhibitor of the coagulation factor Xa (Dunwiddie et al., 1989); antileukoprotease as inhibitor of the stratum corneum chymotryptic enzyme involved in physiological detachment of corneocytes (Franzke et al., 1996); a cleavage product of von Willebrand factor as inhibitor of ADAMTS13, a metallopeptidase that mediates platelet adhesion (Gao et al., 2006); sulfated glycosaminoglycans as inhibitors of human leukocyte elastase, which participate in compartmentalization and inhibition of this and similar enzymes in lysosomes (Kostoulas et al., 1997); a designed ankyrin repeat protein, inhibitor of caspase-2 as a potential agent to control apoptosis (Schweizer et al., 2007).

Taking advantage of modern information technology, forecasting synergy, antagonism or zero-interaction is a simple task with the aid of the general equation (5) and its graphical representation in three dimensions with two axes representing the effectors I and X and the third axis representing v_{IX}, i.e. the effect. At the same time, equieffective concentrations of the two modifiers, the isoboles, can be obtained as projection of the effects on the I–X plane. All three-dimensional graphics in this article were produced with Matlab® software.

Generalized predictions on synergy and antagonism are difficult because dozens of possible combinations should be listed. However, based on our exhaustive analysis of all possible combinations of modifiers, the following statements can be made (Scheme 2b and Eq. (5)). Any combination of mutually exclusive inhibitors ($c = e = \infty$, $\beta_{IX} = 0$) invariably results in zero-interactions. The isoboles consist of parallel straight lines if both inhibitors are linear and of straight lines intersecting at a common point if at least one of the two modifiers is a hyperbolic inhibitor. An example is shown in Fig. 1a. With $0 < c < 1$ (facilitation) or $c = 1$ (independence), any combination of inhibitors (competitive, uncompetitive or mixed) results in synergy with the exception of particular cases of two mixed inhibitors, where at least one of the two modifiers is hyperbolic and the ESIX complex is catalytically active (see Section 3.1). An example with $c = 1$ is shown in Fig. 1b. With $1 < c < \infty$ (hindrance) combinations of inhibitors result in synergy with the exception resulting from two linear mixed or one linear and one hyperbolic mixed inhibitors with predominantly uncompetitive character, and for combinations of two hyperbolic inhibitors. In such cases an indefinite number of effects can be observed, which depend on the coefficients a, b, c, e, β_I, β_X and β_{IX}, as well as on the substrate and inhibitor concentrations. We show here two examples in Fig. 1c (only synergy in the whole inhibitor concentration range) and in Fig. 1d (zero-interaction at low concentration changes into antagonism by increasing the concentration of the inhibitors, see also Section 3.1).

3.1. Reactivation following inhibition and the inhibition paradox

An apparently odd effect can be observed when all paths shown in Scheme 2b exist, including the four catalytic steps, which consists of enzyme inhibition in a low concentration range of the two modifiers, and reactivation by further increasing their concentrations. This effect was predicted by Fajszi and Keleti and what follows is our interpretation of the phenomenon. Although Fajszi and Keleti's treatment is only partially valid because it is affected by mathematical mistakes (reasons discussed above), we wish to credit these authors with the fatherhood of the concept described in this section. The concentration of modifier for which the inhibitory phase changes into reactivation has been called characteristic inhibitor concentration (Fajszi and Keleti, 1974).

In our analysis there are three possibilities for this behavior, and their distinction depends on the nature and availability of the modifiers I and X. If the two compounds are individually available, experiments can first be performed at various substrate concentrations and various I and X concentrations separately, and then using combinations of their concentrations. However, two or more modifiers may be the constituents of a complex mixture, from which they cannot be separated. In this case measurements can only be performed by increasing the concentration of the modifiers at a constant ratio.

Case 1 (I and X are separately available): the ESIX complex is catalytically more efficient than ESI and ESX; case 2 (I and X are separately available): either I or X is a liberator (Appendix B); and case 3 (I and X are components of an inseparable mixture): the individual contributions of the various components to enzyme modification cannot be evaluated, and only a two-dimensional representation of the effect can be produced. In case 1, besides observing a recovery of activity by increasing the concentration of the modifiers in combination over a certain threshold, it may happen that the rate in the presence of both modifiers exceeds the rate measured in the absence of modifiers, i.e. $v_{IX} > v_0$ despite the values of β_I, β_X and β_{IX} being ≤ 1. This property has been called *inhibition paradox* (Fajszi and Keleti, 1974). An example of activity recovery by increasing the concentrations of inhibitors is shown in Fig. 2a, and the inhibition paradox is illustrated in Fig. 2b. In

case 2 the liberator I has no effect whatsoever on enzyme activity ($a = 1$ and $\beta_I = 1$ in Scheme 2b) unless a genuine inhibitor X is also present (Fig. 2c). Experimentally, a distinction of case 2 towards case 1 is straightforward because the liberator I does not influence enzyme activity in the absence of the other modifier. A further difference with respect to case 1 is that a liberator can reverse inhibition maximally to the rate in the absence of modifier, v_0, but cannot enhance the rate to values exceeding those in the absence of modifiers. To illustrate the great variety of effects that can arise from combinations of modifiers, we show in Fig. 2d the case of a non-essential activator with a hyperbolic mixed inhibitor.

Besides the three mentioned cases, a special effect is observed when an initial activation in presence of two modifiers is followed by inhibition after increasing their concentration. To explain this effect we examine the properties of one of the modifiers, say I, whose behavior as inhibitor or activator depends on the coefficients in Scheme 1. If $\alpha < 1$, $\beta \leq 1$ and $\beta > \alpha$, I behaves as a hyperbolic mixed modifier with predominantly uncompetitive character and has a higher affinity for ES than for E (Frieden, 1964, non-limiting case 3). When $[S]/K_m = (\beta-\alpha)/(1-\beta)$ the modifier has no effect on the enzyme. This critical substrate concentration is obtained by differentiating the equation for the mechanism in Scheme 1 (the reciprocal of Eq. (1)) with respect to modifier concentration, setting the derivative equal to zero and solving for [S]. Below this value the modifier behaves as activator and above it as inhibitor. Increasing the substrate concentration favors the formation of ESI rather than EI and results in activation or inhibition depending on substrate concentration (Fig. 3). When such a modifier I is used concomitantly with an inhibitor X at various substrate concentrations, the resulting effects are as those shown in the example of Fig. 4. The three-dimensional plots, which show the change of character of modifier I from inhibitor to

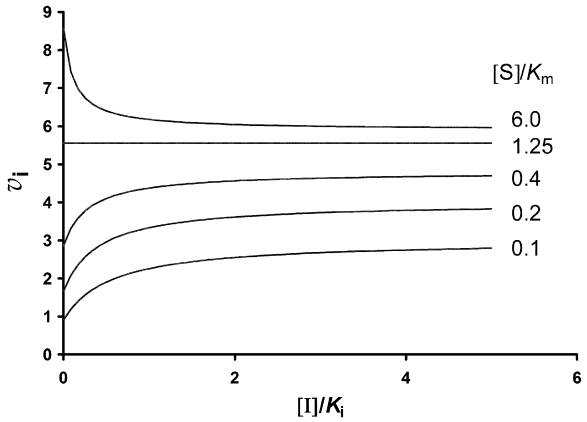

Fig. 3. A modifier activates at low substrate concentration and inhibits at high substrate concentration. Drawn according to Scheme 1 with the rate in arbitrary units and $\alpha = 0.1$, $\beta = 0.6$. At the characteristic ratio $[S]/K_m = (\beta-\alpha)/(1-\beta)$, which is 1.25 in this specific example, the modifier has no effect on the enzyme.

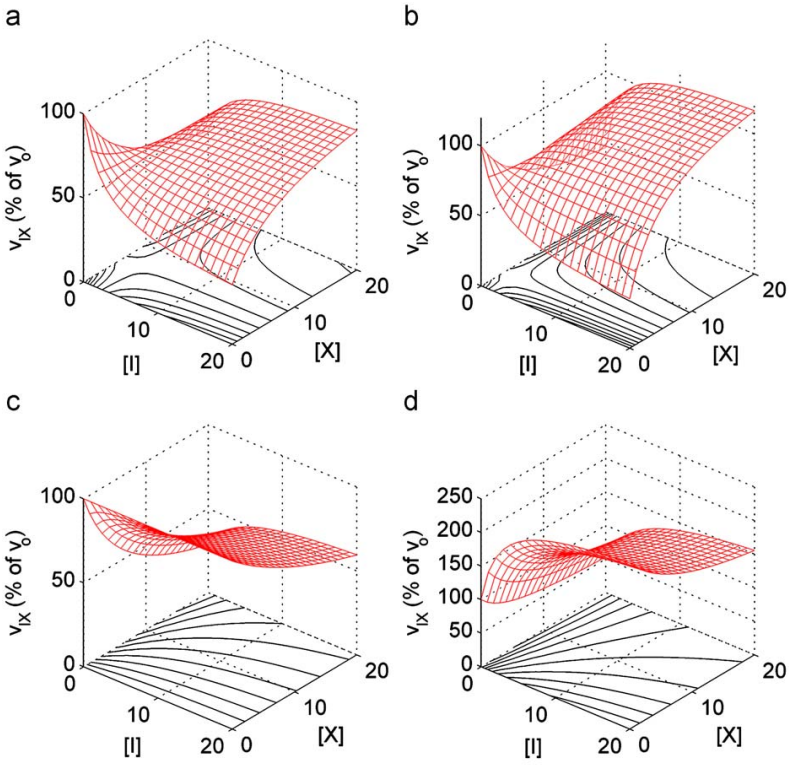

Fig. 2. Plots of the reaction rate as a function of the concentration of two modifiers in special cases. Concentrations and inhibition constants are in μM units, coefficients as defined in Scheme 2b. In all examples shown here $\alpha_I = \alpha_X = \alpha_S = 1$. (a) I is and X are hyperbolic, non-exclusive mixed inhibitors, $a = 2$, $b = 4$, $c = 3.5$ (hindrance), $e = 1.5$, $\sigma = 1$, $\beta_I = 0.4$, $\beta_X = 0.6$, $\beta_{IX} = 0.8$, $K_I = 2$, $K_X = 3$. (b) The same parameters as in (a) but $e = 0.8$ and $\beta_{IX} = 0.9$ (a case of inhibition paradox). (c) I is a liberator and X a linear competitive inhibitor, $a = 1$, $b = \infty$, $c = 5$ (hindrance), $e = \infty$, $\sigma = 1$, $\beta_I = 1$, $\beta_X = \beta_{IX} = 0$, $K_I = 2$, $K_X = 4$. (d) I is a non-essential activator and X is a hyperbolic mixed inhibitor, $a = 2$, $b = 2$, $c = 4$ (hindrance), $e = 5$, $\sigma = 1$, $\beta_I = 4$, $\beta_X = 0.6$, $\beta_{IX} = 1.4$, $K_I = 2$, $K_X = 4$.

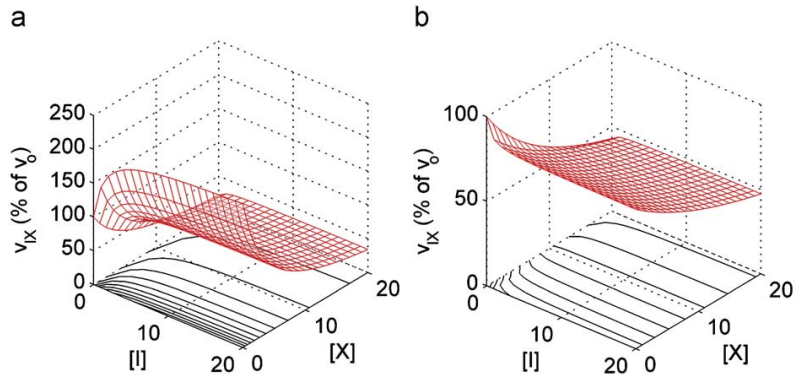

Fig. 4. Hyperbolic mixed-type modifier (I) together with a linear competitive inhibitor (X). The modifier I has the same properties shown in Fig. 3. I and X are non-exclusive on E. Concentrations and inhibition constants are in μM units, coefficients as defined in Scheme 2b with values (for both panels a and b): a = 0.2, b = ∞, c = 0.5, e = ∞, $\beta_I = 0.6$, $\beta_X = \beta_{IX} = 0$, $K_I = 2$, $K_X = 5$. The plots differ only in the value of σ, which is 0.1 in a and 2.0 in b.

activator, differ only in the $[S]/K_m$ ratio (0.1 or 2.0), whereas all other parameters are the same. Depending on how much the [I]:[X] ratio is shifted in favor of [I], the activation effect of this modifier becomes more evident as the substrate concentration decreases.

Acknowledgments

This work was supported by Grant 31-113345/1 of the Swiss National Science Foundation and by the Albert Böni Foundation.

Appendix A

A.1. Essential activator and linear competitive inhibitor

Let X be an essential activator of the enzyme E, S a substrate and I a linear competitive inhibitor, which does not share the same binding site with the activator and is therefore non-exclusive with X. In the absence of X, S would not productively bind the enzyme. This is one of two possible mechanisms of essential activation as described by Frieden (1964), namely his limiting case 1b. With the notation in Scheme 2b, this situation implies $K_S = \infty$ and this may sound mathematically strange because at the same time bK_S must have a finite value. Using the unambiguous nomenclature in Scheme 2a for the mechanism under consideration, this can be sketched as shown in Scheme 3a, where the ES complex is missing because $\alpha_S = \infty$ and therefore also $\alpha_S\alpha_{SX} = \infty$. The relationship $\alpha_I \cdot K_I \cdot \alpha_{IX} \cdot K_X = \alpha_X \cdot K_X \cdot \alpha_{XI} \cdot K_I$ holds (thermodynamic box), and from the definitions in (2) and (3) the mechanism can be simplified as shown in Scheme 3b, with $\alpha_I = \alpha_X = 1$, $\alpha_S = \infty$, a = ∞, $b = \alpha_{XS}$, $c = \alpha_{XI} = \alpha_{IX}$ ($c < \infty$), e = ∞, $\beta_I = \beta_{IX} = 0$, and $\beta_x \neq 0$.

The rate equation can be deduced from (5) by introducing these coefficients:

$$v_{IX} = v_0(1+\sigma)\frac{\beta_X\frac{[X]}{bK_X}}{1+\frac{[I]}{K_I}+\frac{[X]}{K_X}+\frac{[I][X]}{cK_IK_X}+\sigma\frac{[X]}{bK_X}}. \quad (16)$$

The 'K_m' for the path $S + EX \rightleftharpoons ESX \rightarrow EX + P$ corresponds for this mechanism to 'bK_m'. A graphic representation of this system is shown in Fig. 5a.

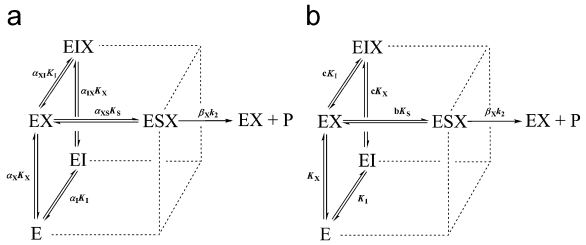

Scheme 3. X is an essential activator and I a linear competitive inhibitor. (a) Explicit symbols as in Scheme 2a and (b) simplified symbols with definitions (2) and (3) as in Scheme 2b.

A.2. Two hyperbolic mixed inhibitors mutually exclusive on ES

Let I and X be two hyperbolic mixed inhibitors which exclude each other in presence of the substrate but not on the free enzyme. Scheme 2a corresponds in this case to Scheme 4a. The thermodynamic boxes imply that $\alpha_S = \alpha_I = \alpha_X = 1$, $a = \alpha_{IS} = \alpha_{SI}$, $b = \alpha_{XS} = \alpha_{SX}$, $c = \alpha_{XI} = \alpha_{IX}$. Since the simultaneous presence of I and X is not possible when S is bound, all three γ-interaction constants are infinite. This reduces symbols as shown in Scheme 4b and the rate equation is given by (17). A graphic representation of this system is shown in Fig. 5b.

$$v_{IX} = v_0(1+\sigma)\frac{1+\beta_I\frac{[I]}{aK_I}+\beta_X\frac{[X]}{bK_X}}{1+\frac{[I]}{K_I}+\frac{[X]}{K_X}+\frac{[I][X]}{cK_IK_X}+\sigma\left(1+\frac{[I]}{aK_I}+\frac{[X]}{bK_X}\right)}. \quad (17)$$

A.3. Linear competitive and hyperbolic, mixed inhibitor, mutually exclusive on ES

The species I is considered to be the competitive inhibitor and the hyperbolic mixed inhibitor is X: I and X are non-exclusive on E ($c < \infty$) but exclusive on ES ($\gamma_S = \gamma_I = \gamma_X = \infty$). Using the same reasoning of the two preceding examples, the reaction schemes using the detailed and the simplified nomenclature are shown in Scheme 5 and the rate equation is expression (18). A plot is shown in Fig. 5c.

$$v_{IX} = v_0(1+\sigma)\frac{1+\beta_X\frac{[X]}{bK_X}}{1+\frac{[I]}{K_I}+\frac{[X]}{K_X}+\frac{[I][X]}{cK_IK_X}+\sigma\left(1+\frac{[X]}{bK_X}\right)}. \quad (18)$$

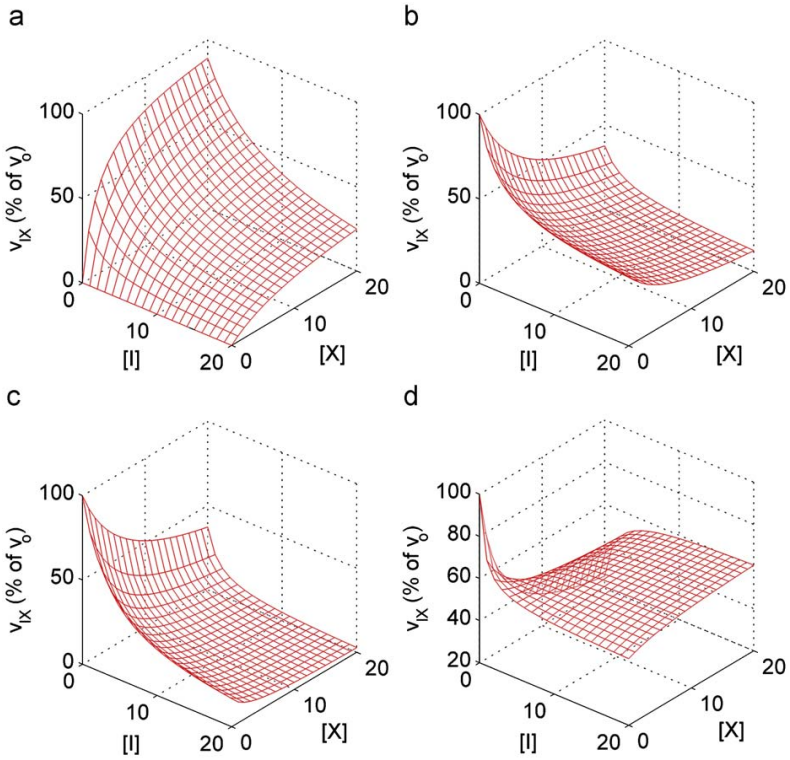

Fig. 5. Plots of the reaction rate as a function of the concentration of two modifiers. Concentrations and inhibition constants are in μM units. (a) An essential activator (X) and a linear competitive inhibitor (I) as shown in Scheme 3, $\alpha_I = \alpha_X = 1$, $\alpha_S = \infty$, a = ∞, b = 1, c = 3 (hindrance), e = ∞, $\sigma = 1$, $\beta_I = 0$, $\beta_X = 1$, $\beta_{IX} = 0$, $K_I = 2$, $K_X = 5$. (b) Two hyperbolic mixed inhibitors exclusive on ES (Scheme 4), $\alpha_I = \alpha_X = \alpha_S = 1$, a = 2, b = 4, c = 1 (independence), e = ∞, $\sigma = 1$, $\beta_I = 0.5$, $\beta_X = 0.3$, $\beta_{IX} = 0$, $K_I = 2$, $K_X = 5$. (c) A linear competitive inhibitor (I) and a hyperbolic mixed inhibitor (X) mutually exclusive on ES (Scheme 5), $\alpha_I = \alpha_X = \alpha_S = 1$, a = ∞, b = 4, c = 0.5 (facilitation), e = ∞, $\sigma = 1$, $\beta_I = 0$, $\beta_X = 0.3$, $\beta_{IX} = 0$, $K_I = 2$, $K_X = 5$. (d) Two non-exclusive hyperbolic mixed inhibitors, both have a predominantly uncompetitive character (Scheme 2), $\alpha_I = \alpha_X = \alpha_S = 1$, a = 0.2, b = 0.5, c = 0.5 (facilitation), e = 0.8, $\sigma = 1$, $\beta_I = 0.3$, $\beta_X = 0.1$, $\beta_{IX} = 0.9$, $K_I = 2$, $K_X = 5$.

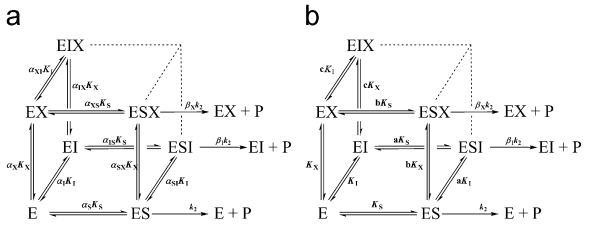

Scheme 4. Two hyperbolic mixed inhibitors. I and X exclude each other when substrate is bound but can coexist in complex with the enzyme alone. Terminology of Scheme 2a (a) and of Scheme 2b (b).

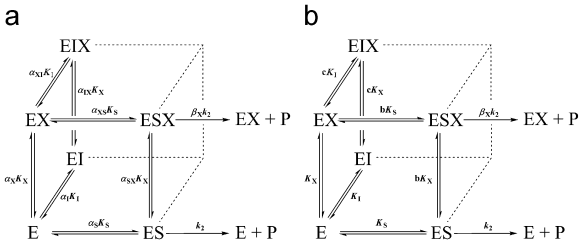

Scheme 5. Reaction paths for a double modifier system consisting of a linear competitive inhibitor (I) and a hyperbolic, mixed inhibitor (X), which can coexist in complex with the enzyme alone. Terminology of Scheme 2a (a) and of Scheme 2b (b).

A.4. Two non-exclusive, hyperbolic mixed inhibitors

The reactions are those shown in Scheme 2b and the rate equation is

$$v_{IX} = v_0(1+\sigma)\frac{1+\beta_I\frac{[I]}{aK_I}+\beta_X\frac{[X]}{bK_X}+\beta_{IX}\frac{[I][X]}{eK_IK_X}}{1+\frac{[I]}{K_I}+\frac{[X]}{K_X}+\frac{[I][X]}{cK_IK_X}+\sigma\left(1+\frac{[I]}{aK_I}+\frac{[X]}{bK_X}+\frac{[I][X]}{eK_IK_X}\right)}. \tag{19}$$

Depending on the interaction coefficients a, b, c, and e, on the residual activities characterized by the three β-values in the numerator of (19), as well as on substrate concentration, this model gives rise to manifold effects that include bizarre results, such as inhibition in a given range of inhibitor concentrations and re-activation from the inhibited state in another (plot in Fig. 5d). An extreme case is the inhibition paradox discussed in Section 3.1.

Appendix B

In the early literature on double inhibition systems, reaction schemes were not always explicitly shown, making readability and interpretation difficult. Therefore, in discussing previous

contributions to this topic in comparison with the present treatment we will show the reaction schemes by sketching them with reactants placed at the eight corners of a cube in the same positions as shown in Scheme 2 even if this was not explicitly done in the original publications. Non-existing paths will be substituted by dashed lines and kinetic parameters will be those of the original publications. For clarity, however, the original rate equations will be written using our present terminology.

B.1. Two competitive inhibitors

Slater and Bonner studied the simultaneous action of fluoride and phosphate on the 'succinic oxidase' system (Slater and Bonner, 1952). This paper dealt with two non-exclusive, linear competitive inhibitors as shown in Scheme 6b. The rate equation (10) by Slater and Bonner in the presence of the two inhibitors, rewritten using our terminology, is the following:

$$v_{IX} = \frac{v_0(1+\sigma)}{1+\frac{[I]}{K_I}+\frac{[X]}{K_X}+\frac{[I][X]}{cK_IK_X}+\sigma}. \tag{20}$$

The four parameters for fluoride and phosphate, K_F, K_{FP}, K_P and K_{PF}, corresponding to our K_X, cK_I, K_I and cK_X, respectively (Scheme 6a) were calculated graphically using double reciprocal plots. The interaction constant between phosphate and fluoride, c in our terminology, can thus be calculated from the data of Slater and Bonner as $K_{PF}/K_F = K_{FP}/K_P = 3.3\times10^{-3}$ (facilitation).

While investigating the inhibition of D-amino acid oxidase, Yagi and Ozawa (1960a) proposed a graphical method for establishing if any interaction occurred between two simultaneously bound inhibitors with the mechanism shown in Scheme 6c. Eq. (6) in Yagi–Ozawa's paper can be rewritten using our general equation (5) and rearranging it with v_0/v_{IX} as the independent variable. This gives

$$\frac{v_0}{v_{IX}} = \frac{1+\frac{[I]}{K_I}+\frac{[X]}{K_X}+\frac{[I][X]}{cK_IK_X}+\sigma}{1+\sigma} \tag{21}$$

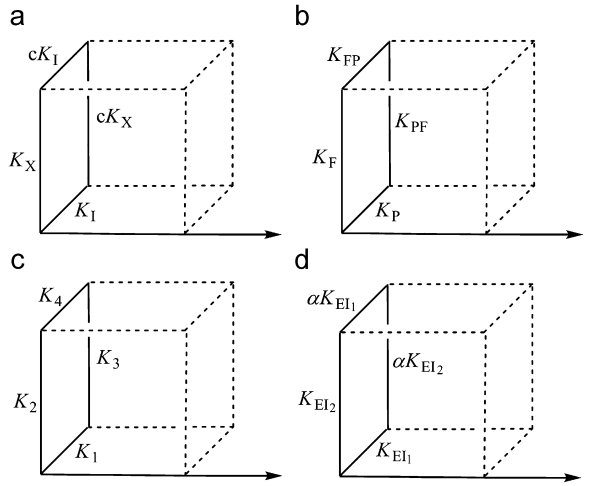

Scheme 6. Abridged reaction schemes for double inhibition by two linear competitive inhibitors described in the literature. Paths from the original publications are compared with the symbolism in this paper. (a) Symbolism in this paper (Scheme 2b); (b) Slater and Bonner (1952); (c) Yagi and Ozawa (1960a); and (d) Yonetani and Theorell (1964).

and Eq. (5) in Yagi and Ozawa (1960a) is obtained by setting $c = \infty$ in (21):

$$\frac{v_0}{v_{IX}} = \frac{1+\frac{[I]}{K_I}+\frac{[X]}{K_X}+\sigma}{1+\sigma}. \tag{22}$$

Eq. (21) is identical with Eq. (20) published eight years before (Slater and Bonner, 1952), which Yagi and Ozawa overlooked. The plot proposed by these authors, v_0/v_{IX} versus a mixture of two inhibitors I and X gives a straight line if the EIX complex is not formed, Eq. (22), or a second-order curve if both inhibitors coexist in a complex with the enzyme, Eq. (21). This method was successful for determining the mechanism of action of antibiotics on D-amino acid oxidase (Yagi and Ozawa, 1960a, 1960b) and was later used by several investigators.

The theoretical issues of the two studies mentioned above were extended to describe double inhibition of liver alcohol dehydrogenase by coenzyme–competitive inhibitor pairs with the reaction scheme shown in Scheme 6d (Yonetani and Theorell, 1964). The interaction coefficient between the two inhibitors, α, is equivalent to the coefficient c in our present symbolism and the equation derived by the authors (their Eq. (13)) is identical to Eq. (10) of (Slater and Bonner, 1952), i.e. Eq. (20) in our terminology. As an elegant variant, Yonetani and Theorell devised a graphical method in which the v_0/v_i ratio is plotted versus the concentration of I_1 while I_2 is kept constant, and versus I_2 at constant I_1. This plot results in a family of parallel straight lines if $c = \infty$ (the two inhibitors exclude each other) and in a set of straight lines converging to a common point in the second quadrant if $0 < c < \infty$ (the two inhibitors are non-exclusive). The Yagi–Ozawa plot can be represented within the Yonetani–Theorell plot by connecting ordinate values for successively increasing I_1 and I_2 concentrations. Among numerous other practical applications, the Yonetani–Theorell plot was used to demonstrate allosteric regulation of α-oxoglutarate dehydrogenase by NAD_{red} (Hall and Weitzman, 1977), and synergism in the inhibition of the HIV type 1 protease by couples of inhibitors (Asante-Appiah and Chan, 1996b). Nevertheless, the Yonetani–Theorell plot cannot be generalized because it is valid only for two linear competitive inhibitors.

In a study of acetylcholinesterase, Allen and Abeles (1989) did not consider any of the previous contributions on double inhibition and re-published the equation for the simultaneous action of two competitive inhibitors discussed above, which was originally derived by Slater and Bonner. The plot used by the authors was based on the reciprocal of Eq. (21) and their coefficient M is equivalent to our 1/c. While nothing is wrong in this paper, the use of the terms positive cooperativity and negative cooperativity to describe the concepts of synergism and antagonism, respectively, cannot be recommended (see Section 3).

B.2. More complex systems

We discuss here double inhibition in a more general context, which includes mixed-type and hyperbolic inhibitors. The basic theories are mainly due to Webb (1963, Chapter 10), Keleti and Fajszi (1971), Fajszi (1974), and Segel (1975, Chapter 8). To facilitate comparison of different treatments, Table 1 lists the elementary steps at the edges of the cube in Scheme 2a, and shows the symbolism used by us and by the authors mentioned in this section. Also, Table 3 lists the interactions that may occur between inhibitors, the free enzyme and the ES complex, their meaning and the symbolism used by different authors.

Chronologically, Webb (1963, Chapter 10) was the first to consider combinations of inhibitions other than competitive. Besides discussing the combination of two competitive inhibitors,

Table 3
Interaction coefficients for the double modifier mechanism when all paths exist (Scheme 2b).

Interaction	This work	Keleti and Fajszi (1971)	Segel (1975)	Webb (1963)
I and X on E	c	$\alpha = \frac{K_{12}}{K_2} = \frac{K_{21}}{K_1}$	γ	α
I and X on ES	$\frac{\gamma_X}{b} = \frac{\gamma_I}{a}$	$\beta = \frac{K_{012}}{K_{02}} = \frac{K_{021}}{K_{01}}$	γ	α
S and X on EI	$\frac{\gamma_S}{a} = \frac{\gamma_X}{c}$	$\gamma = \frac{K_{012}}{K_{12}} = \frac{K_{120}}{K_{10}}$	β	γ
S and I on EX	$\frac{\gamma_I}{c} = \frac{\gamma_S}{b}$	$\delta = \frac{K_{021}}{K_{21}} = \frac{K_{120}}{K_{20}}$	α	β
S on EIX	γ_S	Built-in in K_{120}	$\alpha\beta$	$\beta\gamma$
I on ESX	γ_I	Built-in in K_{021}	$\alpha\gamma$	$\alpha\beta$
X on ESI	γ_X	Built-in in K_{012}	$\beta\gamma$	$\alpha\gamma$

Comparison of symbols and coefficients used by different authors.

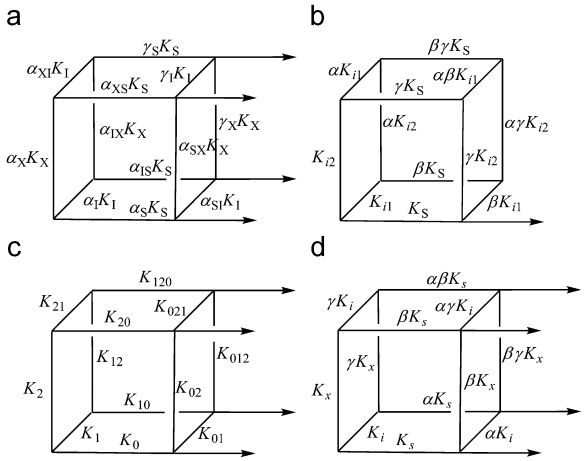

Scheme 7. Abridged reaction schemes for generalized double inhibitions described in the literature. Paths from the original publications are compared with the symbolism in this paper. (a) Symbolism in this paper (Scheme 2a); (b) Webb (1963, Chapter 10); (c) Keleti and Fajszi (1971); and (d) Segel (1975, Chapter 8). Arrows indicate the catalytic steps without symbols.

he derived kinetic equations based on the mechanism shown in Scheme 7b also for the combination of two non-competitive inhibitors or one competitive and one non-competitive inhibitor. On the basis of the coefficient α, the interactions between the two inhibitors were classified as negative ($1<\alpha<\infty$) or positive ($\alpha<1$). The latter case was exemplified by Webb using results discussed above on succinic oxidase (Slater and Bonner, 1952).

Keleti and Fajszi (1971) published a comprehensive treatment of double inhibitions by taking into account all preceding literature and extending the theory to include hyperbolic inhibition. Their reaction scheme is shown in Scheme 7c, which is again written in a way to match the orientation of reactants in our symbolism (Scheme 7a). Keleti and Fajszi used individual symbols for each of the twelve edges of the cube. Apart K_0, K_1 and K_2, which correspond to our K_S, K_I and K_X, respectively, the other symbols include the coefficients of interaction, which can be calculated as the ratio of the constants of two reaction steps on opposite edges on the same face of the cube. For instance, $K_{12}/K_2 = \alpha$ is equivalent to our coefficient c. Using the interaction coefficients, Keleti and Fajszi defined the types of interaction that may occur in double inhibition systems as independence, facilitation, hindrance and exclusion, as specified in the main text (6). A subsequent publication (Fajszi, 1974) was a review of the 1971-paper and included a critical survey of graphical methods for the analysis of double inhibition data.

In the context of double modifier interactions, Keleti (1967) defined *liberator* 'a substance which may liberate the enzyme from the action of an inhibitor without affecting the enzyme activity alone', which is characterized by $\alpha = \beta = 1$ in Scheme 1. This definition was extended also to include the neutralizing action towards activators. In this paper, the author created the mathematical basis and derived equations for describing the kinetics of compounds that were known to act as liberators from a few examples, e.g. the reversible competitive liberation by urea of N-acetylglutamate 5-phosphotransferase from inhibition by arginine (Faragó and Dénes, 1967). Keleti pointed out that a liberator may be competitive, non-competitive or uncompetitive with an inhibitor, and worked out criteria for the differentiation of these mechanisms by considering nine combinations of liberator and inhibitor. There are no mistakes in this interesting treatment, but an attempt at unifying the particular cases in a general scheme is impossible, since Keleti used the same notation of kinetic constants for different paths in nine individually analyzed particular cases. For instance, the symbol K_s' was used for different, unrelated equilibria such as EL+S⇌ELS and EI+S⇌ESI. However, Keleti's treatment for the liberator action can be implemented by using our general Scheme 2a and its simplified variant in Scheme 2b as applicable, as well as the general equation for two modifiers (5), from which the particular cases can be derived in unambiguously. For instance it is sufficient to consider our modifier X to be the liberator, L, described by Keleti.

Segel (1975, Chapter 8) published another thorough scrutiny of double inhibition systems on the basis of the general mechanism shown in Scheme 7d. His theory exactly reproduces the results discussed above (Keleti and Fajszi, 1971; Webb, 1963, Chapter 10), although explicit reference to these previous contributions was not made. All particular cases discussed by Segel can be derived from the general mechanism in Scheme 2 and the corresponding equations can be deduced as particular cases of Eq. (5).

Other contributions to the analysis of combined effects dealt with linear inhibitors (Martinez-Irujo et al., 1998; Reynolds et al., 1970; Semenza and von Balthazar, 1974; Thoma and Crook, 1982). Useful graphical methods for the analysis of the effects produced by two linear inhibitors have been developed (Asante-Appiah and Chan, 1996a; Palatini, 1983a) or for a linear inhibitor combined with a hyperbolic inhibitor (Palatini, 1983b).

The studies mentioned in this section created the frame for a modern interpretation of double inhibition systems. The only difficulty that readers less experienced in enzyme kinetics may encounter with the equations published in these papers is the labor necessary to decipher symbols and to put equations to work in practical cases. The explicit labeling of interaction coefficients with reactant-related indices, as shown in Scheme 2a, avoids the need of continuous referencing to their definitions and makes them understandable at first sight. When one or more of the paths in the general mechanism (Scheme 2a) do not exist, or if ordered binding is present, our nomenclature provides an unambiguous description of the system. The interpretation of the interaction coefficients is more straightforward in our treatment than in those of Segel and Webb. At first sight, the notation in our nomenclature (Scheme 2b), does not clearly show the property of the thermodynamic boxes. For instance $cK_I\gamma_S K_S$ is seemingly not the same as $bK_S\gamma_I K_I$ in our nomenclature but this apparent discrepancy is removed after considering the relationships (4) in the main text. Segel and Webb notation is on the contrary immediate and clearly reveals the consistency of the thermodynamic boxes. However, as shown in Table 3, the interactions of I and X on E, and of I and X on ES, appear to be the same using the

terminologies of Segel or Webb. This arises from the use of the same symbol (γ by Segel and α by Webb) in two different thermodynamic boxes, which implies that the relationship of the ternary complexes ESI, ESX and EIX with the quaternary complex ESIX can be deduced from the preceding steps.

References

Allen, K.N., Abeles, R.H., 1989. Inhibition kinetics of acetylcholinesterase with fluoromethyl ketones. Biochemistry 28, 8466–8473.

Asante-Appiah, E., Chan, W.W., 1996a. Analysis of the interactions between an enzyme and multiple inhibitors using combination plots. Biochem. J. 320 (Pt 1), 17–26.

Asante-Appiah, E., Chan, W.W., 1996b. Synergistic binding of inhibitors to the protease from HIV type 1. Biochem. J. 315 (Pt 1), 113–137.

Baici, A., 1981. The specific velocity plot. A graphical method for determining inhibition parameters for both linear and hyperbolic enzyme inhibitors. Eur. J. Biochem. 119, 9–14, doi:10.1111/j.1432-1033.1981.tb05570.x.

Baici, A., 1998. Inhibition of extracellular matrix-degrading endopeptidases: problems, comments, and hypotheses. Biol. Chem. 379, 1007–1018.

Baici, A., Dicházi, C., Neszmélyi, A., Móczár, E., Hornebeck, W., 1993. Inhibition of the human leukocyte endopeptidases elastase and cathepsin G and of porcine pancreatic elastase by N-oleoyl derivatives of heparin. Biochem. Pharmacol. 46, 1545–1549, doi:10.1016/0006-2952(93)90321-M.

Berenbaum, M.C., 1977. Synergy, additivism and antagonism in immunosuppression. A critical review. Clin. Exp. Immunol. 28, 1–18.

Berenbaum, M.C., 1989. What is synergy?. Pharmacol. Rev. 41, 93–141.

Bincoletto, C., Tersariol, I.L.S., Oliveira, C.R., Dreher, S., Fausto, D.M., Soufen, M.A., Nascimento, F.D., Caires, A.C.F., 2005. Chiral cyclopalladated complexes derived from N,N-dimethyl-1-phenethylamine with bridging bis(diphenylphosphine)-ferrocene ligand as inhibitors of the cathepsin B activity and as antitumoral agents. Bioorg. Med. Chem. 13, 3047–3055, doi:10.1016/j.bmc.2005.01.057.

Botts, J., Morales, M., 1953. Analytical description of the effects of modifiers and of enzyme multivalency upon the steady state catalyzed reaction rate. Trans. Faraday Soc. 49, 696–707.

Brandt, M., Greway, A.T., Holt, D.A., Metcalf, B.W., Levy, M.A., 1990. Studies on the mechanism of steroid 5-a-reductase inhibition by 3-carboxy A-ring aryl steroids. J. Steroid Biochem. Mol. Biol. 37, 575–579, doi:10.1016/0960-0760(90)90403-8.

Chou, T.C., Talalay, P., 1977. A simple generalized equation for the analysis of multiple inhibitions of Michaelis–Menten kinetic systems. J. Biol. Chem. 252, 6438–6442.

Chou, T.C., Talalay, P., 1981. Generalized equations for the analysis of inhibitions of Michaelis–Menten and higher-order kinetic systems with two or more mutually exclusive and nonexclusive inhibitors. Eur. J. Biochem. 115, 207–216.

Cornish-Bowden, A., 1986. Why is uncompetitive inhibition so rare? A possible explanation, with implications for the design of drugs and pesticides. FEBS Lett. 203, 3–6, doi:10.1016/0014-5793(86)81424-7.

Cornish-Bowden, A., 2004. Fundamentals of Enzyme Kinetics. Portland Press, London.

Dunwiddie, C., Thornberry, N.A., Bull, H.G., Sardana, M., Friedman, P.A., Jacobs, J.W., Simpson, E., 1989. Antistasin, a leech-derived inhibitor of factor Xa. Kinetic analysis of enzyme inhibition and identification of the reactive site. J. Biol. Chem. 264, 16694–16699.

Fajszi, C., 1974. Methods of analysis of double inhibition experiments. Symp. Biol. Hung. 18, 77–103.

Fajszi, C., Keleti, T., 1974. Kinetic basis of enzyme regulation. The triple-faced enzyme–inhibitor relation and the inhibition paradox. Symp. Biol. Hung. 18, 105–119.

Faragó, A., Dénes, G., 1967. Mechanism of arginine biosynthesis in *Chlamydomonas reindardti*. II. Purification and properties of N-acetylglutamate 5-phosphotransferase, the allosteric enzyme of the pathway. Biochim. Biophys. Acta 136, 6–18, doi:10.1016/0304-4165(67)90315-7.

Franzke, C.W., Baici, A., Bartels, J., Christophers, E., Wiedow, O., 1996. Antileukoprotease inhibits stratum corneum chymotryptic enzyme. Evidence for a regulative function in desquamation. J. Biol. Chem. 271, 21886–21890.

Fraser, T.R., 1870–1871. An experimental research on the antagonism between the actions of physostigma and atropia. Proc. R. Soc. Edin. 7, 506–511.

Frieden, C., 1964. Treatment of enzyme kinetic data. I. The effect of modifiers on the kinetic parameters of single substrate enzymes. J. Biol. Chem. 239, 3522–3531.

Früh, H., Kostoulas, G., Michel, B.A., Baici, A., 1996. Human myeloblastin (leukocyte proteinase 3): reactions with substrates, inactivators and activators in comparison with leukocyte elastase. Biol. Chem. 377, 579–586.

Gao, W.Q., Anderson, P.J., Majerus, E.M., Tuley, E.A., Sadler, J.E., 2006. Exosite interactions contribute to tension-induced cleavage of von Willebrand factor by the antithrombotic ADAMTS13 metalloprotease. Proc. Natl. Acad. Sci. USA 103, 19099–19104.

Hall, E.R., Weitzman, P.D.J., 1977. Evidence for allosteric NADH regulation of acinetobacter a-oxoglutarate dehydrogenase from multiple-inhibition studies. Biochem. Biophys. Res. Commun. 74, 1613–1617, doi:10.1016/0006-291X(77)90627-1.

International Union of Biochemistry, 1982. Symbolism and terminology in enzyme kinetics. Recommendations 1981. Eur. J. Biochem. 128, 281–291.

Keleti, T., 1967. The liberator. J. Theor. Biol. 16, 337–355, doi:10.1016/0022-5193(67)90060-4.

Keleti, T., Fajszi, C., 1971. The system of double inhibitions. Math. Biosci. 12, 197–215, doi:10.1016/0025-5564(71)90016-2.

King, J.B., West, M.B., Cook, P.F., Hanigan, M.H., 2009. A novel, species-specific class of uncompetitive inhibitors of g-glutamyl transpeptidase. J. Biol. Chem. 284, 9059–9065.

Kostoulas, G., Hörler, D., Naggi, A., Casu, B., Baici, A., 1997. Electrostatic interactions between human leukocyte elastase and sulfated glycosaminoglycans: physiological implications. Biol. Chem. 378, 1481–1489.

Leoncini, R., Pagani, R., Marinello, E., Keleti, T., 1989. Double inhibition of L-threonine dehydratase by aminothiols. Biochim. Biophys. Acta 994, 52–58, doi:10.1016/0167-4838(89)90061-7.

Lien, L.V., Ecsedi, G., Keleti, T., 1979a. Double inhibition of D-glyceraldehyde-3-phosphate dehydrogenase and lactate dehydrogenase. Acta Biochim. Biophys. Acad. Sci. Hung. 14, 11–17.

Lien, L.V., Koubakouenda, H., Keleti, T., 1979b. pH and temperature dependence of the double inhibition of D-glyceraldehyde-3-phosphate dehydrogenase by ATP and quinaldate. Acta Biochim. Biophys. Acad. Sci. Hung. 14, 19–24.

Lienhard, G.E., 1971. Enzymatic catalysis and the transition state theory of reaction rates: transition state analogs. Cold Spring Harbor Symp. Quant. Biol. 36, 45–51.

Loewe, S., Muischnek, H., 1926. Über Kombinationswirkungen. I. Mitteilung: Hilfsmittel der Fragestellung. Arch. Exp. Pathol. Pharmakol. 114, 313–326.

Mares-Guia, M., Shaw, E., 1965. Studies on active center of trypsin. The binding of amidines and guanidines as models of the substrate side chain. J. Biol. Chem. 240, 1579–1585.

Martinez-Irujo, J.J., Villahermosa, M.L., Mercapide, J., Cabodevilla, J.F., Santiago, E., 1998. Analysis of the combined effect of two linear inhibitors on a single enzyme. Biochem. J. 329, 689–698.

Mazat, F., Langla, J., Mazat, J.P., 1981. The measure of synergy in enzymatic regulation. A general coefficient. Biochimie 63, 107–111, doi:10.1016/S0300-9084(81)80173-3.

Palatini, P., 1983a. A new plot for multiple enzyme inhibition. Biochem. Int. 7, 247–254.

Palatini, P., 1983b. The interaction between full and partial inhibitors acting on a single enzyme. A theoretical analysis. Mol. Pharmacol. 24, 30–41.

Reynolds, C.H., Morris, D.L., McKinley-McKee, J.S., 1970. Complexes of liver alcohol dehydrogenase. Further studies on the rate of inactivation. Eur. J. Biochem. 14, 14–26.

Schweizer, A., Roschitzki-Voser, H., Amstutz, P., Briand, C., Gulotti-Georgieva, M., Prenosil, E., Binz, H.K., Capitani, G., Baici, A., Plückthun, A., Grütter, M.G., 2007. Inhibition of caspase-2 by a designed ankyrin repeat protein: specificity, structure, and inhibition mechanism. Structure 15, 625–636, doi:10.1016/j.str.2007.03.014.

Segel, I.H., 1975. Enzyme Kinetics. Behavior and Analysis of Rapid Equilibrium and Steady-State Enzyme Systems. Wiley, New York.

Semenza, G., von Balthazar, A.K., 1974. Steady-state kinetics of rabbit-intestinal sucrase. Kinetic mechanism, Na+ activation, inhibition by tris(hydroxymethyl)aminomethane at the glucose subsite. Eur. J. Biochem. 41, 149–162.

Slater, E.C., Bonner Jr., W.D., 1952. The effect of fluoride on the succinic oxidase system. Biochem. J. 52, 185–196.

Thoma, J.A., Crook, C., 1982. Subsite mapping of enzymes. Double inhibition studies. Eur. J. Biochem. 122, 613–618.

Topham, C.M., Brocklehurst, K., 1992. In defence of the general validity of the Cha method of deriving rate equations. The importance of explicit recognition of the thermodynamic box in enzyme kinetics. Biochem. J. 282, 261–265.

Webb, J.L., 1963. Enzyme and Metabolic Inhibitors. General Principles of Inhibition, vol. 1. Academic Press, New York.

Yagi, K., Ozawa, T., 1960a. Mechanism of inhibition of D-amino acid oxidase. III. Kinetic analysis of the behaviour of chloramphenicol, streptomycin and penicillin in their competition with flavin–adenine dinucleotide. Biochim. Biophys. Acta 39, 304–310, doi:10.1016/0006-3002(60)90815-5.

Yagi, K., Ozawa, T., 1960b. Complex formation of apo-enzyme, coenzyme and substrate of D-amino acid oxidase. I. Kinetic analysis using indicators. Biochim. Biophys. Acta 42, 381–387, doi:10.1016/0006-3002(60)90167-0.

Yonetani, T., Theorell, H., 1964. Studies on liver alcohol dehydrogenase complexes. III. Multiple inhibition kinetics in the presence of two competitive inhibitors. Arch. Biochem. Biophys. 106, 243–251, doi:10.1016/0003-9861(64)90184-5.

Paradoxical interactions between modifiers and elastase-2

Manuscript

Abstract

Die Serinendopeptidase Elastase-2 der menschlichen polymorphonuklearen Leukozyten wird in Verbindung gebracht mit der physiologischen Umgestaltung und dem pathologischen Abbau der extrazellulären Matrix. Die während dem proteolytischen Abbau der 'Core'-Proteine freigesetzten Glykosaminoglykane sind potentielle Liganden der Elastase-2. *In vitro* resultiert diese Interaktion bei tiefer Konzentration der Glykosaminoglykane in einer Hemmung der Enzymaktivität. Diese Hemmung wird jedoch bei höheren Konzentrationen der Liganden teilweise oder gar vollständig aufgehoben. Ein solches Verhalten, ausgelöst durch einen Mechanismus welcher mindestens zwei Glykosaminoglykan-Moleküle involviert, kann den Effekt natürlich vorkommender Inhibitoren beeinflussen, insbesondere jener des α_1-Peptidaseinhibitors. Vor allem bei tiefen Konzentrationen wirken die Glykosaminoglykane der Formation eines Enzym-Inhibitor Komplexes entgegen und stimulieren zudem die proteolytische Aktivität. Diese Beeinträchtigung der Hemmung der Elastase-2 im extrazellulären Raum wird in Verbindung gebracht mit einem fein abgestimmten Kontrollmechanismus in der Mikroumgebung eines Enzyms beim Um- und Abbau der extrazellulären Matrix.

MANUSCRIPT

Paradoxical interactions between modifiers and elastase-2

Patricia Schenker and Antonio Baici*
Department of Biochemistry, University of Zurich, Winterthurerstrasse 190, CH-8057 Zurich, Switzerland

*Corresponding author: Department of Biochemistry, University of Zurich, Winterthurerstrasse 190, CH-8057 Zurich, Switzerland. Tel.: +41-44-6355542, Fax: +41-44-6356805, E-mail: abaici@bioc.uzh.ch

Abstract
The serine endopeptidase elastase-2 from human polymorphonuclear leukocytes is associated with physiological remodeling and pathological degradation of the extracellular matrix. Glycosaminoglycans released after proteolytic processing of the core proteins of proteoglycans are potential ligands of elastase-2. In vitro, this interaction results in enzyme inhibition in a low concentration range of the glycosaminoglycans. However, inhibition is reversed and even abolished at high concentrations of the ligands. This behavior, which can be interpreted with a mechanism involving at least two molecules of glycosaminoglycan binding the enzyme at different sites, may cause interferences with the natural protein inhibitors of elastase-2, particularly the α-1-peptidase inhibitor. Especially at low concentrations, glycosaminoglycans contrast the formation of the enzyme-inhibitor complex and stimulate proteolytic activity as well. This negative interference on elastase-2 inhibition in the extracellular space is put in relation with a finely-tuned control mechanism in the microenvironment of the enzyme during remodeling and degradation of the extracellular matrix.

Keywords: Inhibition, Activation, Multiple interactions, Serine peptidases, Electrostatic interactions, Glycosaminoglycans

List of abbreviations: MeOSuc, N-Methoxysuccinyl; pNA, p-nitroanilide; α1-PI, α-1-peptidase inhibitor; Ch4S, chondroitin-4-sulfate; Ch6S, chondroitin-6-sulfate; DS, dermatan sulfate; PPS, pentosan polysulfate. DU, disaccharide units; MU, monomer units.

1 Introduction

The serine endopeptidase elastase-2 (human leukocyte elastase) is a basic protein with an isoelectric point of 10.5. Eighteen of the 19 arginine residues constituting the primary structure of the protein are located at the surface of the molecule [1] and may be engaged in electrostatic interactions with anionic partners [2]. Elastase-2, together with cathepsin G and myeloblastin, released extracellularly from neutrophilic polymorphonuclear leukocytes during inflammation and in a variety of pathological conditions, can be very destructive by degrading several components of the extracellular matrix [3]. Sulfated glycosaminoglycans, constituents of the proteoglycans, have been shown to interact with the three leukocytic enzymes and to modulate their enzymatic activity [2,4-9]. In particular, elastase-2 undergoes inhibition by chondroitin sulfate isomers, dermatan sulfate (DS) and related sulfated polysaccharides with a high-affinity, electrostatically-driven, hyperbolic mixed-type inhibition mechanism with a predominantly competitive character [2]. The evaluation of these interactions was based on measuring enzymatic activity for increasing concentrations of the modifiers at several fixed concentrations of a suitable substrate until a plateau was reached. We and others [10] observed a puzzling reversal of inhibition, and occasionally complete abolishment of the original inhibition, by increasing the concentration of modifiers by orders of magnitude beyond the level that produced inhibition but did not discuss this phenomenon for the lack of a plausible molecular explanation.

After excluding experimental artifacts and in the light of a recent theoretical assessment of multiple interactions between enzymes and modifiers [11], we describe here the varying behavior of sulfated polysaccharides as modulators of elastase-2 activity. These interactions become important at the interface between insoluble extracellular matrix components and physiological fluids, where the enzyme is engaged in multiple interactions with glycosaminoglycans bound to the matrix, or released from it, and naturally-occurring inhibitors.

2 Materials and Methods

2.1 *Materials*

Elastase-2 (EC 3.4.21.37, Merops database S01.131) was obtained from Elastin Product Company (Owensville, USA). The lyophilized enzyme was dissolved at a concentration of 2.5 mg/mL in 0.1 M sodium acetate buffer, pH = 4.50 and stored in aliquots at -20°C. The concentration of enzyme active sites was determined by titration with MeOSuc-AAPV-CH_2Cl and measuring the residual activity with MeOSuc-AAPV-pNA. Inactivator and substrate were purchased from Bachem (Bubendorf, Switzerland).

Chondroitin-4-sulfate (Ch4S) sodium salt from bovine trachea

and chondroitin sulfate (mixed isomers) from whale cartilage, as well as chondroitin-6-sulfate (Ch6S) sodium salt from shark cartilage were obtained by Sigma - Aldrich Chemie (Buchs, Switzerland). DS from porcine intestinal mucosa was purchased from Calbiochem (Nottingham, UK). Although labeled 'chondroitin-4-sulfate' and 'chondroitin-6-sulfate', these compounds are in reality co-polymers of the 4- and 6-isomers along the same chain and contain also sulfate-free sequences. Ch4S from bovine trachea contained 69% of 4-sulfate and 25% of 6-sulfate; Ch6S contained 45% of 4-sulfate and 54% of 6-sulfate; DS contained 98% of 4-sulfate. Balance to 100% was non-sulfated material. Analyses were performed by HPLC of the unsaturated disaccharides after digestion with chondroitinase ABC as described previously [12]. Pentosan polysulfate (PPS, structure shown in Fig. 3F) was a generous gift from Bene PharmaChem (Geretsried, Germany). All sulfated polysaccharides were dried for 4 hours at 95°C to remove water, weighted and immediately dissolved in distilled water to produce stock solutions of known concentrations. The molecular masses were determined at the Istituto di Ricerche Chimiche e Biochimiche G. Ronzoni (Milano, Italy) by the courtesy of Dr. Antonella Bisio. The procedure is based on high performance liquid chromatography combined with a triple detector array composed of right-angle laser light scattering, refractometer and viscometer [13].

Table 1: Molecular mass of the modifiers. Molecular masses are shown as Mn (number-average), Mw (weight-average) and Mp (molecular mass at the top of the chromatographic peak) measured as described by Bertini et al. [13]. The polydispersity index Mw/Mn is a measure of the molecular mass distribution within a sample. Mp would coincide with Mn and Mw for Mn/Mw = 1. DU, disaccharide units; MU, monomeric units. Ch4S was from bovine trachea.

Modifier	**Mn**	**Mw**	**Mp**	**Mw/Mn**	**Average number of units/chain**
DS	22,022	26,488	25,297	1.203	~ 52 DU
Ch4S	18,843	23,229	20,912	1.233	~ 46 DU
Ch6S	58,810	65,668	63,023	1.117	~ 130 DU
PPS	3,687	5,202	3,888	1.411	~ 15 MU

The isomeric composition and molecular mass of chondroitin sulfate from whale cartilage were not determined (this compound was used for qualitative comparisons), while the characteristics of the other polysaccharides are summarized in Table 1. Their concentration will be expressed as the concentration of the basic unit, which is a monosulfated disaccharide for chondroitin sulfates and DS (Mr = 503.36) and a disulfated monosaccharide for PPS (Mr = 336.27).

Eglin c from the leech Hirudo medicinalis (Merops database identifier I13.001) was purified and characterized as described [14,15] and its protein concentration was confirmed by amino acid analysis. A tetrapeptide inhibitor based on the amino acid sequence 60-63 of eglin c, H-TNVV-OMe [16], was obtained from Bachem (Bubendorf, Switzerland). Human α-1-peptidase inhibitor (α1-PI, Merops database identifier I04.001) was from Behring.

2.2 *Kinetic methods*

Kinetic measurements were performed using disposable acrylic cuvettes at 25 ± 1°C in 50 mM Tris/HCl buffer with NaCl added to an ionic strength of 100 mM; the pH was 7.40 and 0.01% Triton X-100 was added to prevent enzyme adsorption to vessels. The buffer was prepared and used at 25°C. The substrate MeOSuc-AAPV-pNA was dissolved in dimethyl sulfoxide before dilution into the assay buffer, and the final assay concentration of dimethyl sulfoxide was less than 0.1% (v/v). K_m was determined by fitting the Michaelis-Menten equation by non-linear regression to data with substrate concentrations ranging from 0.2 K_m to 5 K_m. Reaction progress was monitored at 405 nm with a Cary 50 spectrophotometer and the concentration of released p-nitroaniline was calculated using an absorption coefficient of 9920 $\mathrm{M^{-1}cm^{-1}}$. Regression analysis was performed with GraphPad Prism version 5.02 for Windows (GraphPad Software, San Diego California USA, www.graphpad.com). Inhibition of elastase-2 by sulfated polysaccharides was analyzed with the four parameter logistic equation adapted to kinetic measurements [2]:

$$v_\mathrm{i} = v_0 - \frac{(v_0 - v_\infty)\,[\mathrm{I}]^h}{K_{0.5}^h + [\mathrm{I}]^h} \qquad (1)$$

In equation (1) v_i is the inhibited velocity, v_0 is the velocity in the absence of modifiers, v_∞ is the velocity after reaching the plateau (saturating inhibitor I), $K_{0.5}$ is the inhibitor concentration for which the velocity equals $(v_0\text{-}v_\infty)/2$, and h is the Hill coefficient, usually not an integer. All measurements were performed at a known, fixed substrate concentration.

Double enzyme-modifier interactions were treated according to Schenker and Baici [11] with the mechanism shown in Scheme 1 and equation

(2).

$$v_{\mathrm{IX}} = v_0(1+\sigma)\left(1+\beta_{\mathrm{I}}\frac{[\mathrm{I}]}{\mathrm{a}K_{\mathrm{I}}} +\beta_{\mathrm{X}}\frac{[\mathrm{X}]}{\mathrm{b}K_{\mathrm{X}}}+\beta_{\mathrm{IX}}\frac{[\mathrm{I}][\mathrm{X}]}{\mathrm{e}K_{\mathrm{I}}\mathrm{K}_{\mathrm{X}}}\right)/ \left(1+\frac{[\mathrm{I}]}{K_{\mathrm{I}}}+\frac{[\mathrm{X}]}{K_{\mathrm{X}}}+\frac{[\mathrm{I}][\mathrm{X}]}{\mathrm{c}K_{\mathrm{I}}\mathrm{K}_{\mathrm{X}}}\right) \sigma\left(1+\frac{[\mathrm{I}]}{\mathrm{a}K_{\mathrm{I}}}+\frac{[\mathrm{X}]}{\mathrm{b}K_{\mathrm{X}}}+\frac{[\mathrm{I}][\mathrm{X}]}{\mathrm{e}K_{\mathrm{I}}\mathrm{K}_{\mathrm{X}}}\right) \quad (2)$$

v_{IX} represents the rate in presence of the two modifiers I and X, v_0 the rate in the absence of modifiers, and $\sigma = [\mathrm{S}]/K_{\mathrm{m}}$. The coefficients a, b and c are those in Scheme 1, and $\mathrm{e} = \mathrm{a}\gamma_{\mathrm{X}} = \mathrm{b}\gamma_{\mathrm{I}} = \mathrm{c}\gamma_{\mathrm{S}}$.

3 Results and Discussion

3.1 *Inhibition of elastase-2 by sulfated polysaccharides*

We previously demonstrated that the interaction between elastase-2 and sulfated polysaccharides resulted in concentration-dependent inhibition of the enzyme activity. We used semisynthetic glycosaminoglycan derivatives of precisely defined isomeric composition and molecular mass for interpreting the effects arising from specific structural elements of the polysaccharides [2]. These effects were based on electrostatic interactions between the positively charged arginine residues at the surface of the enzyme molecule and the negatively charged polysaccharides. The general inhibition mechanism was hyperbolic mixed-type with predominantly competitive character but could not be adequately analyzed with the specific velocity equation [17] because of cooperative effects and multiple binding of the modifiers at different sites. Therefore, the affinity between binders and the enzyme was evaluated with the four parameter logistic equation (1). Without assuming a particular mechanism, this empirical model gives a good estimate of the affinity ($K_{0.5}$), an equivalent of the inhibition constant, and of any cooperativity in the binding process described by the Hill coefficient h. This is a useful approach for comparing the properties of structurally related modifiers.

In nature, sulfated glycosaminoglycans are highly polydisperse and the chondroitin sulfates exist as copolymers of the 4- and 6-sulfate isomers with composition and average molecular masses depending on animal species and tissue. Fig. 1 shows the inhibition of elastase-2 by naturally occurring chondroitin and dermatan sulfates and by a semisynthetic sulfated polysaccharide of plant origin (PPS) used as a reference. Solid curves represent fits to data using equation (1) and the best fit parameters $K_{0.5}$ and h are shown in the panels of Fig. 1. Ch4S had the weakest interaction with elastase-2 among the tested polysaccharides and Ch6S the strongest. Two factors contribute to the higher affinity of the 6-isomer: the larger average molecular mass, with about 130 disaccharide units per chain, compared with only 46 for the 4-isomer (Table 1), and more favorable electrostatic interaction with

elastase-2 [2]. DS is sulfated at position 4 of the galactosamine ring and shows higher affinity to elastase-2 compared with chondroitin4-sulfate with a similar average molecular mass. The tighter binding is due to higher conformational flexibility that allows adapting the molecule to strong interactions with several biomolecules [18]. PPS was considered in this study as a reference molecule with a high degree of uniform sulfation and moderate polydispersity. The affinity of this sulfated polysaccharide was high, with $K_{0.5}$ = 49 nM and a Hill coefficient of 2.3, indicating cooperative binding to elastase-2 evidenced by the sigmoid appearance of the saturation curve (Fig. 1D). As discussed previously [2], partial inhibition of elastase-2 by negatively charged polymers can be ascribed to electrostatic interactions between the 18 positively charged arginine residues at the surface of the enzyme (Fig. 2) and the negatively charged polysaccharides. In particular, when Arg^{217A} interacts electrostatically with polyanions, interference with substrate binding causes partial inhibition.

3.2 *Reactivation of elastase-2 following inhibition*

In order to simulate a plausible natural situation, in which glycosaminoglycans are present at high concentration in the microenvironment in which elastase-2 is active, we performed measurements as shown in Fig. 3 with modifier concentrations increased as much as experimentally possible. Partial or full, concentration-dependent reactivation following the original inhibition occurred in all cases and is best represented on a logarithmic scale. In Fig. 3, Ch4S from whale cartilage is shown in addition to the four polysaccharides in Fig. 1 to show that isomer composition and chain length give rise to different effects (compare panels C and D in Fig. 3). The paradoxical effects shown in Fig. 3 can be interpreted by considering at least two molecules of the polyanion concomitantly binding elastase-2 as shown in the double-modifier mechanism in Scheme 1 and equation (2). According to this mechanism, two hyperbolic inhibitors, or two molecules of the same hyperbolic inhibitor, which bind an enzyme at the same time at two different sites, can induce inhibition in the low concentration range of the modifiers and reverse inhibition at higher concentrations [11]. The analysis of such a system with two modifiers that are individually available is straightforward: measurements are first performed with the modifiers separately and then in various combinations of concentrations. In the case of the sulfated polysaccharides, the effector molecules are constituents of the same sample and their effects on enzyme activity can only be measured by increasing their concentration at a constant ratio. The mole fraction of the individual molecules binding the enzyme at either site is unknown and any attempt at calculating the individual kinetic constants by regression analysis would be

arbitrary. Nevertheless, the simulated inhibition-reactivation profiles shown in Fig. 4, which produce the same effects observed in this study, suggest that a double-modifier mechanism is a plausible model to explain the observed effects. The parameters used for simulating the effects in Fig. 4 were chosen arbitrarily to match experimental results such as those shown in Fig. 3.

The heterogeneous composition of the glycosaminoglycans does not allow speculating which molecular species are responsible for inhibition and its reversal. Given the three arginine residue belts at the surface of the enzyme molecule (Fig. 2), even three binding modes can be envisaged. For this reason, PPS, which has a uniform structure (Fig. 3F), was taken as a reference. As shown in Fig. 3E, reversal of inhibition was complete much like the chondroitin sulfates pointing to the suggestion that the same molecule is capable of binding the enzyme at different sites with different effects. Thus, assuming only two binding sites, one binding mode is responsible for partial inhibition and the other acts as either a liberator (Fig. 4A) or produce an antagonistic effect (Fig. 4B). In the absence of inhibitors or activators, a liberator does not interfere with enzyme activity [11,19].

3.3 *Interference of polysaccharides with inhibitors of elastase-2*

The interaction between sulfated polysaccharides and elastase-2 may favor or disfavor the action of naturally occurring protein inhibitors at sites of action of the enzyme. This event is likely to occur at the interface between extracellular matrix and enzyme engaged in the turnover of proteoglycans. We measured the effects of sulfated polysaccharides on inhibition of elastase-2 by eglin c and α1-PI, whose kinetic mechanisms of inhibition are known [14,20]. Furthermore, we considered the low molecular mass tetrapeptide inhibitor H-TNVV-OMe derived from the active site sequence, amino acids 60-63, of eglin c [16]. The goal of these measurements was to evaluate any disturbance to inhibition by added polysaccharides at two fixed concentrations representing their inhibitory and reactivation concentration ranges. Since eglin c and α1-PI are slow acting modifiers of elastase-2, progress curves were collected at five concentrations of the two inhibitors without added polysaccharides and in the presence of Ch4S from whale cartilage as well as PPS. The reaction profiles are shown in Supplementary Material as Suppl. Fig. 1. The information sought with these experiments was to determine the apparent first-order rate constant of the exponential phase (λ) and the steady-state rate (v_s). Therefore, we fitted an equation for exponential

rise followed by steady-state without ascribing results to a particular mechanism (Suppl. Fig. 1). Problems arising from tight-binding did not affect interpretation because the purpose of the experiment was to compare kinetic parameters obtained in the absence or presence of effectors, not to determine absolute values from their dependency on the concentration of eglin c and α1-PI. The effects brought about on inhibition by α1-PI and eglin c by Ch4S, calculated by regression analysis of progress curves, are shown in Fig. 5. For increasing α1-PI and eglin c concentrations the steady-state rate for substrate hydrolysis leveled off to zero as expected but in presence of the glycosaminoglycan the rate was 10 times higher at the highest α1-PI concentration and 4 times higher at the highest eglin c concentration (Fig. 5A,C and insets). The first-order rate constant (λ) for the exponential approach to steady-state (Fig. 5B,D) was significantly smaller in presence of Ch4S, and the effect was more appreciable at a low concentration of Ch4S. This retardation effect on the functionality of α1-PI towards elastase-2 is similar to that caused by heparin, DNA and other polynucleotides on the inhibition of the same enzyme by the secretory leukocyte peptidase inhibitor and α1-PI [21-24]. Lowering the rate for enzyme-inhibitor complex formation, which can arise for a variety of reasons, is a serious drawback for the control of extracellularly acting peptidases [25]. An almost identical behavior with the same trends shown in Fig. 5 was present in PPS added to both α1-PI and eglin c. These data are not shown here but the trend can easily be deduced from the original progress curves shown in Supplementary material.

The effect of PPS on elastase-2 inhibition by H-TNVV-OMe, a classical, fast acting linear competitive inhibitor of elastase-2 corresponding to amino acids 60-63 of eglin c, is shown in Fig. 6. The polysaccharide weakened the effectiveness of the inhibitor at a low concentration and potentiated it at a higher concentration. Such effects are not predictable by considering the action of the polysaccharide alone at the same concentration. In fact, 0.28 µM MU of PPS reduced enzyme activity by about 80% (Fig. 1D) and 5.6 mM MU of this polysaccharide reduced the activity by 40% (Fig. 3E), while in the presence of the tetrapeptide inhibitor, PPS showed an opposite trend. The same experiments were performed also with Ch6S and DS and the equation for linear competitive inhibition was fitted to data to calculate the changes in K_i. Curves are not shown for Ch6S and DS but all numerical results are shown in Table 2.

Due to multiple binding interactions resulting from the binding of eglin c and the modifiers, K_i must be interpreted as an apparent K_i. A common trend of the sulfated polysaccharides was to increase the apparent K_i (thus decreasing the affinity of eglin c for elastase-2) when used at a low concentration, i.e. that producing the maximal in-

hibitory activity when acting on the enzyme alone. At a higher concentration of the polysaccharides, corresponding to the reactivating phase when used alone (Fig. 3), the effects ranged from lowering K_i by PPS, moderately increasing K_i by DS and no effect on K_i by Ch6S (Table 2). The different effects produced by sulfated polysaccharides on inhibition of elastase-2 by eglin c and by the tetrapeptide derived from his sequence, suggest a particular binding mode of the polysaccharides to elastase-2. In the nomenclature of Schechter and Berger [26], the four amino acids of H-TNVV-OMe bind at positions S4-S3-S2-S1 in the same order as written, namely T binds to S4 and so on, while eglin c is expected to occupy also the primed positions. The fact that polysaccharides exert concentration dependent effects on the efficiency of H-TNVV-OMe for the enzyme (Table 2) but always weaken eglin c binding (Fig. 5) suggests an interaction of polysaccharides with the primed sites of elastase-2, where protein substrates and macromolecular protein inhibitors bind.

Table 2: Inhibition of elastase-2 by the eglin c derived tetrapeptide H-TNVV-OMe. Measurement conditions specified in Fig. 6. The equation for classical competitive inhibition was fitted to data and the K_i values, calculated to take into account a $[S]/K_m$ ratio of 1, are expressed as µM of DU (Ch4S and DS) or in µM of MU (PPS). K_i represents the inhibition dissociation constant of the enzyme-inhibitor complex. In the presence of polysaccharides this must be considered a $K_{i,app}$ value.

Modifier	K_i **(µM)**	**fold increase or decrease**
None	87.7 ± 2.2	
PPS, 0.28 µM MU	142.5 ± 9.2	1.62
PPS, 5.6 mM MU	37.7 ± 1.2	0.43
None	79.3 ± 4.5	
DS, 0.1 mM DU	229.9 ± 14.5	2.90
DS, 10 mM DU	112.0 ± 12.4	1.41
None	104.4 ± 12.8	
Ch6S, 0.2 µM DU	147.8 ± 9.7	1.41
Ch6S, 200 µM DU	94.6 ± 23.2	0.91

In conclusion, the pooled results from this study suggest that glycosaminoglycans released from connective tissues by the action of hydrolases during inflammation or tissue remodeling, may contribute to regulation of elastase-2 by themselves and in association with protein inhibitors. As long as tissue degradation is required, such as in wound healing, the efficiency of α1-PI, the major physiological inhibitor of elastase-2, may be finely tuned by the local concentration of glycosaminoglycans resulting in slowing down its activity. After completion of remodeling, glycosaminoglycans are expected to disappear rapidly allowing efficient inhibition of the no longer needed peptidases. If this is true, the same mechanism is likely to be responsible for the inefficient inhibition of elastase-2 in pathological situations.

Acknowledgments
Supported by Grant 31-113345/1 of the Swiss National Science Foundation and by the Albert Böni Foundation.

References

1. Bode, W., Wei, A.Z., Huber, R., Meyer, E., Travis, J. and Neumann, S. (1986). X-ray crystal structure of the complex of human leukocyte elastase (PMN elastase) and the third domain of the turkey ovomucoid inhibitor. EMBO Journal 5, 2453-2458.

2. Kostoulas, G., Hörler, D., Naggi, A., Casu, B. and Baici, A. (1997). Electrostatic interactions between human leukocyte elastase and sulfated glycosaminoglycans: physiological implications. Biological Chemistry 378, 1481-1489.

3. Korkmaz, B., Moreau, T. and Gauthier, F. (2008). Neutrophil elastase, proteinase 3 and cathepsin G: physicochemical properties, activity and physiopathological functions. Biochimie 90, 227-42.

4. Baici, A. and Bradamante, P. (1984). Interaction between human leukocyte elastase and chondroitin sulfate. Chemico Biological Interactions 51, 1-11.

5. Früh, H., Kostoulas, G., Michel, B.A. and Baici, A. (1996). Human myeloblastin (leukocyte proteinase 3): Reactions with substrates, inactivators and activators in comparison with leukocyte elastase. Biological Chemistry 377, 579-586.

6. Marossy, K. (1981). Interaction of the chymotrypsin- and elastase-like enzymes of the human granulocyte with glycosaminoglycans. Biochimica et Biophysica Acta 659, 351-361.

7. Walsh, R.L., Dillon, T.J., Scicchitano, R. and McLennan, G. (1991). Heparin and heparan sulphate are inhibitors of human leucocyte elastase. Clinical Science 81, 341-346.

8. Baici, A., Diczházi, C., Neszmélyi, A., Móczár, E. and Hornebeck, W. (1993). Inhibition of the human leukocyte endopeptidases elastase and cathepsin G and of porcine pancreatic elastase by N-oleoyl derivatives of heparin. Biochemical Pharmacology 46, 1545-1549.

9. Baici, A., Salgam, P., Fehr, K. and Böni, A. (1980). Inhibition of human elastase from polymorphonuclear leucocytes by a glycosaminoglycan polysulfate (Arteparon). Biochemical Pharmacology 29, 1723-1727.

10. Steinmeyer, J. and Kalbhen, D.A. (1991). Influence of some natural and semisynthetic agents on elastase and cathepsin G from polymorphonuclear granulocytes. Arzneimittel-Forschung/Drug Research 41, 77-80.

11. Schenker, P. and Baici, A. (2009). Simultaneous interaction of enzymes with two modifiers: Reappraisal of kinetic models and new paradigms. Journal of Theoretical Biology doi:10.1016/j.jtbi.2009.07.033

12. Baici, A. and Lang, A. (1990). Cathepsin B secretion by rabbit articular chondrocytes: modulation by cycloheximide and glycosaminoglycans. Cell & Tissue Research 259, 567-573.

13. Bertini, S., Bisio, A., Torri, G., Bensi, D. and Terbojevich, M. (2005). Molecular weight determination of heparin and dermatan sulfate by size exclu-

sion chromatography with a triple detector array. Biomacromolecules 6, 168-173.
14. Baici, A. and Seemüller, U. (1984). Kinetics of the inhibition of human leucocyte elastase by eglin from the leech Hirudo medicinalis. Biochemical Journal 218, 829-833.
15. Seemüller, U., Meier, M., Ohlsson, K., Müller, H.P. and Fritz, H. (1977). Isolation and characterisation of a low molecular weight inhibitor (of chymotrypsin and human granulocyte elastase and cathepsin G) from leeches. Hoppe-Seyler's Zeitschrift für Physiologische Chemie 358, 1105-1117.
16. Tsuboi, S., Nakabayashi, K., Matsumoto, Y., Teno, N., Tsuda, Y., Okada, Y., Nagamatsu, Y. and Yamamoto, J. (1990). Amino acids and peptides. XXVIII. Synthesis of peptide fragments related to eglin c and studies on the relationship between their structure and effects on human leukocyte elastase, cathepsin G and α-chymotrypsin. Chemical and Pharmaceutical Bulletin (Tokyo) 38, 2369-2376.
17. Baici, A. (1981). The specific velocity plot. A graphical method for determining inhibition parameters for both linear and hyperbolic enzyme inhibitors. European Journal of Biochemistry 119, 9-14.
18. Casu, B., Petitou, M., Provasoli, M. and Sinaÿ, P. (1988). Conformational flexibility: a new concept for explaining binding and biological properties of iduronic acid-containing glycosaminoglycans. Trends in Biochemical Sciences 13, 221-225.
19. Keleti, T. (1967). The liberator. Journal of Theoretical Biology 16, 337-355.
20. Shin, J.S. and Yu, M.H. (2002). Kinetic dissection of alpha(1)-antitrypsin inhibition mechanism. Journal of Biological Chemistry 277, 11629-11635.
21. Belorgey, D. and Bieth, J.G. (1995). DNA binds neutrophil elastase and mucus proteinase inhibitor and impairs their functional activity. FEBS Letters 361, 265-268.
22. Belorgey, D. and Bieth, J.G. (1998). Effect of polynucleotides on the inhibition of neutrophil elastase by mucus proteinase inhibitor and alpha(1)-proteinase inhibitor. Biochemistry 37, 16416-16422.
23. Frommherz, K.J., Faller, B. and Bieth, J.G. (1991). Heparin strongly decreases the rate of inhibition of neutrophil elastase by α1-proteinase inhibitor. Journal of Biological Chemistry 266, 15356-15362.
24. Cadène, M., Boudier, C., Daney-de Marcillac, G. and Bieth, J.G. (1995). Influence of low molecular mass heparin on the kinetics of neutrophil elastase inhibition by mucus proteinase inhibitor. Journal of Biological Chemistry 270, 13204-13209.
25. Baici, A. (1998). Inhibition of extracellular matrix-degrading endopeptidases: Problems, comments, and hypotheses. Biological Chemistry 379, 1007-1018.
26. Schechter, I. and Berger, A. (1967). On the size of the active sites in proteases. I. Papain. Biochemical & Biophysical Research Communications 27, 157-162.

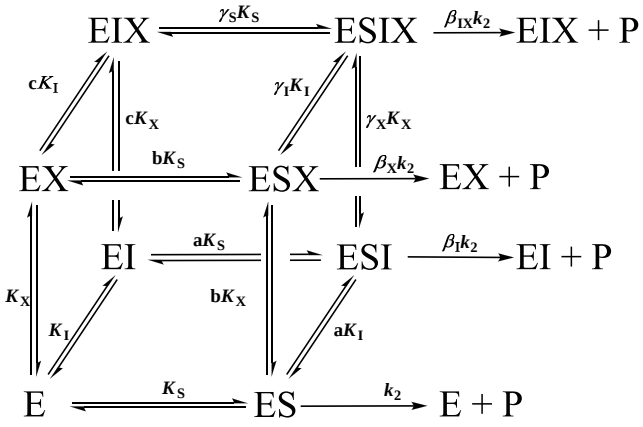

Scheme 1: Simultaneous interaction of two modifiers I and X on the enzyme E [11]. S = substrate, P = product. The coefficients a, b describe the proportion of competitive and uncompetitive inhibition in mixed inhibition. The coefficient c defines four types of interaction between the modifiers I and X on the free enzyme: facilitation ($0 < c < 1$), independence ($c = 1$), hindrance ($1 < c < \infty$) and exclusion ($c = \infty$). The coefficients γ_S, γ_I and γ_X characterize the interactions between reactants in the formation of the quaternary complex ESIX.

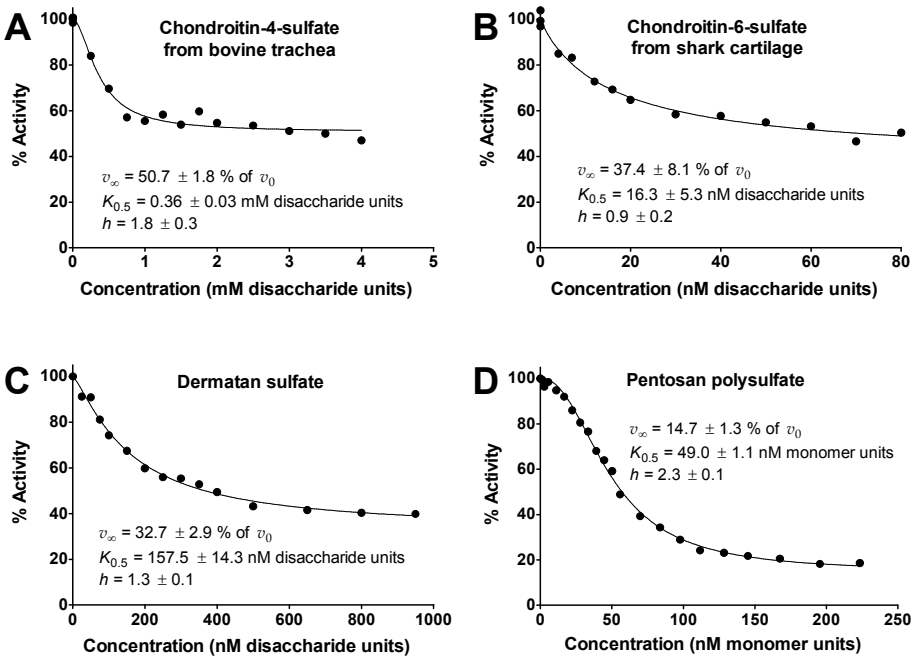

Figure 1: Inhibition of elastase-2 by sulfated polysaccharides. Equation (1) was fitted to data and the solid lines represent the best fit. Parameters from regression analysis are shown together with their standard errors in panels A-D. The substrate was MeOSuc-AAPV-pNA at a fixed concentration [S] = K_{m} = 0.070 mM. 50mM Tris-HCl buffer, pH = 7.40, with NaCl added to an ionic strength of 100 mM and 0.01% (v/v) Triton-X100; temperature 25 ± 1°C. The elastase-2 concentration in all assays was 8.6 nM

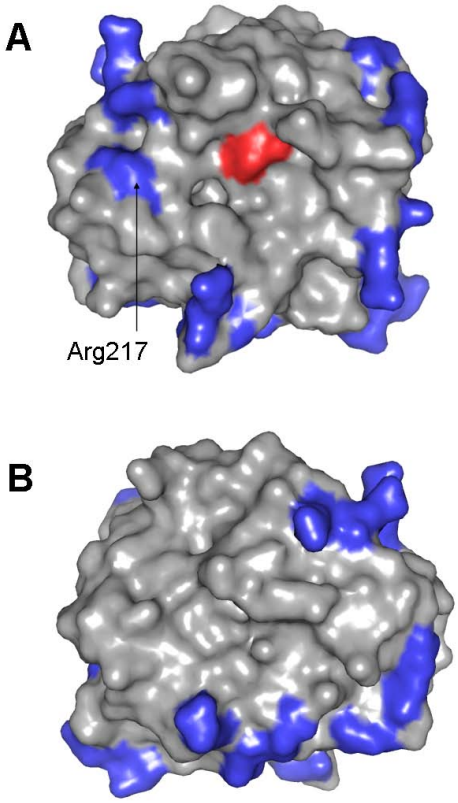

Figure 2: Three-dimensional structure of elastase-2 (protein data bank code 1HNE). Positively charged arginine residues are shown in blue and the active site (His57, Asp102, Ser195) in red. The negative charges form three belts around the enzyme molecule, which is shown here in the front (A) and backside position (B). Arg^{217A} is positioned along the extended hydrophobic substrate binding pocket in such a way to interfere with substrate binding when masked by interaction with polyanions.

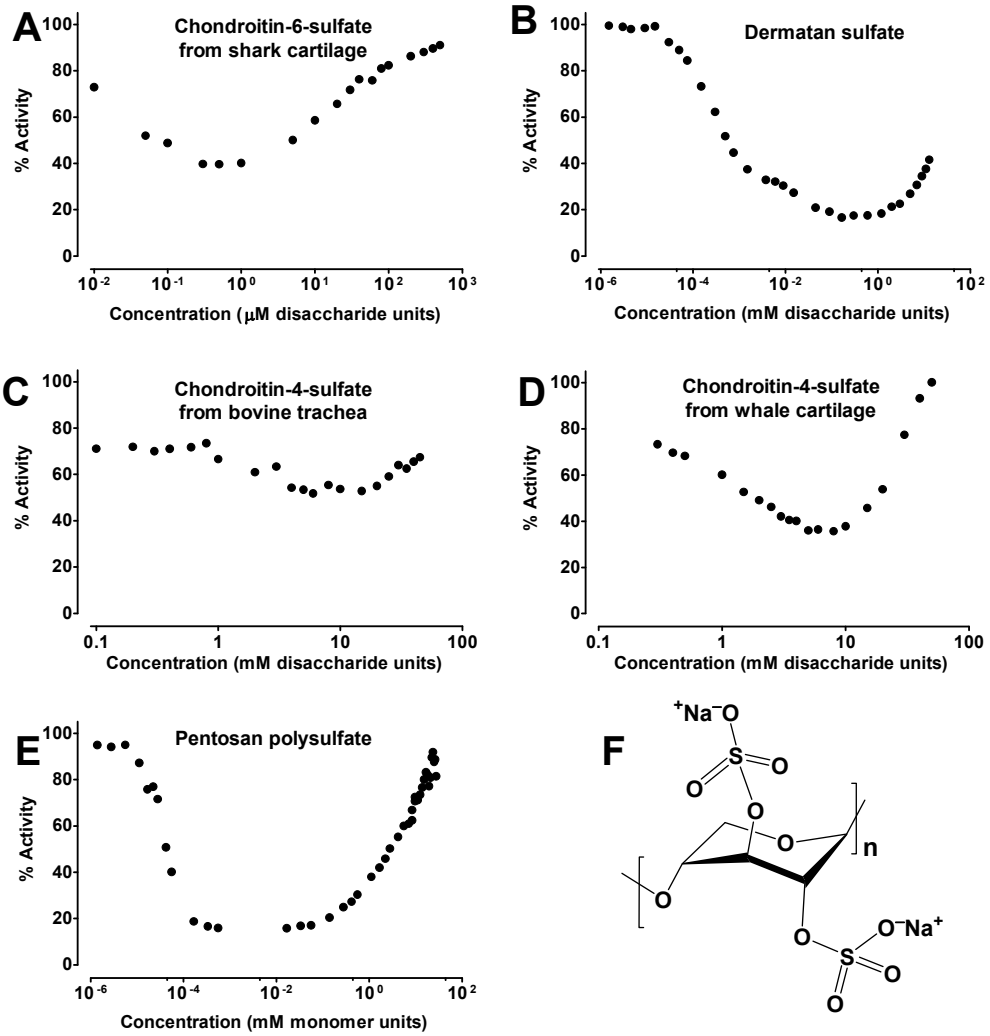

Figure 3: Inhibition and reactivation of elastase-2 by sulfated polysaccharides. Concentration axes are drawn as log10 scale of the constitutive basic units: disaccharide units for chondroitin sulfates and DS (A-D), and monomer units for PPS (E). Experimental conditions as in Fig. 1.

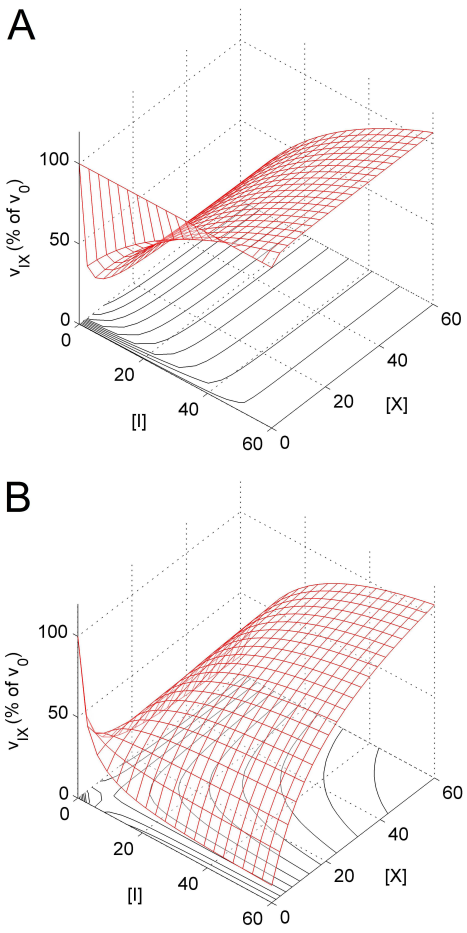

Figure 4: Simulated enzyme inhibition and reactivation by the concomitant action of two modifiers I and X. Plots of the reaction rate as a function of the concentration of two modifiers, which are expressed in mM units. The kinetic parameters and coefficients are defined in Scheme 1 and simulations were performed with Matlab® software using equation (2) as detailed previously [11]. In panel A, I is considered to be a liberator and X a hyperbolic inhibitor with the following parameters: a = 1, b = 7.6, c = ∞ (exclusion), e = 0.77, σ = 1, β_{I} = 1, β_{X} = 0.244, β_{IX} = 1, K_{I} = 63 mM, K_{X} = 0.67 mM. In panel B, I and X are non-exclusive hyperbolic inhibitors, a = b = 0.32, c = ∞ (exclusion), e = 1.42, σ = 1, β_{I} = β_{X} = 0.048, β_{IX} = 1.0, K_{I} = K_{X} = 4.77 mM. The curves in the [I]−[X] plane represent isoboles, i.e. equieffective concentrations of the modifiers, obtained by projection of the three-dimensional graphs.

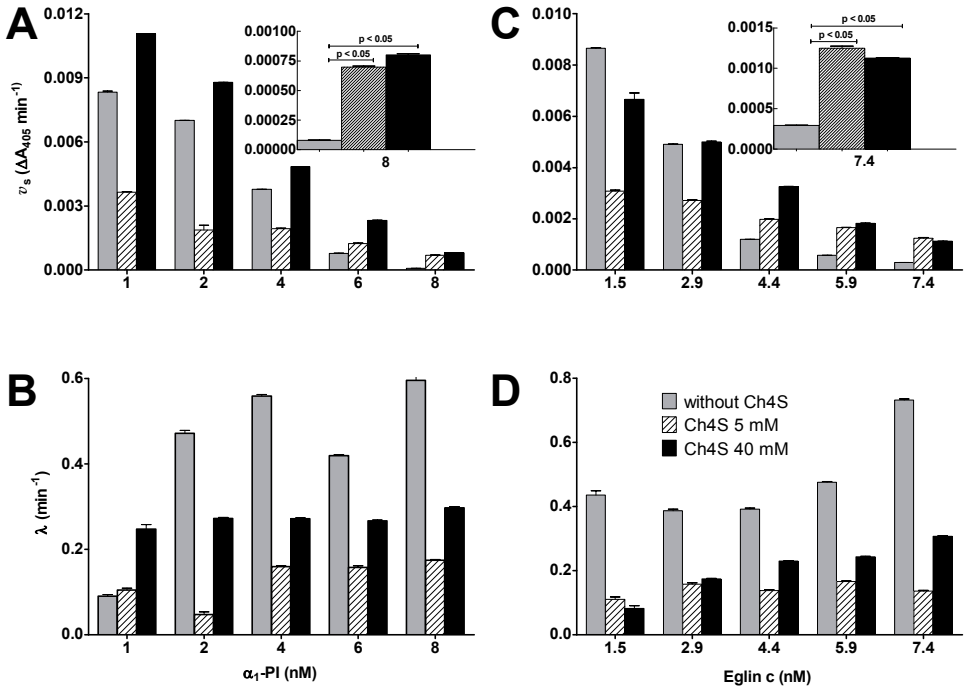

Figure 5: Effect of Ch4S from whale cartilage on the inhibition of elastase-2 by α1-PI. Bars represent the best fits of parameters ± S.E. obtained by non-linear regression to the progress curves shown in Supplementary Material. The insets in panels A and B show the enlarged bars at the highest inhibitor concentrations. The steady-state rates in presence of Ch4S were significantly different from those in their absence (one-way analysis of variance and Tukey multiple comparison test). One-way analysis of variance also showed that all values of λ with the exception of α1-PI at the lowest concentration, were significantly different from one another in all pair combinations ($p < 0.05$). Column legends for all data are shown in panel D.

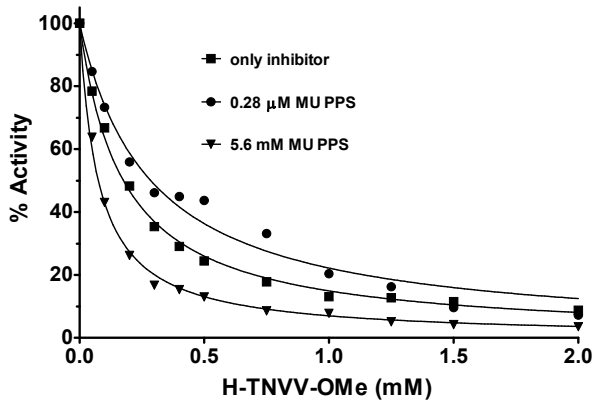

Figure 6: Inhibition of elastase-2 by H-TNVV-OMe (amino acids 60-63 of eglin c) with and without PPS. The elastase-2 concentration in all assays was 6.9 nM of titrated active sites and other experimental conditions were as in Fig. 1.

Supplementary material

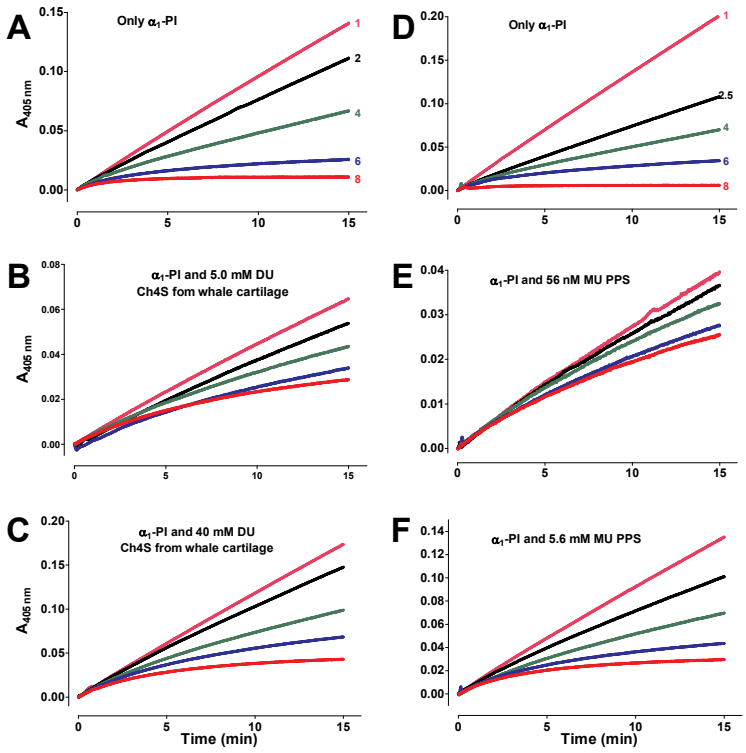

Suppl. Fig. 1: Inhibition of elastase-2 by α1-PI and interference by sulfated polysaccharides. The curves were corrected for baseline. Progress curves in experiments A-C and D-F were performed on different days. A and D, only α1-PI, B and C, chondroitin-4-sulfate (Ch4S) from whale cartilage added at two concentrations; E and F, pentosan polysulfate (PPS) added at two concentrations as indicated. Numbers adjacent to the curves represent nM concentrations of α1-PI and the color codes, shown only on the top panels, also apply to the other curves. The substrate was MeOSuc-AAPV-pNA at a fixed concentration [S] = 0.14 mM (K_m = 0.070 mM). 50mM Tris-HCl buffer, pH = 7.40, with NaCl added to an ionic strength of 100 mM and 0.01% (v/v) Triton-X100; temperature 25 ± 1°C. The final elastase-2 concentration in all assays was 2.3 nM of titrated active sites. The following equation for exponential rise followed by a linear steady-state was fitted to all curves to calculate the apparent first-order constant of the exponential phase (λ) and the steady-state slope (v_s).

$$y = A\left(1 - e^{-\lambda t}\right) + v_\mathrm{s} t + d$$

A is the amplitude of the exponential and d is a displacement factor for any non-zero value of the absorbance at the beginning of the reaction.

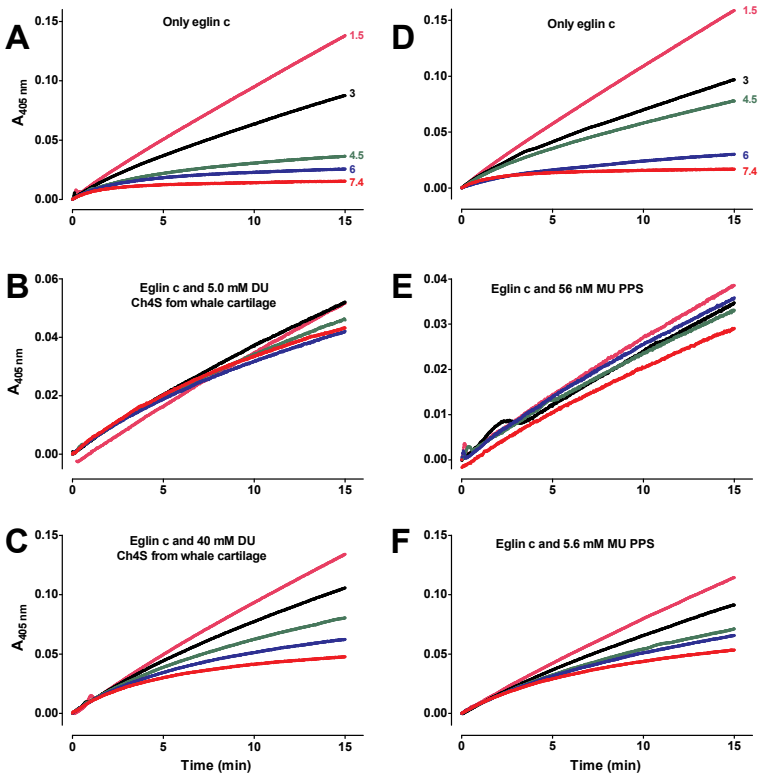

Suppl. Fig. 2: Inhibition of elastase-2 by eglin c and interference by sulfated polysaccharides. Progress curves in experiments A-C and D-F were performed on different days. A and D, only eglin c, B and C, chondroitin-4-sulfate (Ch4S) from whale cartilage added at two concentrations; E and F, PPS added at two concentrations as indicated. Numbers adjacent to the curves represent nM concentrations of eglin c and the color codes, shown only on the top panels, also apply to the other curves. Experimental conditions and kinetic analysis as in Suppl. Fig. 1.

Conclusion

Conclusion

ECM-degrading peptidases are tightly bound to their insoluble substrates in the extracellular space and their active site is barely accessible by exogenous modifiers. We successfully demonstrated that targeting the occluding loop of cathepsin B, a flexible structure outside the active center that governs the exo- and endoproteolytic activity of this enzyme, is a promising strategy deserving further development. One compound, identified by computational docking methods, behaved as a reversible, double-headed competitive inhibitor of cathepsin B that acted by steric hindrance of substrate accessibility to the active site. Effective modification of the cathepsin B activity can thus be achieved through modifiers binding outside the active center. This approach represents an alternative strategy for the development of new inhibitors with potential pharmacological interest.

While developing new, therapeutically useful modifiers, proper kinetic characterization of their interaction mechanism with the target enzymes is vital for any future use. Besides reversible inhibitors, inactivators are synthesized worldwide with a large spectrum of applications. Therefore, we re-evaluated in a systematic way the mechanisms by which inactivators block enzyme activity exploiting model compounds of acetylcholinesterase, here considered as a model target enzyme. The frequently occurring phenomenon of temporary inactivation and the chemical instability of the modifiers were highlighted to allow mechanistic discrimination towards reversible inhibitors. Supported by a large number of measurements with molecules that inactivated acetylcholinesterase by several different mechanisms, we assembled a collection of diagnostic tools, which will serve as a reference for the classification and analysis irreversible enzyme modification reactions.

In vitro studies typically deal with interactions involving a single modifier and one enzyme molecule. Nevertheless, the numerous potential binding partners for peptidases in the ECM raise the question of multiple interactions. In particular, *in vitro* designed modifiers targeted outside the active site are likely to be involved in such interactions. Hence, we re-evaluated the double inhibition concept and proposed a new kinetic model that allows a rigorous mathematical description of the behavior of inhibitors and acti-

vators in multiple interaction systems. This treatment settled discrepancies in the literature on the prediction of synergistic and antagonistic effects of pharmacological importance. Unusual kinetic phenomena, such as reactivation following inhibition and the inhibition paradox, in which two modifiers that produce inhibition when used separately but activation when used simultaneously, can be described quantitatively with the new approach.

Human elastase-2, a key enzyme of neutrophilic leukocytes, is better known for its adverse effects than for a few recognized physiological functions. This enzyme, involved in ECM degradation, is often found at extracellular sites rich in glycosaminoglycans, with which it interacts. At low glycosaminoglycan concentrations elastase-2 is inhibited but is partially or fully reactivated as the glycosaminoglycan concentration increases. Glycosaminoglycans can seriously impair the action of naturally occurring inhibitors of elastase-2 in a glycosaminoglycan-concentration depending manner. The phenomenon, which involves a network of complex interactions, can to some extent be explained with the general model of two modifiers interacting at the same time with one enzyme molecule.

The results of this thesis highlight the importance of methodological procedures in characterizing modifier mechanisms with kinetic techniqes. New paradigms emerged revealing hitherto unpredictable effects. The discovery and correct interpretation of new mechanisms is subordinated to meticulous data collection and analysis as a support in the development of pharmacologically active substances.

Bibliography

[1] P. C. Almeida, I. L. Nantes, J. R. Chagas, C. C. A. Rizzi, A. Faljoni-Alario, E. Carmona, L. Juliano, H. B. Nader, and I. L. S. Tersariol. Cathepsin B activity regulation - Heparin-like glycosaminoglycans protect human cathepsin B from alkaline pH-induced inactivation. *J. Biol. Chem.*, 276:944–951, 2001.

[2] P. C. Almeida, V. Oliveira, J. R. Chagas, M. Meldal, M. A. Juliano, and L. Juliano. Hydrolysis by cathepsin B of fluorescent peptides derived from human prorenin. *Hypertension*, 35:1278–1283, 2000.

[3] M. Alpegiani, A. Baici, P. Bissolino, P. Carminati, G. Cassinelli, S. Del Nero, G. Franceschi, P. Orezzi, E. Perrone, V. Rizzo, and N. Sacchi. Synthesis and evaluation of new elastase inhibitors. I. 1,1-dioxocephem-4-thiolesters. *Eur. J. Med. Chem.*, 27:875–890, 1992.

[4] M. Alpegiani, P. Bissolino, D. Borghi, R. Corigli, S. Del Nero, E. Perrone, G. Razzano, and V. Rizzo. Cephem sulfones as inactivators of human leukocyte elastase. II. Keto-enol tautomerism in cephem-4-ketones. *Bioorg. Med. Chem. Lett.*, 2:1127–1132, 1992.

[5] Jr. Aronson, N. N. and A. J. Barrett. The specificity of cathepsin B. Hydrolysis of glucagon at the C-terminus by a peptidyldipeptidase mechanism. *Biochem. J.*, 171:759–765, 1978.

[6] J. L. Avila. Lysosomes and other related cytoplasmic granules of human neutrophilic polymorphonuclear leukocytes. *Acta Cient. Venezolana*, 28:115–126, 1977.

[7] J. L. Avila and J. Convit. Inhibition of leucocytic lysosomal enzymes by glycosaminoglycans in vitro. *Biochem. J.*, 152:57–64, 1975.

[8] A. Baici. Graphical and statistical analysis of hyperbolic, tight-binding inhibition. *Biochem. J.*, 244:793–796, 1987.

[9] A. Baici. Interaction of human leukocyte elastase with soluble and insoluble protein substrates. A practical kinetic approach. *Biochim. Biophys. Acta*, 1040:355–364, 1990.

[10] A. Baici. Inhibition of extracellular matrix-degrading endopeptidases: Problems, comments, and hypotheses. *Biol. Chem.*, 379:1007–1018, 1998.

[11] A. Baici, M. Knöpfel, and K. Fehr. Cathepsin G from human polymorphonuclear leucocytes cleaves human IgM. *Mol. Immunol.*, 19:719–727, 1982.

[12] A. Baici, M. Knöpfel, and K. Fehr. Cleavage of the four human IgG subclasses with cathepsin G. *Scand. J. Immunol.*, 16:487–498, 1982.

[13] A. Baici, M. Knöpfel, and R. Keist. Tumor-host interactions in the rabbit V2 carcinoma: Stimulation of cathepsin B in host fibroblasts by a tumor-derived cytokine. *Invas. Metast.*, 8:143–158, 1988.

[14] A. Baici, A. Lang, R. Zwicky, and K. Müntener. Beyond matrix proteolysis: Cathepsin B in osteoarthritis. In *New trends in osteoarthritis*, pages 71–76. 2002.

[15] A. Baici and U. Seemüller. Kinetics of the inhibition of human leucocyte elastase by eglin from the leech Hirudo medicinalis. *Biochem. J.*, 218:829–833, 1984.

[16] W. H. Baricos, Y. Zhou, R. W. , and A. J. Barrett. Human kidney cathepsins B and L. Characterization and potential role in degradation of glomerular basement membrane. *Biochem. J.*, 252:301–304, 1988.

[17] A. J. Barrett and H. Kirschke. Cathepsin B, cathepsin H, and cathepsin L. *Meth. Enzymol.*, 80:535–561, 1981.

[18] D. Belorgey and J. G. Bieth. DNA binds neutrophil elastase and mucus proteinase inhibitor and impairs their functional activity. *FEBS Lett.*, 361:265–268, 1995.

[19] D. Belorgey and J. G. Bieth. Effect of polynucleotides on the inhibition of neutrophil elastase by mucus proteinase inhibitor and α_1-proteinase inhibitor. *Biochemistry*, 37:16416–16422, 1998.

[20] S. Berardi, A. Lang, G. Kostoulas, D. Hörler, E. M. Vilei, and A. Baici. Alternative messenger RNA splicing and enzyme forms of cathepsin B in human osteoarthritic cartilage and cultured chondrocytes. *Arthritis Rheum.*, 44:1819–1831, 2001.

[21] R. J. Beynon, G. A. Place, and P. E. Butler. Limited proteolysis of enzymes: the generation of functionally modified derivatives in vitro and in vivo. *Biochem. Soc. Trans.*, 13:306–308, 1985.

[22] H. K. Binz, P. Amstutz, A. Kohl, M. T. Stumpp, C. Briand, P. Forrer, M. G. Grütter, and A. Plückthun. High-affinity binders selected from designed ankyrin repeat protein libraries. *Nat. Biotechnol.*, 22:575–582, 2004.

[23] H. K. Binz, M. T. Stumpp, P. Forrer, P. Amstutz, and A. Plückthun. Designing repeat proteins: Well-expressed, soluble and stable proteins from combinatorial libraries of consensus ankyrin repeat proteins. *J. Mol. Biol.*, 332:489–503, 2003.

[24] J. S. Bond and A. J. Barrett. Degradation of fructose-1,6-bisphosphate aldolase by cathepsin B. A further example of peptidyldipeptidase activity of this proteinase. *Biochem. J.*, 189:17–25, 1980.

[25] J. Botts and M. Morales. Analytical description of the effects of modifiers and of enzyme multivalency upon the steady state catalyzed reaction rate. *Trans. Faraday Soc.*, 49:696–707, 1953.

[26] K. Brix, P. Lemansky, and V. Herzog. Evidence for extracellularly acting cathepsins mediating thyroid hormone liberation in thyroid epithelial cells. *Endocrinology*, 137:1963–74, 1996.

[27] M. R. Buck, D. G. Karustis, N. A. Day, K. V. Honn, and B. F. Sloane. Degradation of extracellular-matrix proteins by human cathepsin B from normal and tumor tissues. *Biochem. J.*, 282:273–278, 1992.

[28] N. Budin, N. Majeux, and A. Caflisch. Fragment-based flexible ligand docking by evolutionary optimization. *Biol. Chem.*, 382:1365–1372, 2001.

[29] D. J. Buttle, M. Abrahamson, D. Burnett, J. S. Mort, A. J. Barrett, P. M. Dando, and S. L. Hill. Human sputum cathepsin B degrades proteoglycan, is inhibited by α_2-macroglobulin and is modulated by neutrophil elastase cleavage of cathepsin B precursor and cystatin C. *Biochem. J.*, 276:325–331, 1991.

[30] D. Campanelli, M. Melchior, Y. Fu, M. Nakata, H. Shuman, C. Nathan, and J. E. Gabay. Cloning of cDNA for proteinase 3: a serine protease, antibiotic, and autoantigen from human neutrophils. *J. Exp. Med.*, 172:1709–1715, 1990.

[31] E. J. Campbell, R. M. Senior, J. A. McDonald, and D. L. Cox. Proteolysis by neutrophils. Relative importance of cell-substrate contact and oxidative inactivation of proteinase inhibitors in vitro. *J. Clin. Invest.*, 70:845–852, 1982.

[32] B. Casu, M. Petitou, M. Provasoli, and P. Sinaÿ. Conformational flexibility: A new concept for explaining binding and biological properties of iduronic acid-containing glycosaminoglycans. *Trends Biochem. Sci.*, 13:221–225, 1988.

[33] M. Cecchini, P. Kolb, N. Majeux, and A. Caflisch. Automated docking of highly flexible ligands by genetic algorithms: A critical assessment. *J. Comput. Chem.*, 25:412–422, 2004.

[34] M. Cegnar, J. Kos, and J. Kristl. Cystatin incorporated in poly(lactide-co-glycolide) nanoparticles: Development and fundamental studies on preservation of its activity. *Eur. J. Pharm. Sci.*, 22:357–364, 2004.

[35] M. Cegnar, A. Premzl, V. Zavasnik-Bergant, J. Kristl, and J. Kos. Poly(lactide-co-glycolide) nanoparticles as a carrier system for delivering cysteine protease inhibitor cystatin into tumor cells. *Exp. Cell Res.*, 301:223–231, 2004.

[36] H. A. Chapman, J. S. Munger, and G. P. Shi. The role of thiol proteases in tissue injury and remodeling. *Amer. J. Respir. Critical Care med.*, 1502:S155–S159, 1994.

[37] V. Dalet-Fumeron, N. Guinec, and M. Pagano. In vitro activation of pro-cathepsin B by three serine proteinases: leucocyte elastase, cathepsin G, and the urokinase-type plasminogen activator. *FEBS Lett.*, 332:251–254, 1993.

[38] R. T. Dean. The roles of cathepsins B1 and D in the digestion of cytoplasmic proteins in vitro by lysosomal extracts. *Biochem. Biophys. Res. Commun.*, 68:518–523, 1976.

[39] L. Debelle and A. M. Tamburro. Elastin: Molecular description and function. *Int. J. Biochem. Cell Biol.*, 31:261–272, 1999.

[40] G. Dubin. Proteinaceous cysteine protease inhibitors. *Cell. Mol. Life Sci.*, 62:653–669, 2005.

[41] J. Duranton, D. Belorgey, J. Carrere, L. Donato, T. Moritz, and J. G. Bieth. Effect of DNase on the activity of neutrophil elastase, cathepsin G and proteinase 3 in the presence of DNA. *FEBS Lett.*, 473:154–156, 2000.

[42] J. Duranton, C. Boudier, D. Belorgey, P. Mellet, and J. G. Bieth. DNA strongly impairs the inhibition of cathepsin G by α_1-antichymotrypsin and α_1-proteinase inhibitor. *J. Biol. Chem.*, 275:3787–3792, 2000.

[43] P. Forrer, M. T. Stumpp, H. K. Binz, and A. Plückthun. A novel strategy to design binding molecules harnessing the modular nature of repeat proteins. *FEBS Lett.*, 539:2–6, 2003.

[44] H. Frauenfelder, B. H. McMahon, R. H. Austin, K. Chu, and J. T. Groves. The role of structure, energy landscape, dynamics, and allostery in the enzymatic function of myoglobin. *Proc. Natl. Acad. Sci. USA*, 98:2370–2374, 2001.

[45] R. Frlan and S. Gobec. Inhibitors of cathepsin B. *Curr. Med. Chem.*, 13:2309–2327, 2006.

[46] H. Früh, G. Kostoulas, B. A. Michel, and A. Baici. Human myeloblastin (leukocyte proteinase 3): Reactions with substrates, inactivators and activators in comparison with leukocyte elastase. *Biol. Chem.*, 377:579–586, 1996.

[47] J. L. Funderburgh. Keratan sulfate: structure, biosynthesis, and function. *Glycobiology*, 10:951–958, 2000.

[48] D. Gabrijelčič, R. Gollwitzer, T. Popovič, and V. Turk. Proteolytic cleavage of human fibrinogen by cathepsin B. *Biol. Chem. Hoppe-Seyler*, 269:287–292, 1988.

[49] J. E. Gadek, G. A. Fells, R. L. Zimmerman, and R. G. Crystal. Role of connective tissue proteases in the pathogenesis of chronic inflammatory lung disease. *Environ. Health Perspect.*, 55:297–306, 1984.

[50] K. Gunasekaran, B. Ma, and R. Nussinov. Is allostery an intrinsic property of all dynamic proteins? *Proteins*, 57:433–443, 2004.

[51] W. Halangk, M. M. Lerch, B. Brandt-Nedelev, W. Roth, M. Ruthenbuerger, T. Reinheckel, W. Domschke, H. Lippert, C. Peters, and J. Deussing. Role of cathepsin B in intracellular trypsinogen activation and the onset of acute pancreatitis. *J. Clin. Invest.*, 106:773–81, 2000.

[52] T. E. Hardingham and A. J. Fosang. Proteoglycans: Many forms and many functions. *FASEB J.*, 6:861–870, 1992.

[53] J. A. Hardy and J. A. Wells. Searching for new allosteric sites in enzymes. *Curr. Opin. Struct. Biol.*, 14:706–715, 2004.

[54] P. A. Hill, D. J. Buttle, S. J. Jones, A. Boyde, M. Murata, J. J. Reynolds, and M. C. Meikle. Inhibition of bone resorption by selective inactivators of cysteine proteinases. *J. Cell. Biochem.*, 56:118–130, 1994.

[55] J. J. Irwin and B. K. Shoichet. ZINC - a free database of commercially available compounds for virtual screening. *J. Chem. Inf. Model.*, 45:177–182, 2005.

[56] K. Ishidoh and E. Kominami. Procathepsin L degrades extracellular matrix proteins in the presence of glycosaminoglycans in vitro. *Biochem. Biophys. Res. Commun.*, 217:624–631, 1995.

[57] M. J. Janusz and N. S. Doherty. Degradation of cartilage matrix proteoglycan by human neutrophils involves both elastase and cathepsin G. *J. Immunol.*, 146:3922–3928, 1991.

[58] D. Kern and E. R. P. Zuiderweg. The role of dynamics in allosteric regulation. *Curr. Opin. Struct. Biol.*, 13:748–757, 2003.

[59] A. R. Khan and M. N. G. James. Molecular mechanisms for the conversion of zymogens to active proteolytic enzymes. *Protein Sci.*, 7:815–836, 1998.

[60] J. E. Koblinski, M. Ahram, and B. F. Sloane. Unraveling the role of proteases in cancer. *Clin. Chim. Acta*, 291:113–135, 2000.

[61] A. Kohl, P. Amstutz, P. Parizek, H. K. Binz, C. Briand, G. Capitani, P. Forrer, A. Plückthun, and M. G. Grütter. Allosteric inhibition of aminoglycoside phosphotransferase by a designed ankyrin repeat protein. *Structure*, 13:1131–1141, 2005.

[62] P. Kolb and A. Caflisch. Automatic and efficient decomposition of two-dimensional structures of small molecules for fragment-based high-throughput docking. *J. Med. Chem.*, 49:7384–7392, 2006.

[63] G. Kostoulas, D. Hörler, A. Naggi, B. Casu, and A. Baici. Electrostatic interactions between human leukocyte elastase and sulfated glycosaminoglycans: Physiological implications. *Biol. Chem.*, 378:1481–1489, 1997.

[64] A. Lang, D. Hörler, and A. Baici. The relative importance of cysteine peptidases in osteoarthritis. *J. Rheumatol.*, 27:1970–1979, 2000.

[65] W. L. Lee and G. P. Downey. Leukocyte elastase - Physiological functions and role in acute lung injury. *Am. J. Respir. Crit. Care Med.*, 164:896–904, 2001.

[66] B. Lenarčič and T. Bevec. Thyropins: new structurally related proteinase inhibitors. *Biol. Chem.*, 379:105–111, 1998.

[67] P. Lestienne and J. G. Bieth. Inhibition of human leukocyte elastase by polynucleotides. *Biochimie*, 65:49–52, 1983.

[68] Z. Q. Li, W. S. Hou, and D. Brömme. Collagenolytic activity of cathepsin K is specifically modulated by cartilage-resident chondroitin sulfates. *Biochemistry*, 39:529–536, 2000.

[69] C. Lopez-Otin and J. S. Bond. Proteases: Multifunctional enzymes in life and disease. *J. Biol. Chem.*, 283:30433–30437, 2008.

[70] R. A. Maciewicz, S. F. Wotton, D. J. Etherington, and V. C. Duance. Susceptibility of the cartilage collagen types II, IX and XI to degradation by the cysteine proteinases, cathepsins B and L. *FEBS Lett.*, 269:189–193, 1990.

[71] J. Mai, Jr. Finley, R. L., D. M. Waisman, and B. F. Sloane. Human procathepsin B interacts with the annexin II tetramer on the surface of tumor cells. *J. Biol. Chem.*, 275:12806–12, 2000.

[72] N. Majeux, M. Scarsi, J. Apostolakis, C. Ehrhardt, and A. Caflisch. Exhaustive docking of molecular fragments with electrostatic solvation. *Proteins*, 37:88–105, 1999.

[73] R. W. Mason and S. D. Massey. Surface activation of pro-cathepsin L. *Biochem. Biophys. Res. Commun.*, 189:1659–1666, 1992.

[74] Y. Matsunaga, T. Saibara, H. Kido, and N. Katunuma. Participation of cathepsin B in processing of antigen presentation to MHC class II. *FEBS Lett.*, 324:325–330, 1993.

[75] M. E. McGrath. The lysosomal cysteine proteases. *Annu. Rev. Biophys. Biomolec. Struct.*, 28:181–204, 1999.

[76] M. M. Mohamed and B. F. Sloane. Cysteine cathepsins: Multifunctional enzymes in cancer. *Nat. Rev. Cancer*, 6:764–775, 2006.

[77] J. F. Morrison. The slow-binding and slow, tight-binding inhibition of enzyme-catalysed reactions. *Trends Biochem. Sci.*, 7:102–105, 1982.

[78] J. S. Mort, M. C. Magny, and E. R. Lee. Cathepsin B: An alternative protease for the generation of an aggrecan 'metalloproteinase' cleavage neoepitope. *Biochem. J.*, 335:491–494, 1998.

[79] K. Müntener, R. Zwicky, G. Csucs, J. Rohrer, and A. Baici. Exon skipping of cathepsin B: Mitochondrial targeting of a lysosomal peptidase provokes cell death. *J. Biol. Chem.*, 279:41012–41017, 2004.

[80] D. Musil, D. Zucic, D. Turk, R. A. Engh, I. Mayr, R. Huber, T. Popovic, V. Turk, T. Towatari, N. Katunuma, and W. Bode. The refined 2.15 Å X-ray crystal structure of human liver cathepsin B: The structural basis for its specificity. *EMBO J.*, 10:2321–2330, 1991.

[81] H. Nagase. Activation mechanisms of matrix metalloproteinases. *Biol. Chem.*, 378:151–160, 1997.

[82] H. Nagase and M. Kashiwagi. Aggrecanases and cartilage matrix degradation. *Arthritis Res. Ther.*, 5:94–103, 2003.

[83] H. Nagase, K. Suzuki, T. E. Cawston, and K. Brew. Involvement of a region near valine-69 of tissue inhibitor of metalloproteinases (TIMP)-1 in the interaction with matrix metalloproteinase 3 (stromelysin 1). *Biochem. J.*, 325:163–167, 1997.

[84] D. K. Nägler, A. C. Storer, F. C. V. Portaro, E. Carmona, L. Juliano, and R. Menard. Major increase in endopeptidase activity of human cathepsin B upon removal of occluding loop contacts. *Biochemistry*, 36:12608–12615, 1997.

[85] M. A. Navia, B. M. McKeever, J. P. Springer, T. Y. Lin, H. R. Williams, E. M. Fluder, C. P. Dorn, and K. Hoogsteen. Structure of human neutrophil elastase in complex with a peptide chloromethyl ketone inhibitor at 1.84-Å resolution. *Proc. Natl. Acad. Sci. USA*, 86:7–11, 1989.

[86] M. Novinec, R. N. Grass, W. J Stark, V. Turk, A. Baici, and B. Lenarčič. Interaction between human cathepsins K, L and S and elastins: Mechanism of elastinolysis and inhibition by macromolecular inhibitors. *J. Biol. Chem.*, 282:7893–7902, 2007.

[87] S. T. Olson and J. D. Shore. Demonstration of a two-step reaction mechanism for inhibition of α-thrombin by antithrombin III and identification of the step affected by heparin. *J. Biol. Chem.*, 257:14891–14895, 1982.

[88] S. T. Olson and J. D. Shore. Transient kinetics of heparin-catalyzed protease inactivation by antithrombin III. the reaction step limiting heparin turnover in thrombin neutralization. *J. Biol. Chem.*, 261:13151–13159, 1986.

[89] J. Otlewski, F. Jelen, M. Zakrzewska, and A. Oleksy. The many faces of protease-protein inhibitor interaction. *EMBO J. 2*, 24:1303–1310, 2005.

[90] H. H. Otto and T. Schirmeister. Cysteine proteases and their inhibitors. *Chem. Rev.*, 97:133–171, 1997.

[91] R. Pankov and K. M. Yamada. Fibronectin at a glance. *J. Cell Sci.*, 115:3861–3863, 2002.

[92] M. Podobnik, R. Kuhelj, V. Turk, and D. Turk. Crystal structure of the wild-type human procathepsin B at 2.5 Ångstrom resolution reveals the native active site of a papain-like cysteine protease zymogen. *J. Mol. Biol.*, 271:774–788, 1997.

[93] O. Quraishi, D. K. Nägler, T. Fox, J. Sivaraman, M. Cygler, J. S. Mort, and A. C. Storer. The occluding loop in cathepsin B defines the pH dependence of inhibition by its propeptide. *Biochemistry*, 38:5017–5023, 1999.

[94] N. D. Rawlings, D. P. Tolle, and A. J. Barrett. Merops: the peptidase database (http://merops.sanger.ac.uk). *Nucleic Acids Res.*, 32 Database issue:D160–D164, 2004. http://merops.sanger.ac.uk.

[95] C. F. Reilly and J. Travis. The degradation of human lung elastin by neutrophil proteinases. *Biochim. Biophys. Acta*, 621:147–157, 1980.

[96] R. J. Riese, P. R. Wolf, D. Brömme, L. R. Natkin, J. A. Villadangos, H. L. Ploegh, and H. A. Chapman. Essential role for cathepsin S in MHC class II - Associated invariant chain processing and peptide loading. *Immunity*, 4:357–366, 1996.

[97] R. Salsas-Escat and C. M. Stultz. The molecular mechanics of collagen degradation: Implications for human disease. *Exp. Mech.*, 49:65–77, 2009.

[98] A. Schweizer, H. Roschitzki-Voser, P. Amstutz, C. Briand, M. Gulotti-Georgieva, E. Prenosil, H. K. Binz, G. Capitani, A. Baici, A. Plückthun, and M. G. Grütter. Inhibition of caspase-2 by a designed ankyrin repeat protein: Specificity, structure, and inhibition mechanism. *Structure*, 15:625–636, 2007.

[99] M. J. Sculley and J. F. Morrison. The determination of kinetic constants governing the slow, tight-binding inhibition of enzyme-catalysed reactions. *Biochim. Biophys. Acta*, 874:44–53, 1986.

[100] U. Seemüller, H. Fritz, and M. Eulitz. Eglin: Elastase - Cathepsin G inhibitor from Leeches. *Meth. Enzymol.*, 80:804–816, 1981.

[101] B. C. Sheu, W. C. Chang, C. Y. Cheng, P. H. Wang, S. Lin, and S. C. Huang. Extracellular matrix proteases - cytokine regulation role in cancer and pregnancy. *Front. Biosci.*, 14:1571–1588, 2009.

[102] G. M. Süel, S. W. Lockless, M. A. Wall, and R. Ranganathan. Evolutionarily conserved networks of residues mediate allosteric communication in proteins. *Nature Structural Biology*, 10:59–69, 2003.

[103] S. E. Szedlacsek and R. G. Duggleby. Kinetics of slow and tight-binding inhibitors. *Meth. Enzymol.*, 249:144–180, 1995.

[104] S. E. Szedlacsek, V. Ostafe, M. Serban, and M. O. Vlad. A re-evaluation of the kinetic equations for hyperbolic tight-binding inhibition. *Biochem. J.*, 254:311–312, 1988.

[105] A. M. Szpaderska and A. Frankfater. An intracellular form of cathepsin B contributes to invasiveness in cancer. *Cancer Res.*, 61:3493–3500, 2001.

[106] C. C. Taggart, G. J. Lowe, C. M. Greene, A. T. Mulgrew, S. J. O'Neill, R. L. Levine, and N. G. McElvaney. Cathepsin B, L, and S cleave and inactivate secretory leucoprotease inhibitor. *J. Biol. Chem.*, 276:33345–33352, 2001.

[107] J. M. Trowbridge and R. L. Gallo. Dermatan sulfate: New functions from an old glycosaminoglycan. *Glycobiology*, 12:117R–125R, 2002.

[108] B. Turk, I. Dolenc, V. Turk, and J. G. Bieth. Kinetics of the pH-induced inactivation of human cathepsin L. *Biochemistry*, 32:375–380, 1993.

[109] B. Turk, I. Dolenc, E. Zerovnik, D. Turk, F. Gubensek, and V. Turk. Human cathepsin B is a metastable enzyme stabilised by specific ionic interactions associated with the active site. *Biochemistry*, 33:14800–14806, 1994.

[110] B. Turk, D. Turk, and V. Turk. Lysosomal cysteine proteases: More than scavengers. *BBA-Protein Struct. Mol. Enzym.*, 1477:98–111, 2000.

[111] A. H. Warfel, C. Cardozo, O. H. Yoo, and D. Zucker-Franklin. Cystatin C and cathepsin B production by alveolar macrophages from smokers and nonsmokers. *J. Leukoc. Biol.*, 49:41–47, 1991.

[112] M. Wolf, I. Clark-Lewis, C. Buri, H. Langen, M. Lis, and L. Mazzucchelli. Cathepsin D specifically cleaves the chemokines macrophage inflammatory protein-1α, macrophage inflammatory protein-1β, and SLC that are expressed in human breast cancer. *Amer. J. Pathol.*, 162:1183–1190, 2003.

[113] W.-F. Xu, X.-Ch. Cheng, Q. Wang, and H. Fang. Advances in matrix metalloproteinase inhibitors based on pyrrolidine scaffold. *Current Medicinal Chemistry*, 15:374–385, 2008.

[114] S. Q. Yan, M. Sameni, and B. F. Sloane. Cathepsin B and human tumor progression. *Biol. Chem.*, 379:113–123, 1998.

[115] W. H. Yu, S. S. C. Yu, Q. Meng, K. Brew, and J. F. Woessner. TIMP-3 binds to sulfated glycosaminoglycans of the extracellular matrix. *J. Biol. Chem.*, 275:31226–31232, 2000.

[116] R. Zwicky and A. Baici. Cytoskeletal architecture and cathepsin B trafficking in human articular chondrocytes. *Histochem. Cell Biol.*, 114:363–372, 2000.

Appendix

Enzyme Inhibition Mechanisms

A.1 Classification

Enzyme inhibitors are classified, whether the enzyme inhibitor complex can freely dissociate or not, into reversible inhibitors and inactivators (Table A.1). Further classification of the different reversible inhibition mechanisms is based on the ratio of $[E]_t$, $[I]_t$ and K_i as well as on the reaction velocity of the formation of the EI complex.

Table A.1: Classification of Enzyme Inhibitors.

type	**characteristics**	**reaction velocity of EI formation**
Reversible		
classical	$[I]_t \gg [E]_t$	fast
slow-binding	$[I]_t \gg [E]_t$	slow
tight binding	$[I]_t \approx [E]_t$ and K_i	fast
slow-tight binding	$[I]_t \approx [E]_t$ and K_i	slow
type	**examples**	
Irreversible		
unspecific	group-specific reactions	
specific	active site binding, mechanism based inactivation (e.g. k_{cat}-inactivators, suicide inhibitors)	

A.2 Reversible Kinetic Inhibition Mechanisms

A.2.1 Classical Inhibition

Scheme A.1, the *General Modifier Mechanism*, is the basic mechanism for the description of all classical reversible inhibition mechanisms [25]. Depending on the value of β, a linear ($\beta = 0$) or a hyperbolic ($0 < \beta \leqslant 1$) inhibitor is described, meaning that at saturating inhibitor concentrations the residual enzyme activity is either fully or partially decreased, respectively. Competitive, uncompetitive or mixed type inhibition is distinguished by the value of α and K_i adopting any positive values (Table A.2).

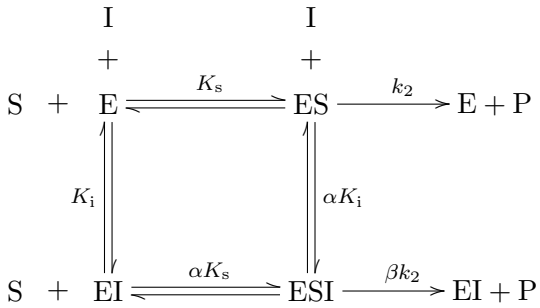

Scheme A.1: The General Modifier Mechanism [25]. E: enzyme, S: substrate, I: inhibitor, K_s: substrate dissociation constant, K_i: inhibitor dissociation constant, k_cat: catalytic activity, α and β: dimensionless constants that define the characteristics of the inhibition mechanism.

Table A.2: Classical Reversible Inhibition Types.

relative values of α and β		**inhibition type**
$\alpha = \infty$	$\beta = 0$	linear competitive
$1 < \alpha < \infty$	$\beta = 1$	hyperbolic competitive
$\alpha \to 0$, $K_\mathrm{i} \to \infty$	$\beta = 0$	linear uncompetitive
$0 < \alpha < 1$	$0 < \beta < 1$ and $\alpha = \beta$	hyperbolic uncompetitive
$1 \leqslant \alpha < \infty$	$\beta = 0$	linear mixed-type
$1 \leqslant \alpha < \infty$	$0 < \beta < 1$	hyperbolic mixed-type

The rate equation A.1 is valid for the *General Modifier Mechanism* (scheme A.1) under the assumption of quasi-equilibrium for the binding of I to E and ES, and steady-state for the fluxes around ES and ESI. v_0 and v_i are the initial rates in absence and presence of the inhibitor and $\sigma = [\mathrm{S}]/\mathrm{K_m}$.

$$v_\mathrm{i} = \frac{v_0(1+\sigma)\left(1+\beta\dfrac{[\mathrm{I}]}{\alpha K_\mathrm{i}}\right)}{1+\dfrac{[\mathrm{I}]}{K_\mathrm{i}}+\sigma\left(1+\dfrac{[\mathrm{I}]}{\alpha K_\mathrm{i}}\right)} \tag{A.1}$$

A.2.2 Slow-Binding Inhibition

The formation of an intermediate during catalysis with structural analogy to the transition state, or the fact that the actual inhibition needs a conformational change in the enzyme that is slow on the steady-state time scale, can result in a slow formation of the enzyme-inhibitor complex.

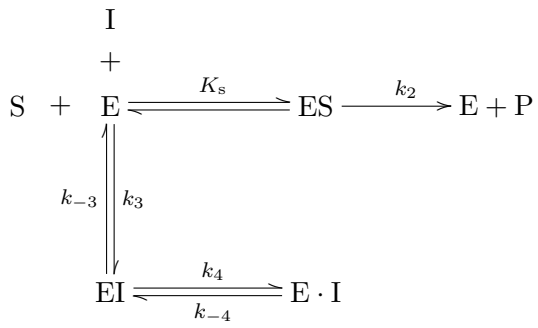

(a) two step mechanism

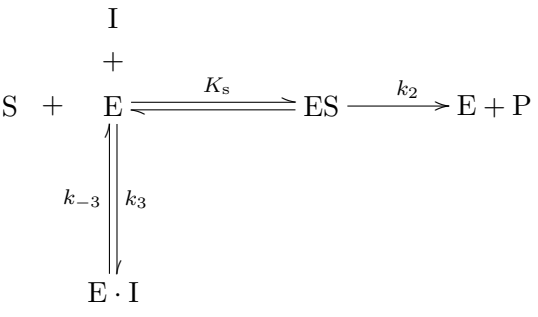

(b) one step mechanism

Scheme A.2: Reversible slow-binding inhibition mechanism in two steps (a) and in one step (b). E: enzyme, S: substrate, I: inhibitor, EI: adsorptive complex, E·I: noncovalent complex. In both cases the formation of E·I is slow.

Two common reaction mechanisms of slow-binding competitive inhibition are shown in Scheme A.2, with EI indicating an adsorptive complex and E·I a stable noncovalent complex. In case of the slow-binding mechanism in two steps (Scheme A.2a) the fast formation of the adsorptive EI complex is

followed by a slow generation of a stable but reversible E·I complex. In the case of Scheme A.2b, a degeneration of Scheme A.2a, already the first step is slow.
The progress curves of both mechanisms are described by the integrated rate equation A.2.

$$P = v_s t + \frac{(v_z - v_s)}{\lambda}(1 - e^{-\lambda t}) \tag{A.2}$$

v_s is the velocity of the reaction at steady state, v_z the velocity at the beginning of the reaction (*zero time*), λ a first order constant, which describes the exponential phase and t indicates time.
To distinguish whether a one or a two step slow-binding inhibition mechanism is present, progress curves with different inhibitor concentrations are analyzed. The behavior of the parameters λ, v_z and v_s in dependence of the inhibitor concentration indicate the proper mechanism. For example, for mechanism A.2a v_z depends on the inhibitor concentration, for mechanism A.2b it does not.

A.2.3 Tight Binding Inhibition

In case of a tight binding inhibitor, $[I]_t \approx [E]_t$ and K_i (Table A.1), the affinity of the inhibitor for the enzyme is very high and the inhibition process fast. In this case, it can not be assumed any longer that the free inhibitor concentration [I] is identical with the total inhibitor concentration $[I]_t$, but its decrease has to be taken into account.
Equation A.3 describes classical reversible tight binding inhibition based on the General Modifier Mechanism (Scheme A.1) [8, 104]. Again, the parameters α, β and K_i determine the characteristics of the inhibitor.

$$\begin{aligned} v_i = & \frac{v_0}{2}\left[\frac{\alpha+\sigma-\beta(1+\sigma)}{\alpha+\sigma}\right]\left[\sqrt{\left[\left(\frac{1+\sigma}{\alpha+\sigma}\frac{\alpha K_i}{[E]_t}+\frac{[I]_t}{[E]_t}-1\right)^2+4\frac{1+\sigma}{\alpha+\sigma}\frac{\alpha K_i}{[E]_t}\right]}\right. \\ & \left.+\frac{\alpha+\sigma+\beta(1+\sigma)}{\alpha+\sigma-\beta(1+\sigma)}-\frac{1+\sigma}{\alpha+\sigma}\frac{\alpha K_i}{[E]_t}-\frac{[I]_t}{[E]_t}\right] \end{aligned} \tag{A.3}$$

It is advantageous that the values for v_0, σ and $[E]_t$ are known, what eases the fitting of the experimental data by nonlinear regression analysis.

A.2.4 Slow, Tight-Binding Inhibition

A tight binding inhibitor can additionally show slow-binding characteristics [77, 99, 103]. Similarly to slow-binding inhibition, the mathematical treatment of such an inhibition is fitting of Eq. A.4 to progress curves. The meaning of the parameters v_z, v_s and λ is the same as in slow-binding mechanisms (Section A.2.2), but Eq. A.4 describes the one step mechanism only.

$$P = v_s t + \frac{(v_z - v_s)(1-\gamma)}{\gamma\lambda} \ln \frac{(1-\gamma e^{-\lambda t})}{1-\gamma} \tag{A.4}$$

$$\gamma = \frac{K_i(1+\sigma) + [E]_t + [I]_t - Q}{K_i(1+\sigma) + [E]_t + [I]_t + Q} \tag{A.5}$$

$$\text{with} \quad Q = \sqrt{(K_i(1+\sigma) + [E]_t + [I]_t)^2 - 4[E]_t[I]_t} \tag{A.6}$$

A.3 Mechanisms of Inactivation

Inactivators have a more drastic effect on the enzyme activity than reversible inhibitors. Similarly to the slow-binding mechanisms, a primary distinction is made between a one and a two step inactivation mechanism (Scheme A.3). In case of a two step mechanism, a reversible step with the formation of an adsorptive EI complex precedes the inactivation step resulting in the covalent binding of the inhibitor to the enzyme (E-I).

Similarly to slow-binding inhibition mechanisms, progress curves in presence of different inactivator concentrations are fitted to Eq. A.7.

$$P = \frac{v_z}{\lambda}\left(1 - e^{-\lambda t}\right) \tag{A.7}$$

The values of λ obtained for different inactivator concentrations are fitted either to Eq. A.8 or A.9, depending on whether the inactivation occurs in two or in one step, respectively.

$$\lambda = \frac{k_4}{1 + \frac{K_3}{[I]}(1+\sigma)} \tag{A.8}$$

$$\lambda = \frac{k_3}{1+\sigma}[I] \tag{A.9}$$

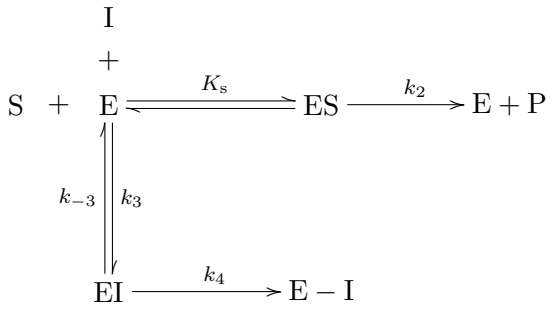

(a) two step mechanism

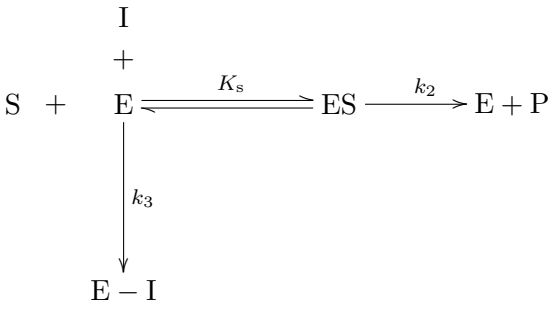

(b) one step mechanism

Scheme A.3: Inactivator mechanisms in two steps (a) and in one step (b). E: enzyme, S: substrate, I: inhibitor, EI: adsorptive complex, E-I: covalent complex.

The meaning of v_z and λ are the same as in slow-binding mechanisms. v_s is not present because after a certain time all enzyme will be covalently bound to the inhibitor and therefore no substrate is transformed and the reaction velocity at steady state is necessarily zero.

Enzyme Activation Mechanisms

B.1 Classification and Mechanisms

Classical activators are as well described by Scheme A.1. Similarly to the inhibition mechanisms, the definition of activation mechanisms is based on the characteristics of the parameters α, β and K_i.
There are two mechanisms worth mentioning in the context of an overview of activation mechanisms, namely the essential (Scheme B.1a) and the mixed activation (Scheme B.1b).

In case of an essential activator, its presence is necessary for substrate binding to the enzyme. The activator is needed only for catalysis of the substrate in case of a mixed activator, but its presence is not necessary for substrate binding to the enzyme.
The rate equations for essential (Eq. B.10) and mixed activation (Eq. B.11), indicate their analogy to linear competitive and mixed type inhibition.

$$v_\mathrm{a} = \frac{v_0(1+\sigma)}{1+\frac{K_\mathrm{x}}{[\mathrm{X}]}+\sigma} \tag{B.10}$$

$$v_\mathrm{a} = \frac{v_0(1+\sigma)}{\alpha\left(1+\frac{K_\mathrm{x}}{[\mathrm{X}]}\right)+\sigma\left(1+\frac{\alpha K_\mathrm{x}}{[\mathrm{X}]}\right)} \tag{B.11}$$

Nevertheless, there are some differences between these mechanisms: Firstly, a competitive inhibitor does most likely not bind simultaneously with substrate, whereas an essential activator does so. Secondly, essential activation are much less frequently observed than competitive inhibition.

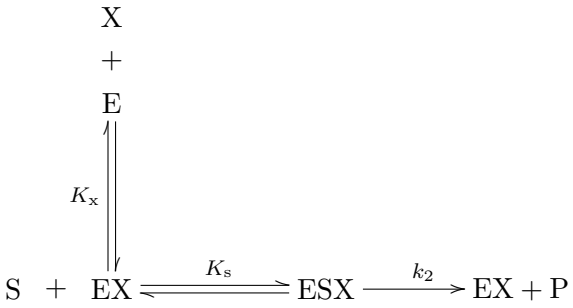

(a) essential activation

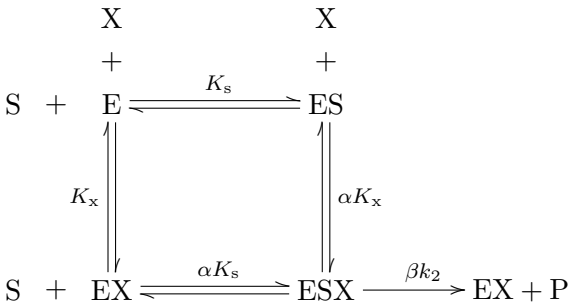

(b) mixed activation

Scheme B.1: Mechanisms of activation.

Curriculum Vitae

Persönliche Daten

Name	SCHENKER
Vorname	Patricia
Geburtsdatum	27. April 1979
Bürgerort	Walterswil SO

Ausbildung

12/2005-heute	Dissertation in Biochemie Universität Zürich
9/2000-11/2005	Studium der Umweltnaturwissenschaften Eidgenössische Technische Hochschule Zürich Umwelthygiene und aquatische Systeme 'Untersuchung der Aussagekraft der $LSWT_{skin}$ bezüglich der $LSWT_{bulk}$ unter Einfluss meteorologischer Bedingungen'
8/1995-3/2000	Wirtschaftsgymnasium Typus E Kantonsschule Olten SO

Publikationen

P. Schenker, A. Baici
Paradoxical interactions between modifiers and elastase-2
Manuscript

P. Schenker, A. Baici
Simultaneous interaction of enzymes with two modifiers: reappraisal of kinetic models and new paradigms
Journal of Theoretical Biology, 2009, 261:318−329

A. Baici, P. Schenker, M. Wächter, P. Rüedi
3-Fluoro-2,4-dioxa-3-phosphadecalins as inhibitors of acetylcholinesterase. A reappraisal of kinetic mechanisms and diagnostic methods
Chemistry and Biodiversity, 2009, 3:261−282

P. Schenker, P. Alfarano, P. Kolb, A. Caflisch, A. Baici
A double-headed cathepsin B inhibitor devoid of warhead
Protein Science, 2008, 17:2145−2155